

**The Synthesis and Characterisation of a Novel  
Polyamine-Terpyridine Ligand and Related  
Complexes**

A thesis submitted in partial fulfilment  
of the requirements for the degree

of

**Master of Science in Chemistry**

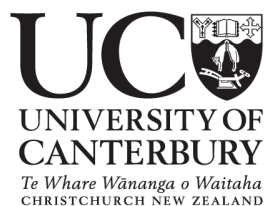
at the

**University of Canterbury**

by

**Paul A. Thornley**

---



**March 2009**

## Abstract

This project was aimed at synthesising, characterising and examining the properties of the novel polyamine ligand 4'-{2'''-(12-Amino-2,6,9-triazadodecyl)-phenyl}-2,2':6',2''-terpyridine and its related complexes. The ligand would be based around the 4'-(*o*-toluyl)-2,2':6',2''-terpyridine framework and have potential applications in analytical chemistry.

The 4'-(*o*-toluyl)-2,2':6',2''-terpyridine framework would have a tail attached on the functionalised *o*-toluyl methyl group. The *ortho* toluyl functionality was chosen so that the donor atom containing tail would be directed back towards the coordination site. This would make it easier for the tail to interact with a central metal ion. There is potential to be able to change the number and type of donor atom in the tail so that the ligand may be metal ion selective. As the tail would contain donor atoms, the denticity of the ligand would be increased making it more applicable for complexometric titrations. The 2,2':6',2'' terpyridines exhibit strong colours when coordinated to selective metal ions and so would have potential applications in colorimetry also.

The ligand was successfully synthesised and characterised. In a multi-step process, the 4'-(*o*-toluyl)-2,2':6',2''-terpyridine underwent radical bromination before the tail was attached. The tail used in this research was N,N'-bis (3-aminopropyl)ethane-1,2-diamine (3,2,3-tet). The secondary amines in this polyamine tail were protected before addition to the brominated 4'-(*o*-toluyl)-2,2':6',2''-terpyridine to ensure terminal addition. After the tail addition, a two step separation process purified a sample of 4'-{2'''-(12-Amino-2,6,9-triazadodecyl)-phenyl}-2,2':6',2''-terpyridine for analysis. Due to the late stage in this research where a successful

separation technique was found, little work was done on examining the properties of this ligand and its complexes.

## **Acknowledgements**

The research presented in this thesis is the result of two years of work and the finale of a five year personal goal. I have many people to thank for their support along this long, and sometimes arduous, journey.

Firstly, I would like to say a very personal thank-you to my supervisor, Dr Richard Hartshorn for his encouragement, support and pursuit of perfection. His commitment to teaching is exemplary and this has ensured my education was to a level second to none.

I would like to thank my family for their encouragement, after an initial period of... apprehension, and for their support. On many occasions I was supplied with items that would be considered a luxury on the student allowance. So, to Mum, Ash, Dad, my brothers, Craig and Grant and their respective partners, Thank-you very much. I will never forget and I have been humbled by your generosity.

To Barb, Georgy and Zoe, I am privileged to have had you all to share in my highs and support me through my lows.

To the Hartshorn group, thank-you for your support and help with learning many of the day to day issues that come with research. It has been a positive experience for me with many social occasions.

The team from the University of Canterbury Chemistry Department have been indispensable.

To:

- ❖ Wayne, Danny and Nick for fixing all things mechanical.
- ❖ Rob for fixing all things glass.
- ❖ Jeni, Matt, Peter and Jan for fixing all things crystal.
- ❖ Marie for fixing all things NMR, UV/Vis and mass spec.

# Table of Contents

<b>ABSTRACT</b>	<b>II</b>
<b>ACKNOWLEDGMENTS</b>	<b>IV</b>
<b>ABBREVIATIONS</b>	<b>VIII</b>
<b>CHAPTER 1: INTRODUCTION</b>	<b>1</b>
1.1 GENERAL OVERVIEW	1
1.2 STRUCTURES OF 2,2':6',2''-TERPYRIDINES	4
1.3 HISTORY OF TERPYRIDINES	8
1.4 SYNTHESIS OF TERPYRIDINES	9
1.5 PROPERTIES AND APPLICATIONS OF TERPYRIDINES	12
<b>CHAPTER 2: LIGAND SYNTHESIS</b>	<b>17</b>
2.1 INTRODUCTION	17
2.2 RESULTS AND DISCUSSION	18
2.2.1 4'-(o-Toluy)-2,2':6',2''-terpyridine Synthesis	18
2.2.2 The Radical Bromination Reaction	28
2.2.3 N,N'-bis (3-aminopropyl)ethane-1,2-diamine (3,2,3 tet) Protection Product: 1,5,8,12-Tetraazadodecane	32
2.2.4 The Amination Reaction	39
2.3 SUMMARY	53
<b>CHAPTER 3: METAL COMPLEXES &amp; CHARACTERISATION</b>	<b>54</b>
3.1.1 [Cu(ottp)Cl <sub>2</sub> ]-CH <sub>3</sub> OH	54
3.1.2 [Co(ottp) <sub>2</sub> ]Cl <sub>2</sub> ·2.25CH <sub>3</sub> OH	58
3.1.3 [Fe(ottp) <sub>2</sub> ][PF <sub>6</sub> ] <sub>2</sub>	62
3.1.4 [(Cl-ottp)Cu(μ-Cl)(μ-Br)Cu(Cl-ottp)][PF <sub>6</sub> ] <sub>2</sub>	66
3.1.5 The Iron(II) 2'''-patottp Complex	72
3.1.6 Miscellaneous 2'''-patottp Complexes	75
3.2 SUMMARY	75
<b>CHAPTER 4: CONCLUSIONS AND FUTURE WORK</b>	<b>77</b>
<b>CHAPTER 5: EXPERIMENTAL</b>	<b>79</b>
5.1 MATERIALS	79
5.2 NUCLEAR MAGNETIC RESONANCE (NMR)	79
5.3 SYNTHESIS OF 4'-(O-TOLUYL)-2,2':6',2''-TERPYRIDINE.	80
5.4 BROMINATION OF 4'-(O-TOLUYL)-2,2':6',2''-TERPYRIDINE.	84
5.5 PROTECTION CHEMISTRY FOR N,N'-BIS(3-AMINOPROPYL)ETHANE-1,2-DIAMINE (3,2,3-tet)	85
5.6 ADDITION OF PROTECTED TETRAAMINE TO BROMINATED TERPYRIDINE AND DEPROTECTION	86
5.7 PURIFICATION OF 4'-{2'''-(12-AMINO-2,6,9-TRIAZADODECYL)-PHENYL}-2,2':6',2''-TERPYRIDINE.	87
5.8 METAL COMPLEXES OF 4'-(O-TOLUYL)-2,2':6',2''-TERPYRIDINE (OTTP) AND DERIVATIVES	88
5.8.1 Cu(ottp)Cl <sub>2</sub> ·CH <sub>3</sub> OH	88
5.8.2 [Co(ottp) <sub>2</sub> ]Cl <sub>2</sub> ·2.25CH <sub>3</sub> OH	88
5.8.3 [Fe(ottp) <sub>2</sub> ][PF <sub>6</sub> ] <sub>2</sub>	88

5.8.4	$[(\text{Cl-ottp})\text{Cu}(\mu\text{-Cl})(\mu\text{-Br})\text{Cu}(\text{Cl-ottp})][\text{PF}_6]_2$	89
5.8.5	The Iron(II) 2 <sup>'''</sup> -patottp Complex	90
<b>REFERENCES</b>		<b>92</b>
<b>APPENDIX</b>		<b>95</b>
<b>X-RAY CRYSTALLOGRAPHIC TABLES</b>		<b>95</b>
1.1	1,5,8,12-TETRAAZADODECANE	95
2.1	$\text{CU}(\text{OTTP})\text{CL}_2 \cdot \text{CH}_3\text{OH}$	104
3.1	$[\text{CO}(\text{OTTP})_2]\text{CL}_2 \cdot 2.25\text{CH}_3\text{OH}$	111
4.1	$[(\text{CL-OTTP})\text{CU}(\text{M-CL})(\text{M-BR})\text{CU}(\text{CL-OTTP})][\text{PF}_6]_2$	123
<b>REFERENCES</b>		<b>134</b>

## ABBREVIATIONS

2,2,2-tet	N,N'-bis(2-aminoethyl)-ethane-1,2-diamine
2'''-patottp	4'-{2'''-(12-amino-2,6,9-triazadodecyl)-phenyl}-2,2':6',2'''-terpyridine
3,2,3-tet	N,N'-bis-(3-aminopropyl)-ethane-1,2-diamine
<sup>1</sup> H	Proton NMR
<sup>13</sup> C{ <sup>1</sup> H}	Proton decoupled Carbon-13 NMR
atms	atmospheres
COSY	2D <sup>1</sup> H NMR correlation spectroscopy
H.S	high spin
HSQC	Heteronuclear Single Quantum Coherence ADiabatic
Lit.	Literature
L.S	low spin
MHz	megahertz
NMR	Nuclear Magnetic Resonance
NOESY	nuclear Overhauser effect spectroscopy
O.S.	oxidation state
ottp	4'-( <i>o</i> -toluyl)-2,2':6',2'''-terpyridine
pos <sup>n</sup>	position
ppm	parts per million
ppt	precipitate
R <sub>1</sub>	Refinement factor
S.C.	spin crossover
TMPS	3-(trimethylsilyl)propane-1-sulfonic acid

TMS	trimethylsilane
tpy/s	terpyridine/s
Z	number of asymmetric units per cell
$\delta$	chemical shift
$\epsilon_{\max}$	extinction coefficient at maximum absorbance
$\lambda_{\max}$	wavelength at maximum absorbance

# Chapter 1: Introduction

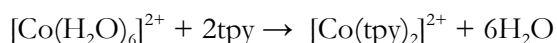
## 1.1 General Overview

This thesis describes the synthesis and study of a new polydentate ligand, 4'-{2''-(12-amino-2,6,9-triazadodecyl)-phenyl}-2,2':6',2''-terpyridine, which contains a terpyridine fragment along with additional amine donor groups in a flexible tail. This introductory chapter therefore discusses the background chemistry relevant to the synthesis and potential applications for this type of ligand.

Denticity is a term used in coordination chemistry which describes the type and number of donor atoms on a ligand which can coordinate to a central atom, usually a metal ion. Ambidentate, monodentate, bidentate and polydentate are the most commonly used related expressions. Ambidentate indicates more than one type of donor or heteroatom is included in the ligand. An example of an ambidentate ligand would be the thiocyanate ion ( $\text{NCS}^-$ ) as it is able to bind through the N atom or the S atom. A ligand which has three or more donor atoms for coordination is often called polydentate. An example of a polydentate ligand is terpyridine. This ligand has three N atoms and frequently binds in a meridional manner around an octahedral metal ion.

Polydentate ligands are able to form one or more chelate rings (from the Greek word *chelè*, meaning claw). This is where two of the donor atoms together with other atoms of the ligand form a ring with the central metal atom. The chelate effect is the name given to the extra stability that is observed for complexes of chelating ligands compared to those of the

equivalent number of monodentate ligands<sup>1</sup>. The extra stability can be understood in two ways. For example, if an ammonia ligand dissociates from a metal ion, it is easily lost into the solution surrounding the complex. If, however, one of the donor atoms of a tridentate ligand dissociates, it is far less likely that the second and/or third donor atom/s would dissociate at the same time so that the ligand would be lost into the surrounding solution. The donor atom that had dissociated is held close and is therefore more likely to re-coordinate than if it was free in solution. Secondly, there is a gain in stability that is achieved through the more positive entropy change associated with complexation of a polydentate compared to that for monodentate ligands. When a polydentate ligand replaces some or all of the monodentate ligands on a metal ion, more disorder is generated<sup>2</sup>. In a reaction where the number of product molecules are greater than the number of starting reagent molecules, there are more degrees of freedom in the product, greater disorder, and therefore the reaction has a positive change in entropy. In the reaction between cobalt(II) hexahydrate and tpy, three molecules on the left produce the seven molecules on the right:



There are effects which can reduce the stability of the chelates. These include ring strain, especially in rigid ligands, ligand to ligand repulsion and the effective positive charge of the metal ion being reduced as more ligands are attached to the metal ion. The strength of metal-ligand ( $d-\pi^*$ ) back donation in terpyridine's enables them to bind strongly to a variety of metal ions<sup>3</sup>. This characteristic, the chelate effect and the tuned properties, through functionalised substituents (Fig 1-3), facilitate terpyridine's use in many applications.

For example, polydentate ligands can be exploited in the area of complexometric titrations and colorimetry. These two analytical techniques can be used to determine the concentration of metal ions in aqueous solutions. In the field of complexometric titrations, polydentate ligands are able to react more completely and often react with metal ions in a single step process. This gives the titration curves a sharper end point<sup>4</sup> (Figure 1-1).

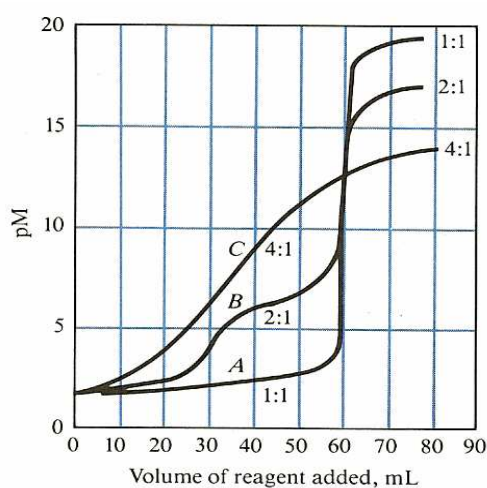


**Figure 1-1** Titration curves of a tetradentate ligand (A), a bidentate ligand (B) and a monodentate ligand (C). Douglas A. Skoog, Donald M. West, F. James Holler. *Analytical Chemistry. An Introduction*. Saunders College Publishing, U.S.A. 1994, p 239.

The end point is distinguished by observing a significant change in colour or, more commonly, by detecting the activity (concentration) of anionic species using an ion-selective electrode (ISE). The ISE can detect the activity of the metal ion directly ( $\text{pM}^{n+}$ ). Detection can also be through pH by using an indicator, such as erichrome black, which consumes  $\text{H}^+$  ions at specific pHs when it is displaced from the metal ion by the complexing agent<sup>5</sup>.

Colorimetry is used to determine the concentration of metal ions in aqueous solution. This technique can also detect the presence of a particular metal by visual means<sup>6</sup>. The concentration is established using a spectrophotometer which operates in the UV/Visible

region (200 – 800nm). From a series of complexes of known concentration, a set of absorbance values are established and a graph constructed. An absorbance reading from a sample of unknown concentration can then be obtained. This reading can then be interpolated directly from the graph or inserted into the equation, for the slope of the graph, to find the unknown concentration.

Terpyridines, or more specifically, 2,2':6',2''-terpyridine (tpy), is a ligand that is polydentate. Tpy can be modified with substituents, as we will show later, so that the denticity can be increased. Tpy also contains a conjugated system. A conjugated system generally enables a ligand to give a range of strong colours in the visible region when coordinated with a variety of metal ions. These intense colours facilitate ease of detection, as the presence of a particular metal ion can be identified by the human eye without the need for expensive diagnostic equipment. It is well documented that tpy gives an array of intense colours with a variety of metal ions<sup>7, 8 & 9</sup>. These characteristics make tpy ideal for use in colorimetry and could also provide applications in complexometric titrations.

## 1.2 Structures of 2,2':6',2''-Terpyridines

The tpy molecule contains three coupled pyridine rings. The central pyridine is coupled at the 2 and 6 positions to the other two pyridine rings. Both the outer two pyridine groups are coupled to the central pyridine at their 2 position. Rotation about the 2-2' and 6'-2'' bonds enables tpy to act as a tridentate ligand (Fig. 1 -2). The rigid planar geometry forces tpy to bind to a central octahedral metal ion in a meridional manner. For nomenclature purposes, positions on the left hand pyridine ring will be numbered 1 – 6, the central pyridine ring 1' – 6' and the right hand pyridine ring 1'' – 6''. In the case of presence of a 4'-aryl group,

positions will be numbered 1''' – 6''', and any major substituents will be labelled *ortho* (*o*), *meta* (*m*) or *para* (*p*) according to their position on the 4'-aryl ring.

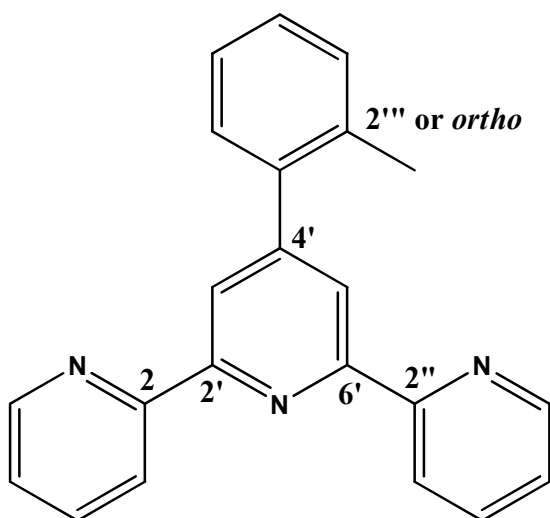


**Figure 1-2** The unsubstituted structure of *o*-toluy-2,2':6',2''-terpyridine.

There are many positions where the tpy ligand can have different substituents added (Fig. 1-3). These substituents are usually already part of tpy precursors<sup>10</sup>. Substituents in the 3 – 6 and 3'' – 6'' positions are called terminally substituted 2,2':6',2''-terpyridines as they are on the terminal rings. These substituents can be symmetrical or unsymmetrical. Terminal substitutions have, so far, been reported only in very limited numbers<sup>11, 12 & 13</sup>.

By far the most substitutions have been in the 4' position. In this position, the substituent is directed away from the meridional coordination site of the ligand. There are two main synthetic pathways for adding substituents in the 4' position after construction of the tpy framework, shown in the scheme below. Firstly (route a), 4'-terpyridinoxy derivatives are easily accessible *via* a nucleophilic aromatic substitution of 4'-haloterpyridines by primary

alcohols and analogs and secondly (route b) by  $S_N2$ -type nucleophilic substitution of the alcoholates of 4'-hydroxyterpyridines<sup>14</sup>.

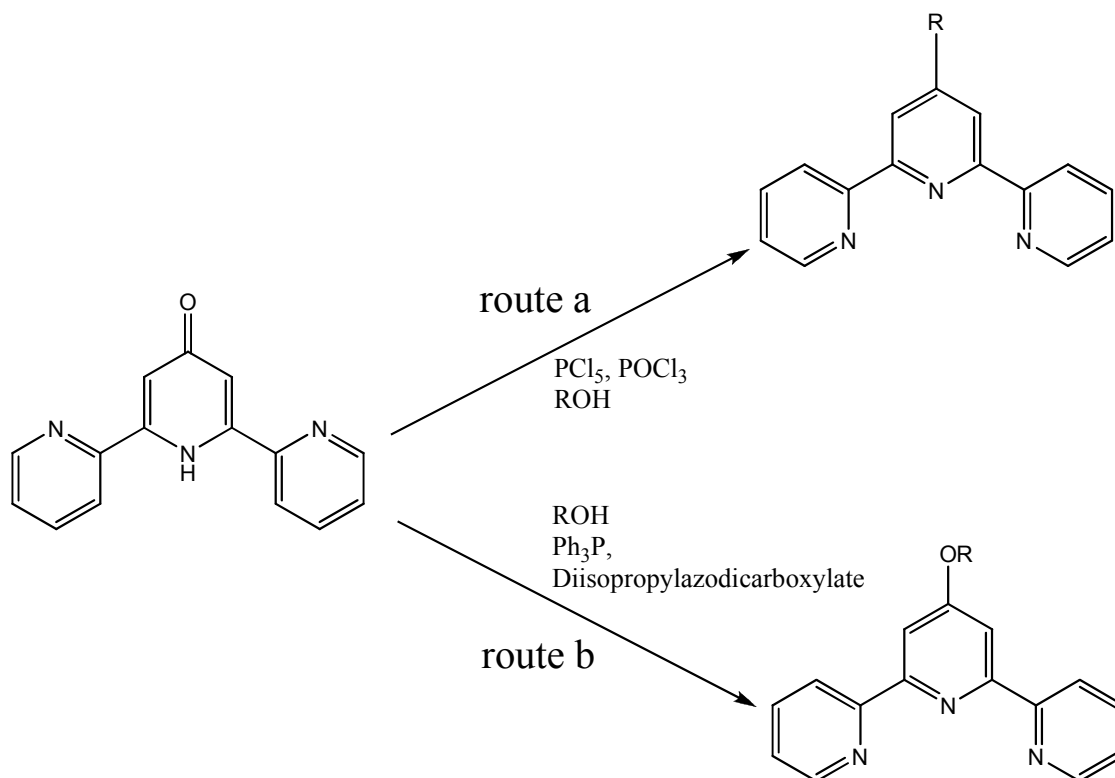


**Figure 1-3** 2,6-bis(2-pyridyl)-4(1H)-pyridone with route a) the nucleophilic aromatic substitution via a 4'-halo terpyridine and route b) an  $S_N2$ -type nucleophilic substitution.

4'-Arylterpyridines can also be synthesised from the starting materials *via* the Kröhnke ring closure method (Figure 1-4). More details on these reactions are given in Section 1.4, Synthesis of Terpyridines.

Once again the majority of the functional substituents, of the aryl group are in the *para* position and, point directly away from the coordination site. The *ortho* site could be exploited so that a “tail” containing donor atoms would be directed back towards the coordination site (Figure 1-5). The “R” group, or tail, would now be able to interact with the metal ion and

more closely to the rest of the ligand. This close interaction with the tail could thereby influence the properties, such as fluorescence, redox potential and colour intensity of the complex.

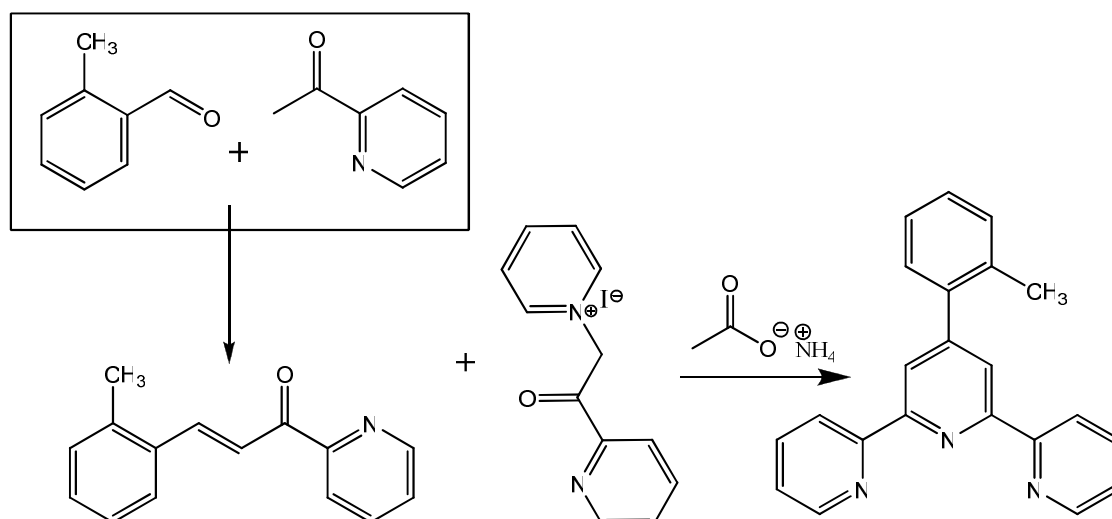


**Figure 1-4** The Kröhnke ring closure synthetic route of a 4'-aryl-terpyridine. Inset shows the origin of the 4'-aryl substituent, *o*-toluyl aldehyde.

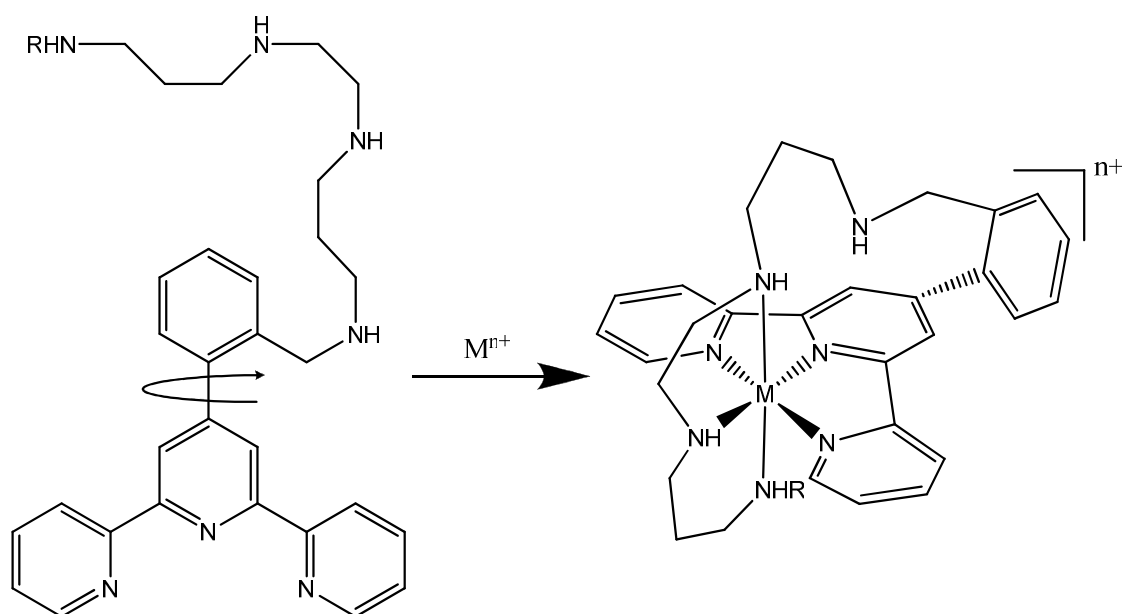


**Figure 1-5** Terpyridine with a poly heteroatom “tail” interacting with a central metal ion.

With the addition of the tail, the shape of this molecule is reminiscent of a scorpion as it bites through the three pyridine nitrogen atoms and the tail comes over the top to “sting” the metal centre. It could be said that this molecule is more scorpion-like than the classes of ligands called scorpionates<sup>15</sup> or scoriands<sup>16</sup> (Figure 1-6).

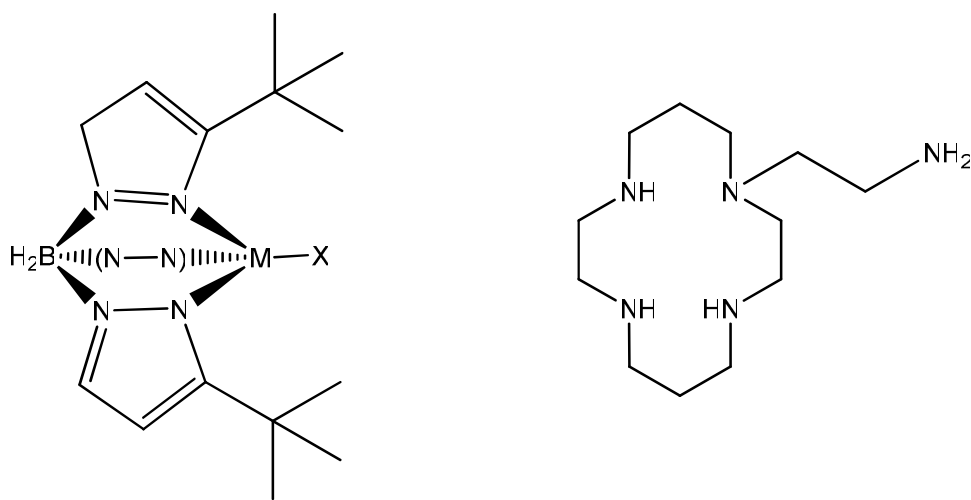


**Figure 1-6** Examples from the classes of ligands called scorpionates<sup>15</sup> (left) and scoriands<sup>16</sup> (right)

### 1.3 History of Terpyridines

Sir Gilbert Morgan and Francis H. Burstall were the first to isolate terpyridine in the 1930's. They achieved this by heating between one and eight litres of pyridine in a steel autoclave to 340°C, at 50 atms, with anhydrous ferric chloride for 36 hours<sup>17</sup>. Since this discovery, terpyridines have been widely studied. As of the late 1980's, research into terpyridines and their applications has grown exponentially (Fig. 1-4). The application of tpy's in supramolecular chemistry has certainly contributed to this growth<sup>18</sup>.

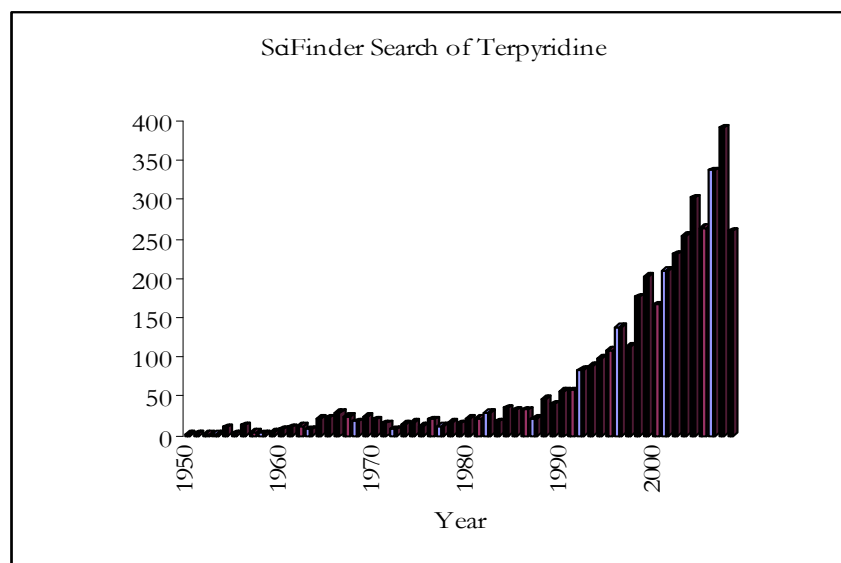
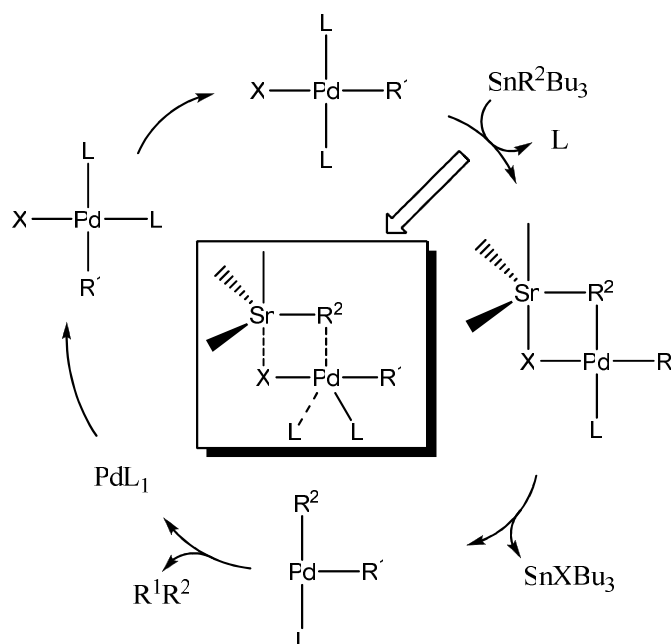
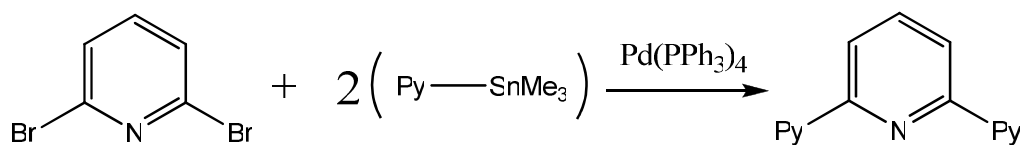


Figure 1-7 A graph of a search done using SciFinder on articles containing the term terpyridine as of 30/10/2008

## 1.4 Synthesis of Terpyridines

There are two commonly used synthetic routes for the production of terpyridines. These are the cross-coupling and the ring assembly methods. The cross-coupling method has mostly given poor conversions and has been the less favoured of the two. The Kröhnke ring assembly method has, to date, been the more popular method.

The Stille cross-coupling reaction is a palladium catalysed carbon-carbon bond generation from the reaction of organotin reagents<sup>19</sup>. The mechanism of the reaction is still the subject of debate<sup>20,21</sup> (Fig. 1-7). It appears that the 2,6-dibromo-pyridine completes two cycles to form the 2,2':6',2''-terpyridine. It is also possible that there are two palladium catalysts acting simultaneously on the 2,6-dibromo-pyridine.



**Figure 1-8** A generic Stille coupling synthesis of 2,2':6',2'' terpyridine. (Py = pyridine). Below is a mechanism proposed by Espinet and associates Arturo L. Casado, Pablo Espinet and Ana M. Gallego. *J. Am. Chem. Soc.* 2000, 122, p 11771 – 11782.

This method of tpy synthesis could become more popular than the conventional ring closure method as cross-coupling becomes more efficient. Schubert and Eschbaumer recently described the formation of 5,5''-dimethyl-2,2':6',2''-terpyridine with a yield of 68% using the Stille cross-coupling method<sup>22</sup>. Efficiency aside, the fact remains that organotin compounds are volatile and toxic which creates environmental issues<sup>23</sup>.

The Kröhnke ring closure synthesis<sup>24</sup> is well known and widely used<sup>25,26,27,28&29</sup>. The ring closure is facilitated by ammonia condensation with the appropriate enone or a 1,5 diketone (Figure 1-9).

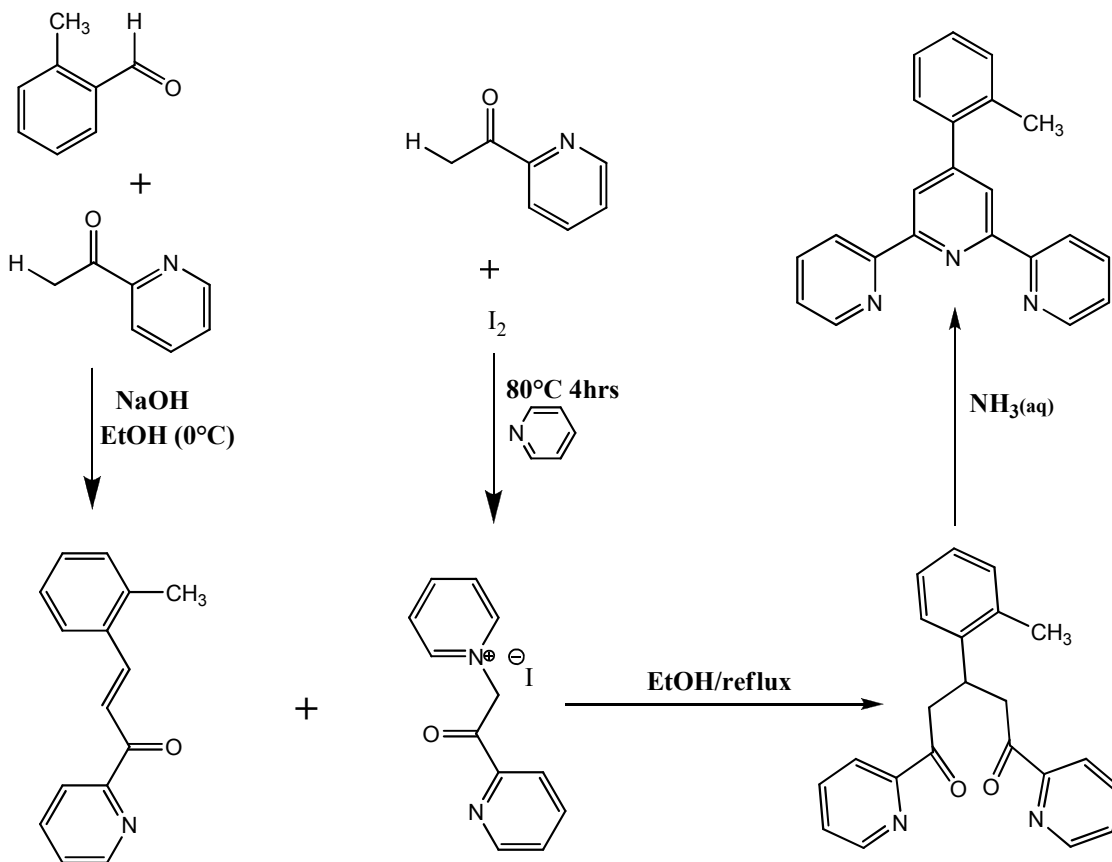


**Figure 1-9** The Kröhnke style synthesis for 4'-(*o*-touyl)-2,2':6',2''-terpyridine.

Sasaki *et al.* reports yields of up to 85% from some Kröhnke style condensations for synthesizing tpy<sup>30</sup>. Wang and Hanan describe a facile “one-pot” Kröhnke style synthesis of 4'-aryl-2,2':6',2''-terpyridines<sup>31</sup>. Cave and associates have investigated ‘green’ solvent free alternatives to the Kröhnke synthesis<sup>32,33</sup>.

These different syntheses have enabled substitution of the tpy ligand at most positions. This has allowed their application in many areas of structural chemistry such as coordination chemistry, polymer and supramolecular chemistry. The different substituents, in different positions, also change the properties of tpy. Much tpy research is based around the changes in properties that the addition of different substituents gives this ligand and its complexes.

The substituents can change the electronic and spectroscopic properties of tpy complexes. The change in tpy properties depends upon the electron donating and withdrawing characteristics and the position of the substituents<sup>34</sup>.

## 1.5 Properties and Applications of Terpyridines

The properties of tpy complexes are wide, varied and interesting. These properties are the reason that tpy complexes potentially have many practical applications<sup>35</sup>. Some examples are a conjugated polymer with pendant ruthenium tpy trithiocyanato complexes with charge carrier properties for potential application in photovoltaic cells<sup>36</sup>. A redox active bis (tpy) iron complex for charge storage which can be applied to the field of electronic memory storage<sup>37</sup>. The photoactive properties of tpy complexes lead to potential applications in organic light emitting diodes<sup>38</sup> and plastic solar cells<sup>39</sup>. Only the examples more important and relevant to this project will be described in more detail.

Luminescence is an important property that has potential applications in sensors. Luminescence is the emission of radiation/photons from a complex after the electronic excitation of the complex by radiation. The two mechanistic categories of luminescence are fluorescence and phosphorescence. Fluorescence is the emission of a photon with a lower energy (longer wavelength) than the radiation that was absorbed to increase the energy of the system. This mechanism is spin allowed and typically has half-lives in the order of nanoseconds. Phosphorescence is also the emission of a photon lower in energy than the radiation that was absorbed. This mechanism is spin forbidden, which usually results in a

significantly longer lifetime than in fluorescence. There are many complexes containing tpy that display luminescent behaviour and could be applied in the field of sensors. The choice of metal center is somewhat limited as most transition metals ( $d^1 - d^9$ ) are able to quench any luminophore in close proximity. They achieve this via electron transfer, redox, or by energy transfer due to partially filled d shells of low energy<sup>40</sup>.

Kumar and Singh recently described an eight coordinate complex of samarium and terpyridine  $[\text{SmCl}_2(\text{tpy})(\text{CH}_3\text{OH})_2]\text{Cl}$ . Although the emission spectrum was not shown in this paper for this complex, it was stated that all four samarium derivatives displayed the same emission features. Therefore  $[\text{SmCl}_2(\text{terpy})(\text{CH}_3\text{OH})_2]\text{Cl}$  has similar features to the spectrum for  $[\text{SmCl}_3(\text{bipy})_2(\text{CH}_3\text{OH})]$  which showed metal centered emission peaks at 562.0, 597.0, 664.0 and 715nm<sup>41</sup>. Zhang *et al* describe their spectroscopic studies of a multitopic tpy ligand, 4'-(4-pyridyl)-2,2':6',2''-terpyridine with a range of metal ions. They show that this ligand shows increasing luminescence, with increasing concentration, when coordinated to cobalt(II) and iron(II). The complexes then experienced luminescence quenching once the concentration exceeded  $1.3 \times 10^{-5} \text{ mol L}^{-1}$ . When 4'-(4-pyridyl)-2,2':6',2''-terpyridine was coordinated to samarium(III), europium(III) and terbium(III), the complexes showed both ligand and lanthanide ion emission<sup>42</sup>.

Redox potential is another reported property of tpy complexes. Molecules that display redox properties have prospective applications in charge storage<sup>43</sup>, solar cells<sup>44</sup> and photocatalysis<sup>45</sup>. Houarner-Rassin *et al* investigate a new heteroleptic bis(tpy) ruthenium complex that has improved photovoltaic photoconversion efficiency because of an appended oligothiophene on the tpy ligand. It was proposed that the appended oligothiophene unit decreased the rate

of the charge recombination process. Equally important, is the development of solid state strategies for real world applications. This is because the presence of liquid electrolyte in cells limits the industrial application due to the electrolytes long term stability<sup>46</sup>. This polymer coating has the potential to replace the liquid electrolytes are currently used in solar panels. Alternative sources of energy become increasingly important, especially as the worlds resources come under increasing pressure<sup>47</sup>

Molecular storage/switches are another area of importance. Advances in research give us the ability to develop applications with ever decreasing energy requirements using nanoscale technology<sup>48</sup>. Pipes and Meyer report on a terpyridine osmium complex  $[(\text{tpy})\text{Os}^{\text{VI}}(\text{O})_2(\text{OH})]^+$  that has a reversible three electron couple at the same potential<sup>49</sup>.

Colorimetry is the measurement of the change in the colour or intensity of light because of a chemical reaction. Metal ions are able to undergo a significant colour change when they exchange ligands. Detection can be identified by the naked human eye or the detection limit can be lowered significantly and read more precisely with an absorbance spectrometer<sup>50</sup>. This is a field in which this project could have potential applications. Kröhnke has already mentioned that some tpys are highly sensitive reagents for detecting iron(II)<sup>51</sup>. Zuo-Qin Liang *et al* developed a novel colorimetric chemosensor containing terpyridine capable of detecting relative amounts of both iron (II) and iron (III) in solution using light-absorption ratio variation approach<sup>52</sup>. Previous chemosensors have only been able to detect the total amount of Fe(II) + Fe(III) in solution. Coronado *et al* described a tpy ruthenium dye,  $[(2,2':6',2''\text{-terpyridine-4,4',4''-tricarboxylate})\text{ruthenium(II)} \quad \text{tris(tetrabutylammonium)}$

tris(isothiocyanate)]. The dye was able to detect and be specific for mercury(II) ions to 150 ppb<sup>53</sup>. From the crystals of a similar complex, where bis(2,2'-bipyridyl-4,4'-dicarboxylate) replaced (2,2':6',2''-terpyridine-4,4',4''-tricarboxylate), it was found that the mercury ions bound to the sulphur atom of the dye's thiocyanate group. This sensor also exhibited reversible binding by washing with potassium iodide. It was postulated that the iodide ions from the potassium iodide formed a stable complex with the mercury ions thereby releasing them from the ruthenium-tpy complex. In a later paper, Shunmugam and associates<sup>54</sup> detail tpy ligand derivatives able to detect mercury(II) ions in aqueous solution. The tpy ligands are able to selectively detect mercury(II) ions over other environmentally relevant metal ions such as Ca<sup>II</sup>, Ba<sup>II</sup>, Pb<sup>II</sup>, Co<sup>II</sup>, Cd<sup>II</sup>, Ni<sup>II</sup>, Mg<sup>II</sup>, Zn<sup>II</sup>, and Cu<sup>II</sup>. They report a detection limit of 2 ppb, the EPA standard for mercury(II) in drinking water.

There's no doubt that tpys have potential applications in the field of colorimetry. An area that has yet to reach its full potential is complexometry. Complexometry traditionally uses polydentate ligands and the closer the denticity to the coordination number of the target metal ion, the sharper the end-point<sup>55</sup>. The deprotonated form of EDTA is a typical agent, as it is hexadentate. This enables the ligand to completely encapsulate the target metal ion. Why have tpys been overlooked in the field of complexometric titrations? Perhaps it is because they are only tridentate and this is considered insufficient because if tridentate tpy was titrated against a metal ion with a coordination number of 6, two end points would be detected with each stepwise formation<sup>56</sup>. What if the denticity of tpys could be increased so that they too, could encapsulate the entire target metal ion? And, what if, tpys could be 'tuned' to suit a particular metal ion? We could use our knowledge of chemistry, such as hard soft acid base theory and preferential coordination number, to design these adaptations.

With the substituent in the 4' position, tpy has this functional group directed away from the coordination site. This may have been because the researchers were only interested in the effect these substituents had on the properties of the complex with tridentate binding. In this project we describe a tpy ligand that has been designed so that the substituent is directed back towards the coordination site. This tpy ligand is based on 2,2':6',2'' terpyridine with a 4'-aryl substituent. The difference with the 4'-aryl group on this tpy is that its functional group is in the *ortho* position. Most previously reported tpy ligand derivatives with a 4'-aryl group have had the functional group in the *para* position. If this functional group was in the *ortho* position of the 4' aryl substituent, it would now be positioned back towards the tridentate coordination site and could also be further functionalised. This *ortho* substituent could also contain donor atoms which would increase the denticity of the tpy ligand. There is scope to change the type and number of donor atoms in the substituent and as a result the tpy could be tuned to be specific for a particular metal ion.

There is a possibility that this ligand could form dimers, trimers or even undergo polymerisation when coordinating with metal ions. Formation of monomeric complexes may well be entropically favoured, but other effects may overcome this. Polymerisation could happen when the three terpyridine nitrogen atoms bind to one metal and the tail to a second. Then, three terpyridine nitrogen atoms from a second ligand bind to that second metal atom and its tail to a third metal atom and so on.

## Chapter 2: Ligand Synthesis

### 2.1 Introduction

The aim of the research presented in this thesis was to synthesise and characterise a new polydentate ligand based on the 4'-(*o*-toluyl)-2,2':6',2''-terpyridine framework and explore its coordination chemistry. The 4'-(*o*-toluyl)-2,2':6',2''-terpyridine was chosen because there was potential for the methyl group on the 4' toluyl ring to cause this ring to twist because of steric effects. This twist and the position of the methyl group on the ring means that the methyl group will now be directed back over the top of the ligand towards the tridentate tpy binding site. A tail containing donor atoms can now be attached to increase the denticity of the ligand and therefore binding to a central metal ion.

The plan to synthesise this new polydentate ligand is shown in the retrosynthetic analysis in the figure below (Figure 2-1). The tail addition is achieved *via* a radical bromination of 4'-(*o*-toluyl)-2,2':6',2''-terpyridine which in turn comes from the Kröhnke style ring closure of 2-methyl-1-[3-(2-pyridyl)-3-oxypropenyl]-benzene and (2-pyridacyl)-pyridinium iodide.

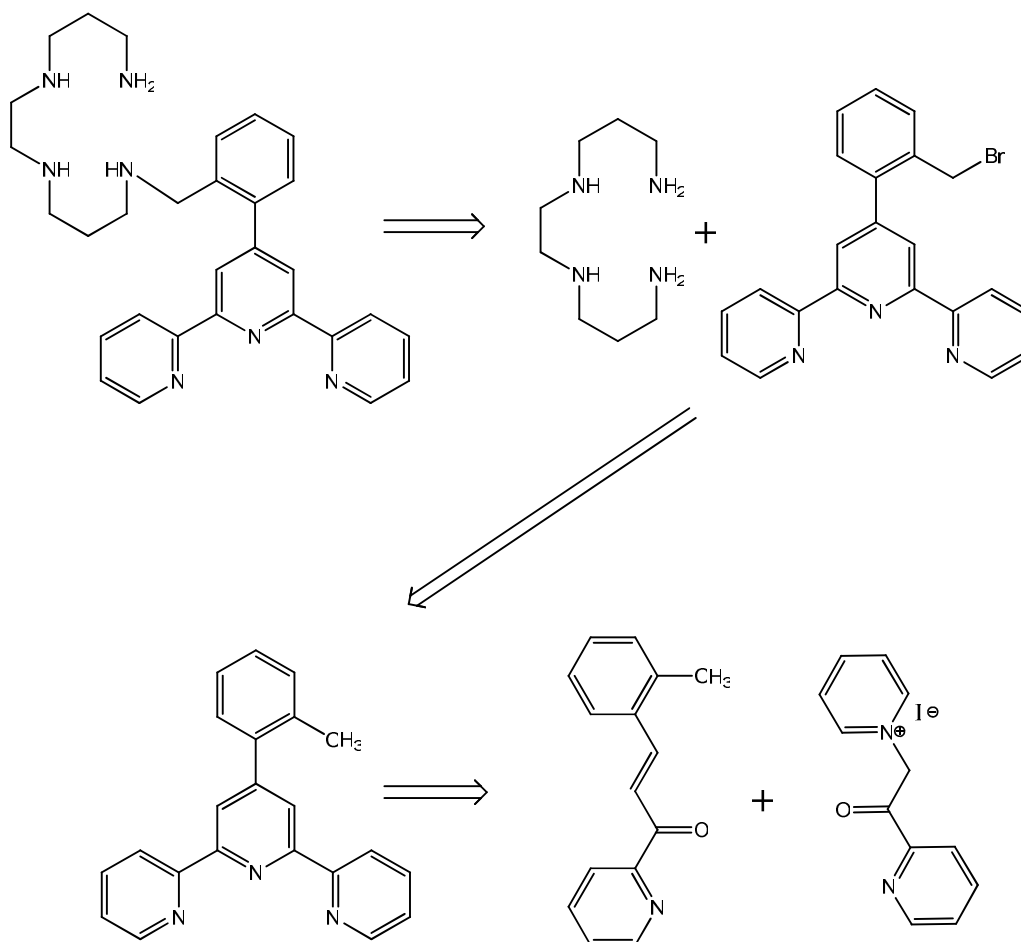


**Figure 2-1** The retrosynthetic analysis of 4'-(2''-(12-amino-2,6,9-triazadodecyl)-phenyl)-2,2':6',2''-terpyridine

## 2.2 Results and Discussion

### 2.2.1 4'-(*o*-Toluyyl)-2,2':6',2''-terpyridine Synthesis

Two methods were explored for the synthesis of 4'-(*o*-toluyyl)-2,2':6',2''-terpyridine. The three step Field *et al* method<sup>76</sup> gave a very pure product, after recrystallisation, but I obtained only poor overall yield at just 4% and it was very labour intensive. The second method is the Hanan “1 pot” synthesis<sup>75</sup>. I could increase the scale of that synthesis 5-fold without compromising the better yield, of over 51%. This synthesis gave a far greater yield and could

be produced in larger individual quantities with less time being consumed than with the three step method.

The  $^1\text{H}$  NMR spectra of the two precursors in the three step method, 2-methyl-1-[3-(2-pyridyl)-3-oxypropenyl]-benzene (Figure 2-3) and (2-pyridacyl)-pyridinium iodide (Figure 2-5) were compared with the literature results of Field *et al*<sup>76</sup> and Ballardini *et al*<sup>77</sup>, respectively, to confirm that the correct product had formed.

2-Methyl-1-[3-(2-pyridyl)-3-oxypropenyl]-benzene is a key intermediate in the three step synthesis of 4'-(*o*-toluyl)-2,2':6',2''-terpyridine. It is obtained through a reaction of equal molar amounts of 2-acetylpyridine and *o*-tolualdehyde. A yield of 34% was recorded and the product was off-white in colour and its physical appearance fluffy or fibrous.

The assignment of proton positions will be made using the numbering system for 2-methyl-1-[3-(2-pyridyl)-3-oxypropenyl]-benzene shown in Figure 2-2. In the  $^1\text{H}$  NMR spectrum for 2-methyl-1-[3-(2-pyridyl)-3-oxypropenyl]-benzene (Figure 2-3), there are 11 proton environments for the 13 protons. The signals assigned to the methyl group (pos<sup>n</sup> 16) and methylene proton (pos<sup>n</sup> 8) adjacent to the carbonyl carbon are the most obvious, with chemical shifts of 2.56 ppm and 8.80 ppm, and relative integral values of 3 and 1 respectively. The large downfield chemical shift of the peak at 8.80 ppm is due to the deshielding nature of the carbonyl group. The doublet for the alkene proton adjacent to the carbonyl carbon arises from the coupling to the single alkene proton (pos<sup>n</sup> 9) on the adjacent carbon atom. The remaining peaks, from 7.26 ppm to 8.30 ppm correspond to the aryl and pyridine protons (pos<sup>ns</sup> 2 – 5 and 11 – 14).

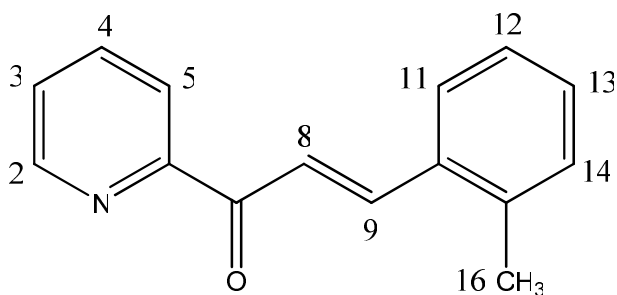


**Figure 2-2** The numbering system for 2-Methyl-1-[3-(2-pyridyl)-3-oxopropenyl]-benzene

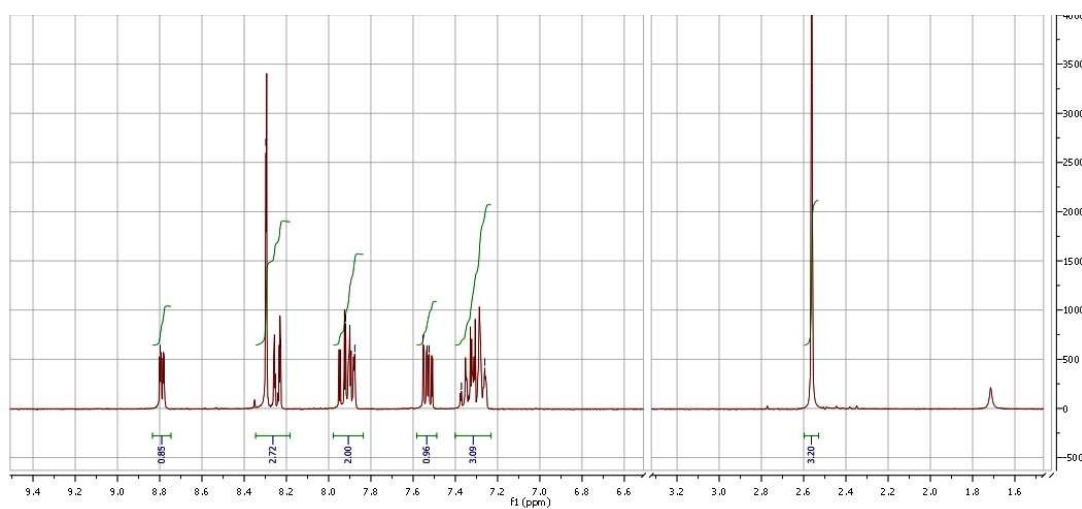


**Figure 2-3** The  $^1\text{H}$  NMR spectrum of 2-methyl-1-[3-(2-pyridyl)-3-oxopropenyl]-benzene

(2-Pyridacyl)-pyridinium iodide is the second intermediate required in the three step synthesis of 4'-(*o*-toluyl)-2,2':6',2''-terpyridine. It is obtained from reaction between iodine, pyridine and 2-acetylpyridine under inert conditions. A yield of 26% was obtained and the product was yellow/green and crystalline in appearance.

The numbering system for (2-pyridacyl)-pyridinium iodide is shown in Figure 2-4. The  $^1\text{H}$  NMR spectrum for (2-pyridacyl)-pyridinium iodide (Figure 2-5) shows there are 8 proton environments for the 11 protons. The singlet peak at 4.60 ppm was assigned to the two

protons on the carbon (pos<sup>n</sup> 8) adjacent to the carbonyl carbon (pos<sup>n</sup> 7) as no coupling to others protons is observed. This spectrum is consistent with the description in the literature<sup>77</sup>.

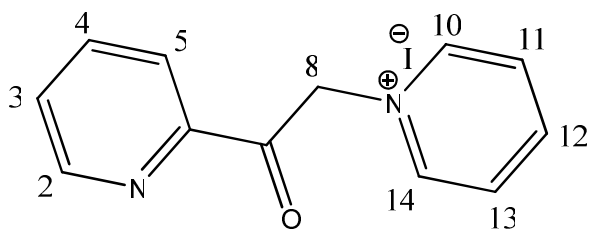


**Figure 2-4** The numbering system for (2-pyridacyl)-pyridinium iodide

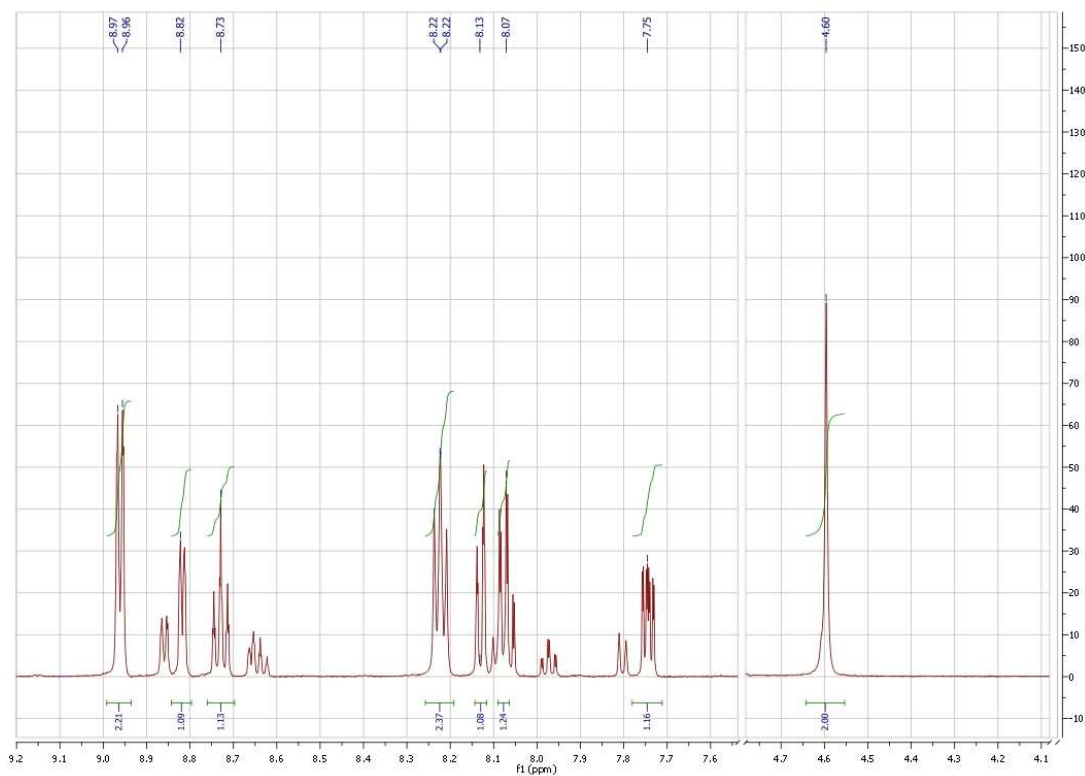


**Figure 2-5** The <sup>1</sup>H NMR spectrum for (2-pyridacyl)-pyridinium iodide

4'-(*o*-Toluy)-2,2':6',2''-terpyridine was synthesised by two methods as mentioned previously. The third step, in the three step method, involves a Michael addition followed by an aldol condensation between 2-methyl-1-[3-(2-pyridyl)-3-oxopropenyl]-benzene and (2-pyridacyl)-pyridinium iodide. The “1 pot” method is a reaction between 1 molar equivalent of *o*-tolualdehyde and 2 molar equivalents of 2-acetylpyridine. In both cases the product was a yellowish white precipitate.

Complete assignments of  $^1\text{H}$  and  $^{13}\text{C}$  NMR spectra were made and were consistent with the values given in the literature<sup>76</sup>. COSY, NOESY and HSQC spectra were also obtained. The  $^1\text{H}$  NMR spectrum (Figure 2-7) shows a total of 17 protons in the 10 environments. The *o*-toluy methyl group has a singlet peak at 2.38 ppm. The only other singlet peak in this spectrum is for the 3' and 5' protons at 8.49 ppm. The doublet peak at 8.70 – 8.72 ppm shows four protons in similar environments. Previous papers have assigned these peaks to 6,6'' at 8.72 ppm and for 3,3'' at 8.71 ppm<sup>51, 76</sup>.

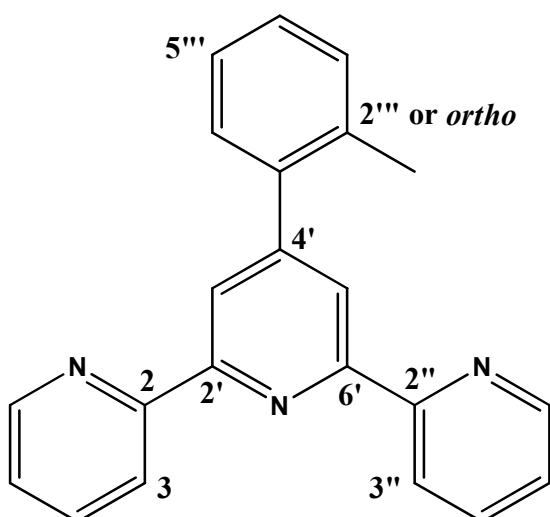


**Figure 2-6** The numbering system for 4'-(*o*-toluy)-2,2':6',2''-terpyridine

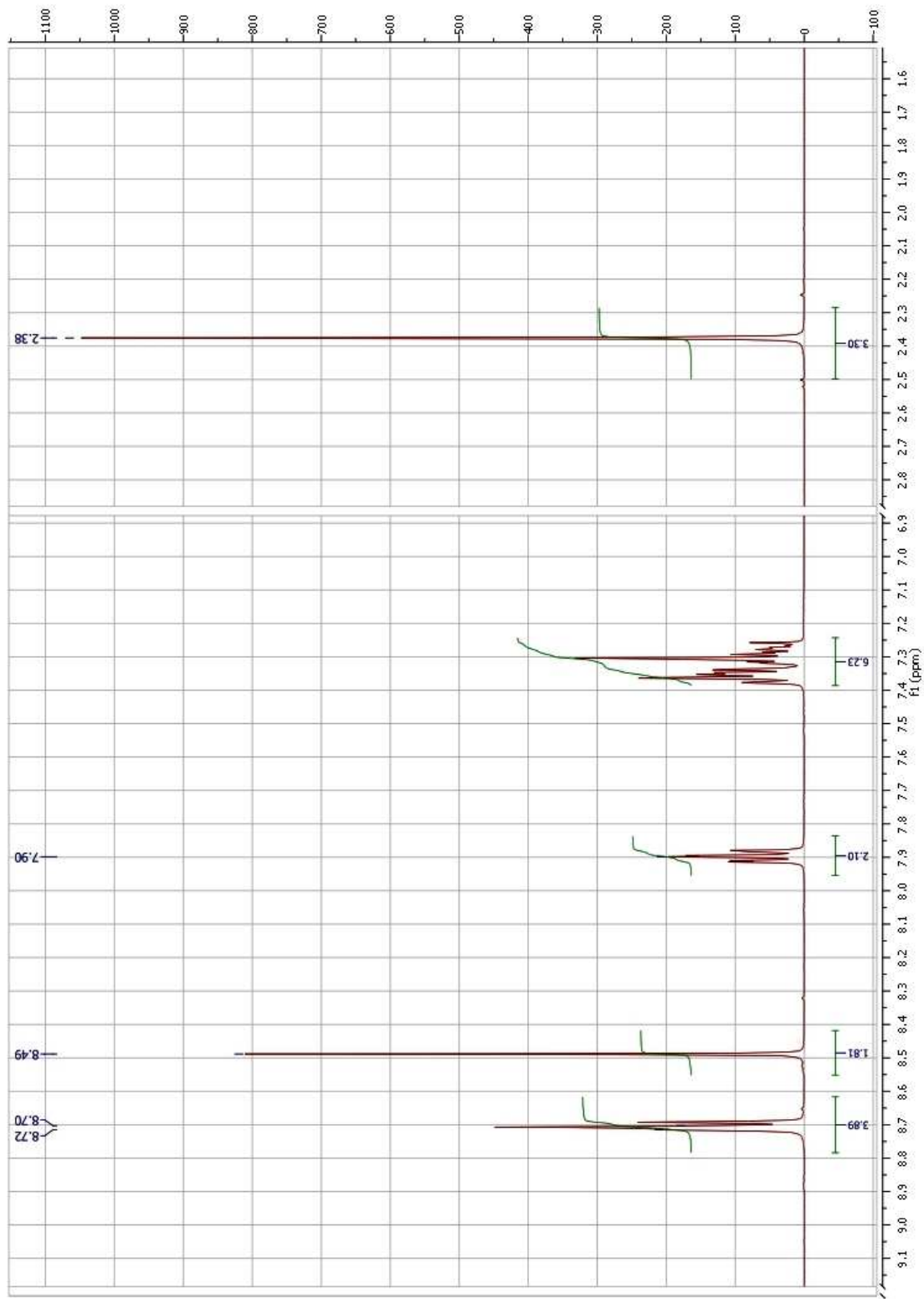


Figure 2-7 The <sup>1</sup>H NMR spectrum for 4-(*o*-toluy)-2,2':6',2''-terpyridine.

The COSY spectrum (Figure 2-8) shows that the overlapping doublets at 8.70 to 8.72 ppm both have couplings to protons at 7.90 ppm and around 7.30 ppm. The triplet at 7.90 ppm is coupled to the doublet peak for 3,3'' protons and so can be assigned to the 4,4'' protons. In a similar way the peaks at around 7.30 ppm can then be assigned 5,5'' protons. All the peaks for the pyridyl rings have now been assigned. The remaining peaks are assigned to the 4'-toluyl ring. This group of peaks wasn't able to be distinguished further by the other spectroscopic methods used.

The two NOESY spectra gave no useful results for *o*-toluyl-2,2':6',2''-terpyridine after the molecule was irradiated at 8.49 ppm and 2.38 ppm.

The HSQC spectrum (Figure 2-9) shows 9 carbon atoms, with protons attached, in the aromatic region. Four of these have the protons at 7.30 to 7.34 ppm. The methyl group can be assigned to the peak at 20.74 ppm.

The <sup>13</sup>C NMR spectrum (Figure 2-10) gives information on the quaternary carbon atoms which can be assigned based on them typically having lower peak heights and through cross-referencing with the HSQC spectrum. There are five environments for the quaternary carbon atoms which is consistent with the five shorter peaks in the spectrum. These peaks we found at 156.5, 155.6, 152.2, 139.9 and 135.4 ppm. Three of these peaks are the shortest, 152.2, 139.9 and 135.4 ppm. These can be assigned to the quaternary carbon atoms, 4', 1''' and 6'''. The other two peaks at 156.5 and 155.6 ppm, which have double the peak heights due to symmetry in the molecule, represent the quaternary carbons 2,2'' and 2',6'.

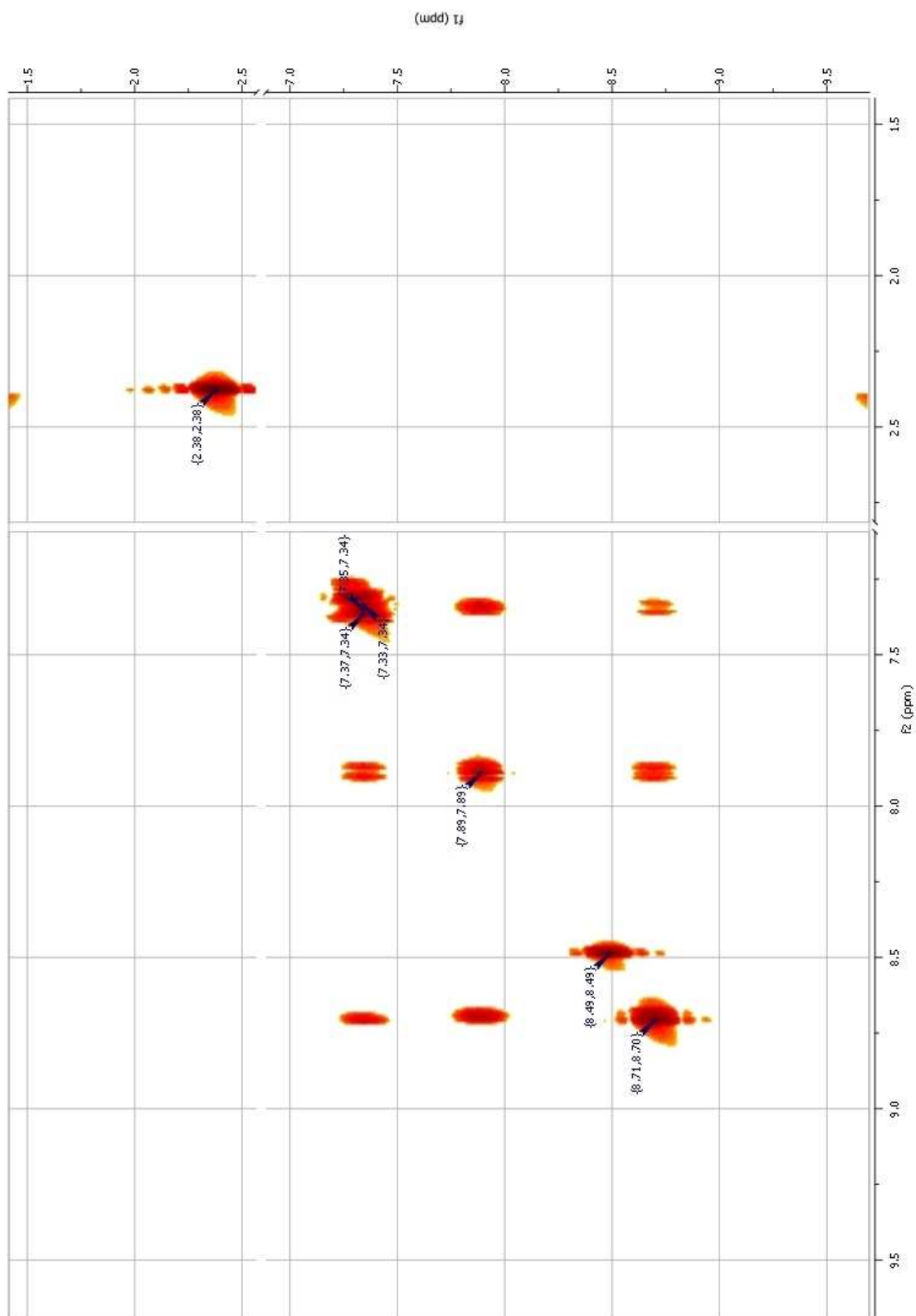
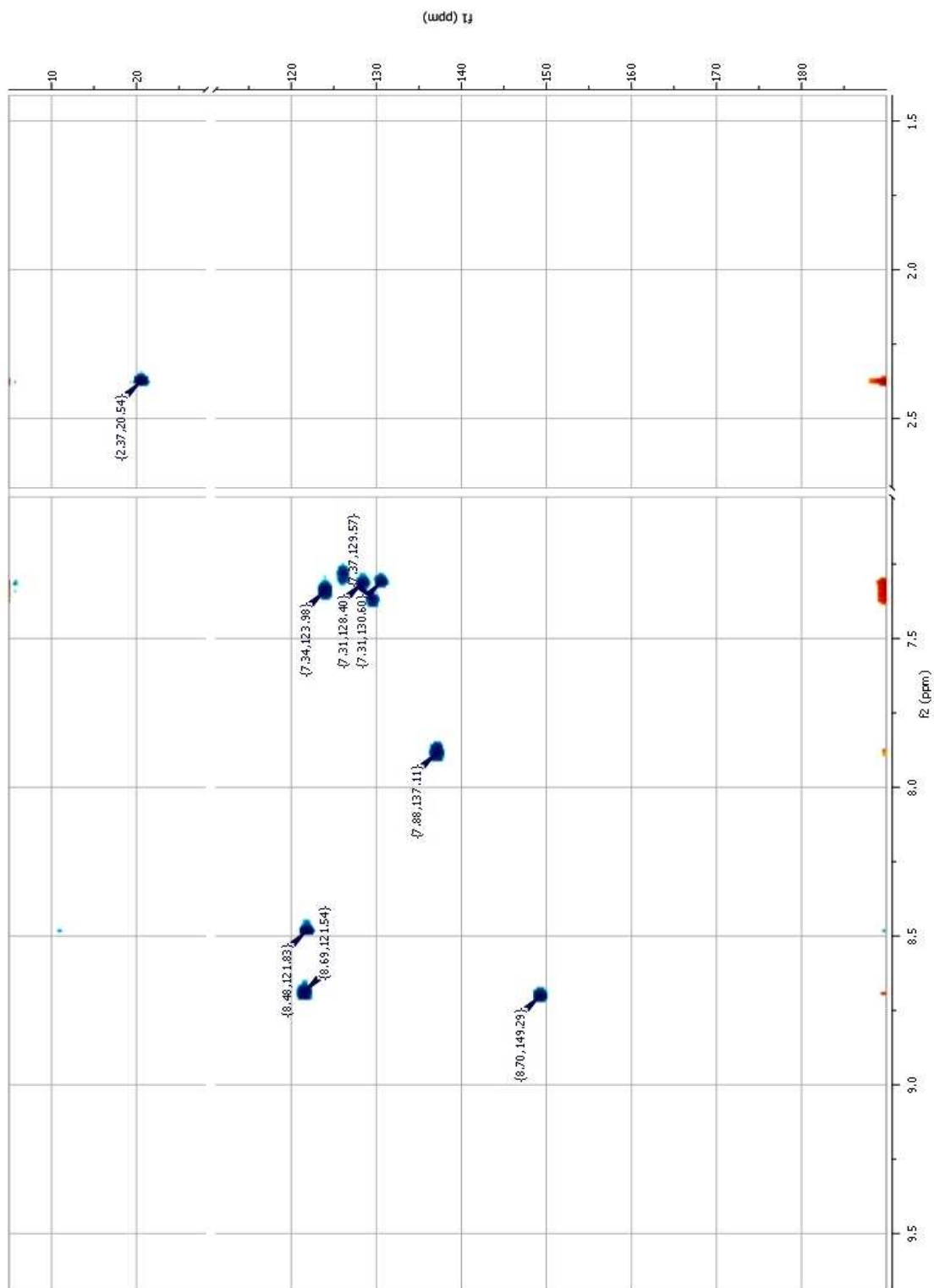


Figure 2-8 The COSY spectrum for 4'-(*o*-toluy)-2,2':6',2''-terpyridine.



**Figure 2-9** The HSQC spectrum for 4'-(*o*-toluy)-2,2':6',2''-terpyridine.

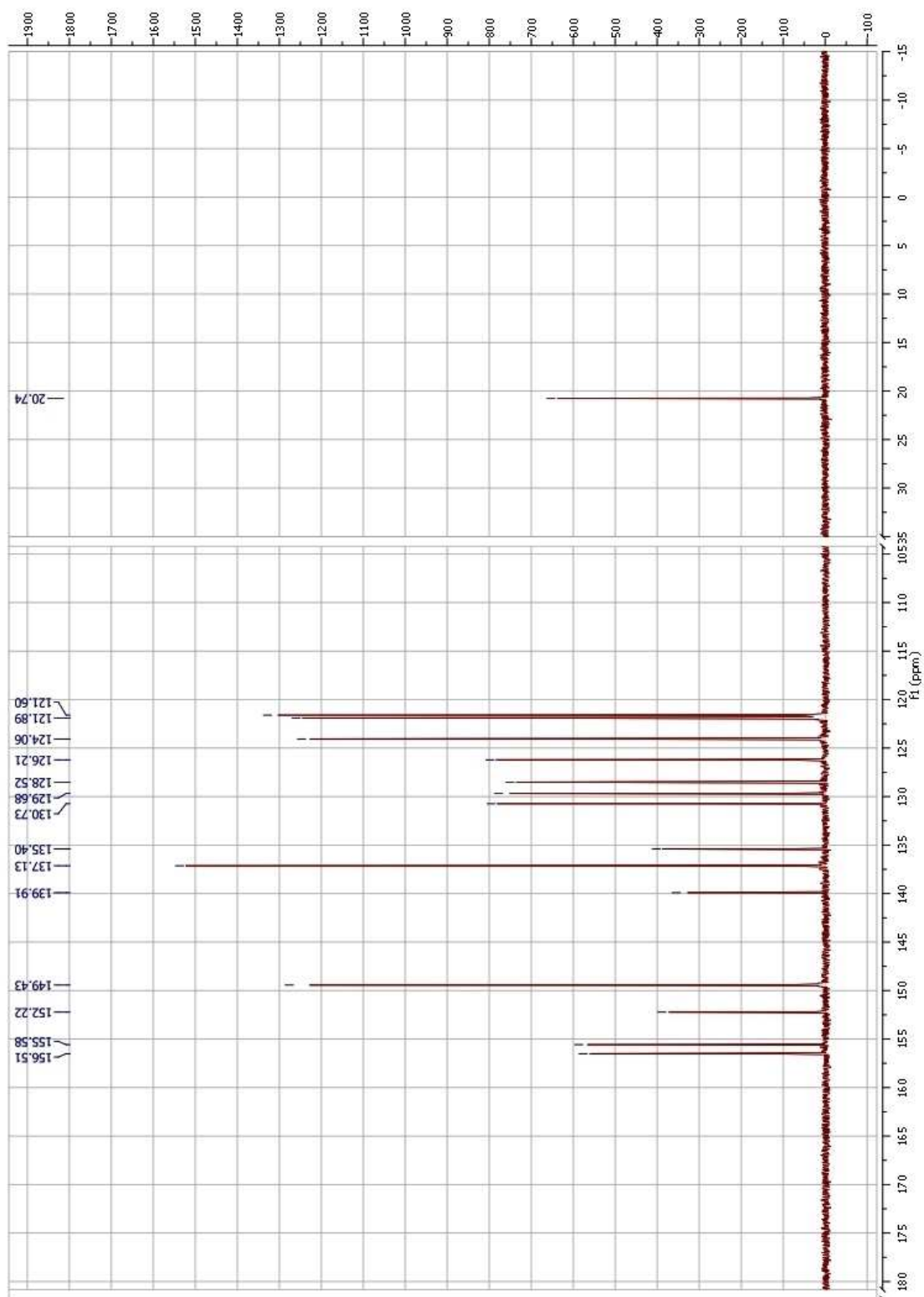


Figure 2-10 The  $^{13}\text{C}$  NMR spectrum for 4'-(*o*-toluy)-2,2':6',2''-terpyridine.

## 2.2.2 The Radical Bromination Reaction

The radical bromination step was initially performed in benzene and gave only mediocre results. Yields were low and there was always some starting material present, approximately 10%, in the final product. Carbon tetrachloride solvent was tried next in attempts to improve yields as it has no C-H bonds and doesn't easily undergo free radical reactions<sup>57</sup>. This approach was tried and found to be a great success. Not only were yields increased, but the final product was found to be of higher purity.

The radical bromination was a delicate reaction that required more care than with the previous reactions in this sequence. This reaction was carried out under inert conditions. Special care was also taken with all reaction vessels and solvent to remove the maximum amount of moisture content. The reaction vessels were stored in an oven (70°C) prior to the reaction. The carbon tetrachloride was dried over phosphorous pentoxide and this mixture was then heated at reflux in a still under inert conditions for four hours prior to use. The crude product of this reaction, 4'-(2-(bromomethyl)phenyl)-2,2':6',2''-terpyridine, was used directly because of its tendency to decompose. When benzene was the solvent, the yield was 38% and when using carbon tetrachloride, yields of up to 64% were achieved.

Crude samples of this molecule were characterized using <sup>1</sup>H NMR, COSY, HSQC and <sup>13</sup>C NMR spectroscopy. Only <sup>1</sup>H NMR and COSY spectra will be discussed as interest was principally focused on the extent of the radical bromination. Assignment of proton positions on this molecule follows the same numbering system of 4'-(*o*-toluyl)-2,2':6',2''-terpyridine (Figure 2-6). The <sup>1</sup>H NMR spectrum (Figure 2-11) clearly shows a new peak, in comparison to the <sup>1</sup>H NMR spectrum for 4'-(*o*-toluyl)-2,2':6',2''-terpyridine, at 4.45 ppm for the

brominated *o*-toluyl methyl group. There is also a small peak at 2.30 ppm in the spectrum which can be assigned to the *o*-toluyl-methyl group of unreacted 4'-(*o*-toluyl)-2,2':6',2''-terpyridine. A doublet peak has appeared at 7.42 ppm out of the cluster of peaks representing the 4'-toluyl and 5,5'' protons. The integral for this peak is consistent with it being due to a single proton and it is therefore assigned to the 4' toluyl proton. There are only two possibilities for doublets in the 4' toluyl ring, 3''' and 6''' protons, as the 4''' and 5''' proton peaks will appear to be triplets. This doublet most likely represents the 3''' proton and has moved downfield, presumably due to the electronegativity of the bromine atom.

The COSY spectrum (Figure 2-12) shows coupling of the new doublet peak at 7.42 ppm and the cluster of peaks but no coupling to the other terpyridine protons. This confirms that this proton is part of the 4'-toluyl ring.

The mass spectrum of 4'-(2-(bromomethyl)phenyl)-2,2':6',2''-terpyridine (Figure 2-13) showed good results with peaks at 402.0603 and at 404.0605. This two peak set, two units apart, is typical of mass spectra for bromine containing molecules. The isotope pattern was in agreement with the calculated isotope pattern.

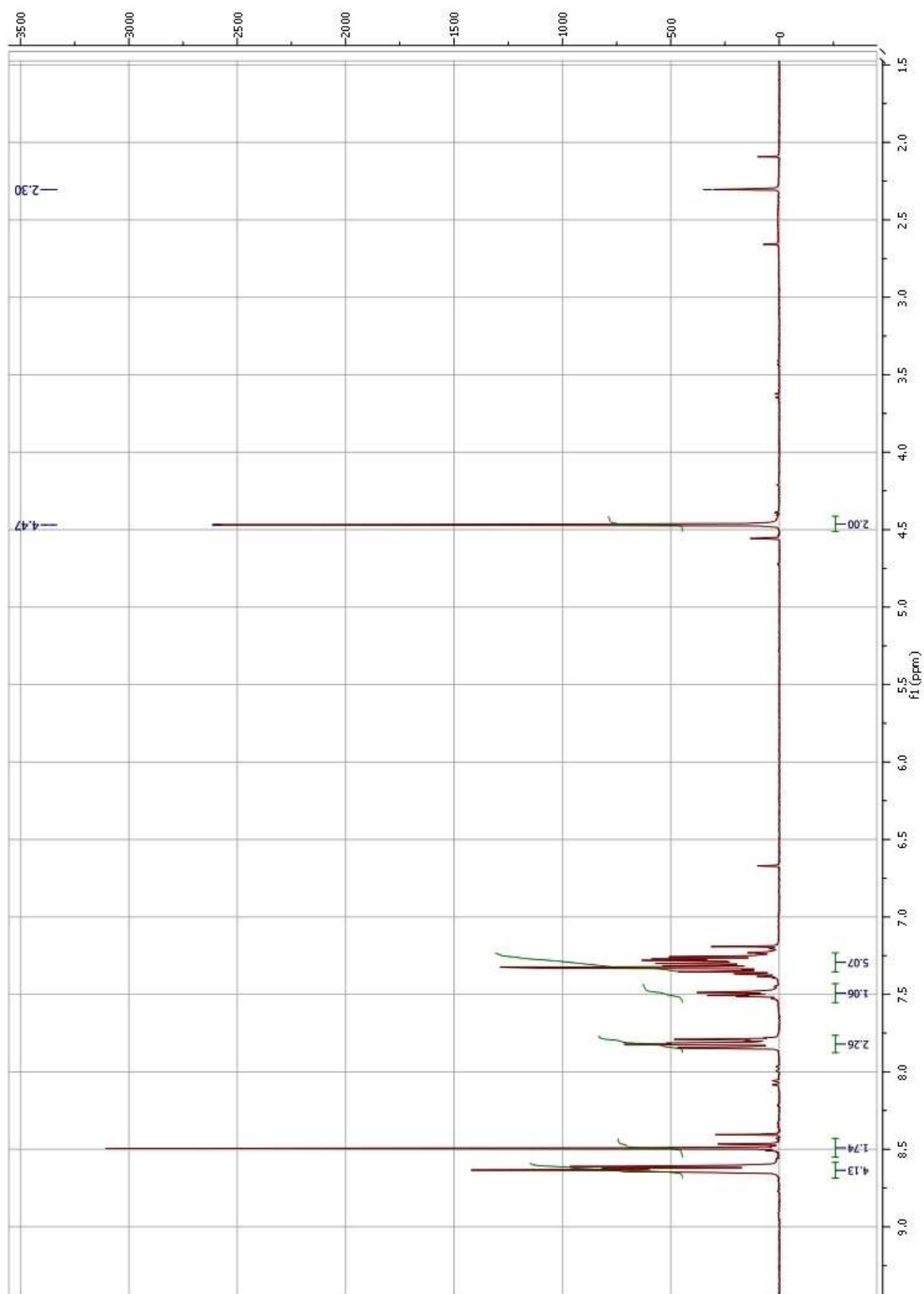


**Figure 2-11** The <sup>1</sup>H NMR spectrum for 4'-(2-(bromomethyl)phenyl)-2,2':6',2''-terpyridine



Figure 2-12 The COSY spectrum for 4'-(2-(bromomethyl)phenyl)-2,2':6',2''-terpyridine

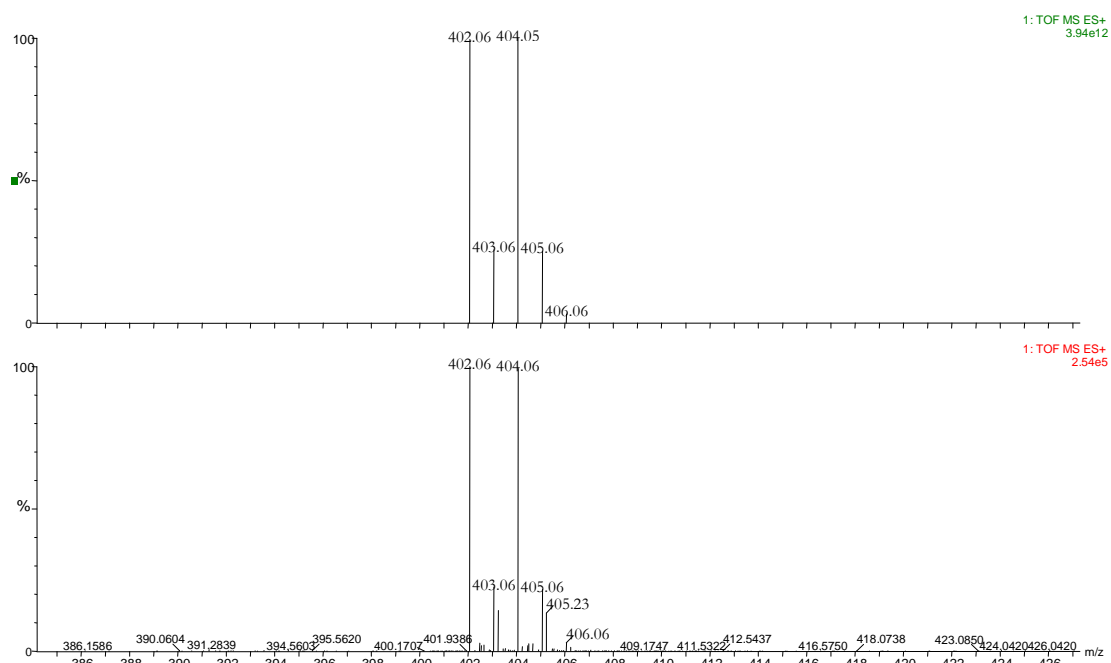


Figure 2-13 4'-(2-(bromomethyl)phenyl)-2,2':6',2''-terpyridine mass spectrum (bottom) and calculated isotope pattern (top)

### **2.2.3 N,N'-bis (3-aminopropyl)ethane-1,2-diamine (3,2,3 tet) Protection Product: 1,5,8,12-Tetraazadodecane**

The addition of the tail or more precisely, the site at which the addition took place on the polyamine tail was the next challenge. The site was an issue because we wanted a terminal addition to take place, but secondary amines are often more reactive than primary amines because of their higher basicity. There is, however more steric hindrance involved with the secondary amines. Mixtures would likely result and these may prove difficult to separate. The direct approach was attempted in case it did prove to be straight-forward but mixtures were produced, and separation attempts failed.

A way of protecting these secondary amines was needed. A route similar to that which has been employed for the production of macrocyclic polyamines was used (Figure 5-6). In this reaction, the polyamine underwent a double condensation reaction with glyoxal and formed a ring-like structure called a bisaminal. This produced tertiary amines from the secondary amines and secondary amines from the primary amines. The reaction had the two-fold effect of protecting the secondary amines and producing more reactive terminal amines. The plan was to use N,N'-bis(3-aminopropyl)ethane-1,2-diamine (3,2,3-tet) for the tail of the ligand. In the protection reaction, it was predicted that the glyoxal would add in a vicinal manner (Figure 2-14). If this protection chemistry was done on N,N'-bis(2-aminoethyl)-ethane-1,2-diamine (2,2,2 tet), the dialdehyde can add in a vicinal or geminal manner giving a mixture of isomers. Previous studies have shown that the dialdehyde adds in such a manner that products with as many six-membered rings as possible are preferentially formed<sup>58</sup>. The

dialdehyde adds in a vicinal manner with 3,2,3 tet because if the glyoxal added in a geminal fashion, two seven membered rings would form on the propanyl sections of the 3,2,3-tet rather than two six membered rings.

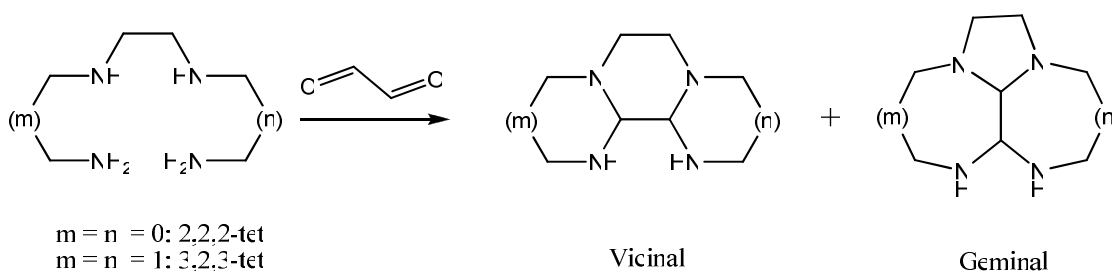


**Figure 2-14** The vicinal and geminal isomer formation from the protection chemistry of 2,2,2 tet and 3,2,3 tet

A good yield of 82% of the bisaminal was obtained.

For the assignment of proton positions on this molecule, refer to Figure 2-15. The  $^1\text{H}$  NMR spectrum (Figure 2-16) shows eight similar environments for the 18 protons. The only likely assignment that can be made from this spectrum is for the singlet peak at 2.57 ppm. These peaks can be assigned to the two protons on the methine carbon atoms (pos<sup>n</sup> 13 and pos<sup>n</sup> 14) that originated from the glyoxal.

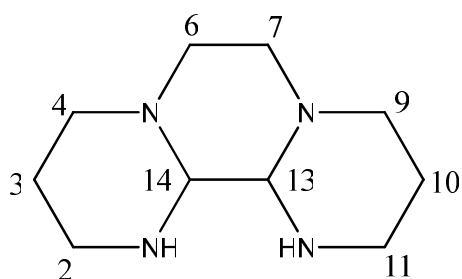


**Figure 2-15** The numbering system of the bisaminal, 1,5,8,12-tetraazadodecane, for the assignment of protons

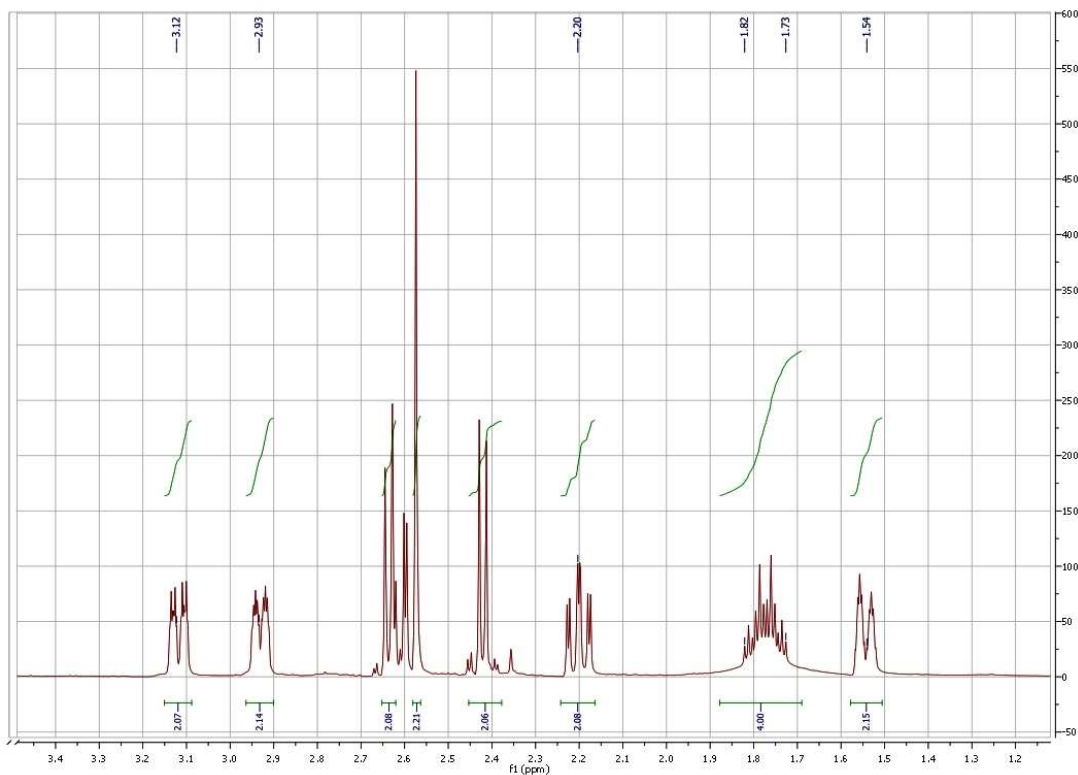


**Figure 2-16** The  $^1\text{H}$  NMR spectrum for the bisaminal 1,5,8,12-tetraazadodecane

The COSY spectrum (Figure 2-17) gives us a little more information. The peak for pos<sup>n</sup> 13 and 14 protons is just visible at 2.57 ppm and shows no coupling to another proton. Immediately beside this is a peak at 2.63 ppm with coupling to one other proton at 2.43 ppm only. These two peaks can be assigned to the ethane-1,2-diyl section of the polyamine (pos<sup>n</sup> 6 and pos<sup>n</sup> 7), on the bisaminal.

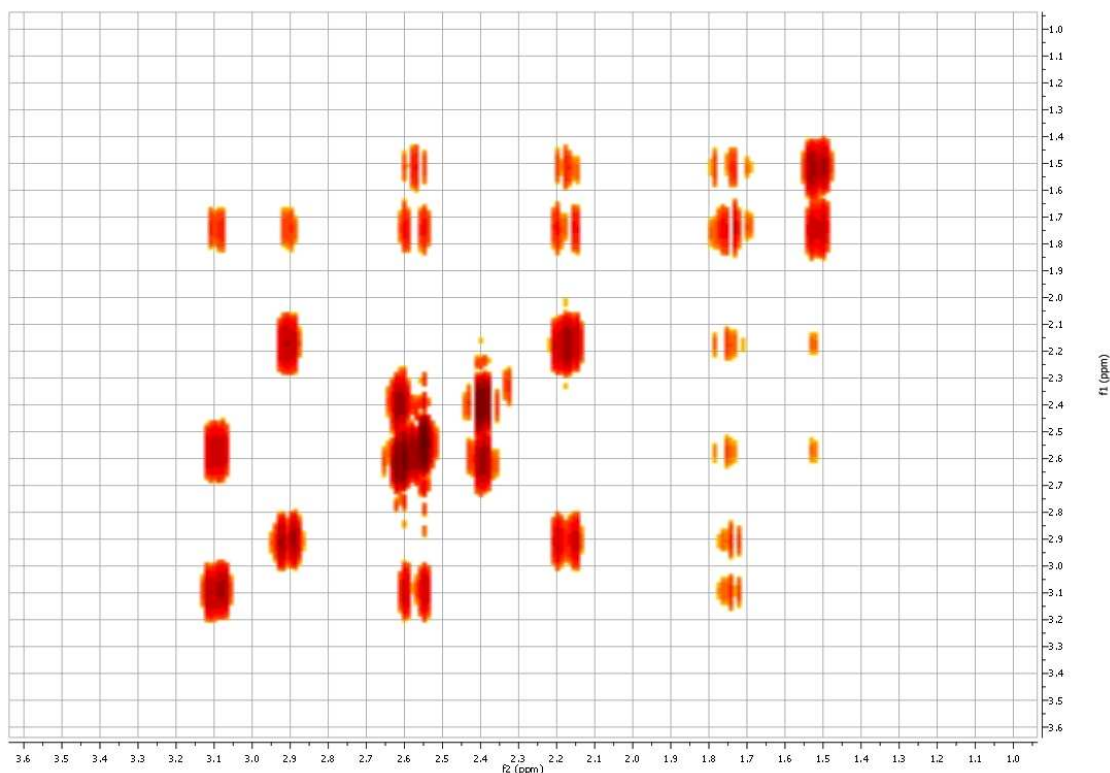


**Figure 2-17** The COSY spectrum for the bisaminal 1,5,8,12-tetraazadodecane

Single crystals suitable for X-ray diffraction studies grew on standing the oily product. The X-ray crystal structure for the bisaminal, 1,5,8,12-tetraazadodecane, (Figure 2-18) shows the carbon atom, C10, bonded to atoms N1 and N2, and the carbon atom, C9, bonded to atoms N3 and N4. This confirms the vicinal addition of the dialdehyde, glyoxal, to the tetraamine, 3,2,3 tet. Atoms C9 and C10 originate from glyoxal. This vicinal addition gives results in the structure having all of its three rings being six-membered, which is the preferred outcome for this type of reaction<sup>58</sup>.

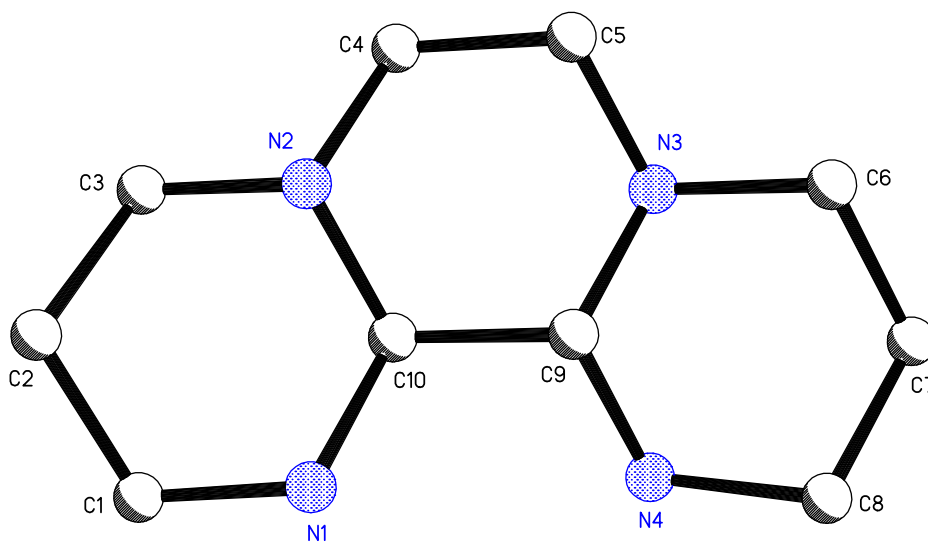


**Figure 2-18** The X-ray crystal structure for the bisaminal, 1,5,8,12-tetraazadodecane, excluding hydrogen atoms for clarity

The X-ray structure showing attached hydrogen atoms (Figure 2-19) reveals their different environments and is consistent with the complexity of the  $^1\text{H}$  NMR spectrum. For a proton bonded to C7, rather than give a simple triplet signal, it instead gives a multiplet as both protons attached to C7 are in different environments, albeit very similar. They still show coupling to the adjacent protons of C6 and C8, which themselves are in different environments. Figure 2-19 also shows the conformation of the three rings to be all chair structures.

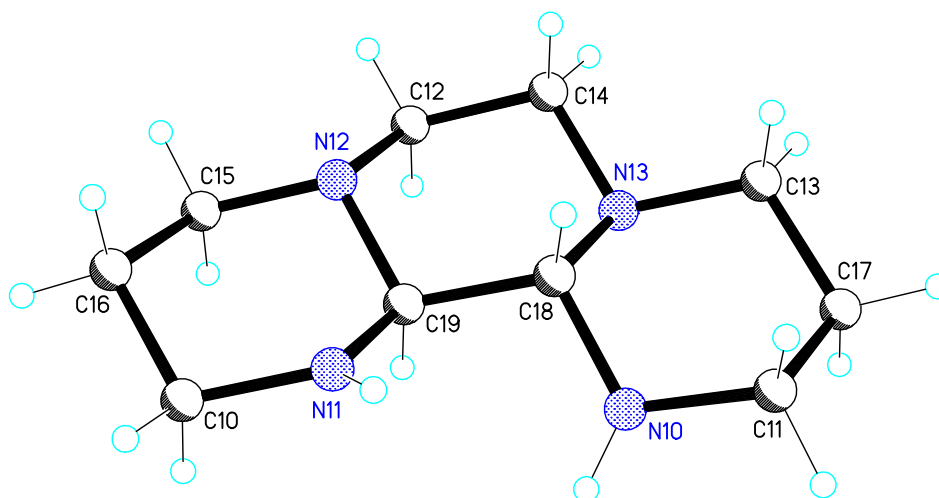


**Figure 2-19** The X-ray crystal structure for the bisaminal, 1,5,8,12-tetraazadodecane, including protons.

The X-ray crystal packing diagrams are shown in Figure 2-20 and Figure 2-21 and the space group is R3c. The total occupancy of the unit cell is four with a volume of 4858.5 Å<sup>3</sup> and angles of  $\alpha$  90°  $\beta$  90°  $\gamma$  120°. There is no evidence of hydrogen bonding between molecules as the smallest distance between a hydrogen atom and a nitrogen atom on another molecule is greater than 2.9 Å. It is possible the molecules are held together *via* van der Waals interactions.

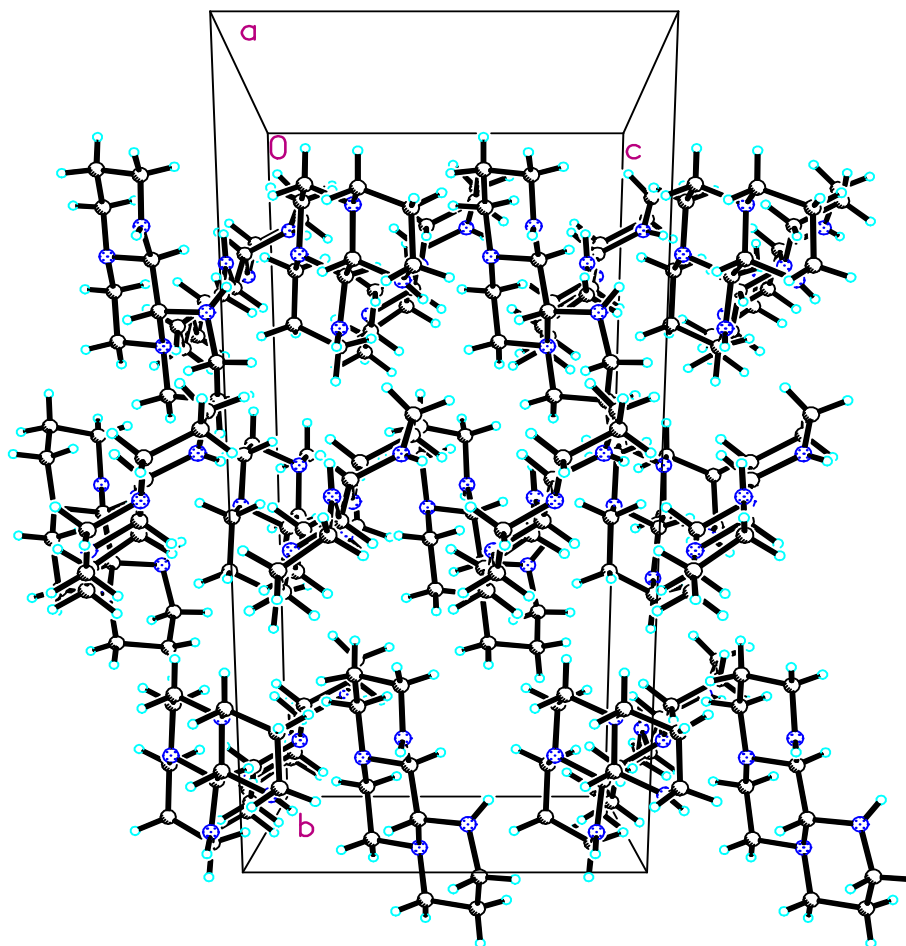


**Figure 2-20** The X-ray crystal packing diagram for the bisaminal, 1,5,8,12-tetraazadodecane, extended outside the unit cell

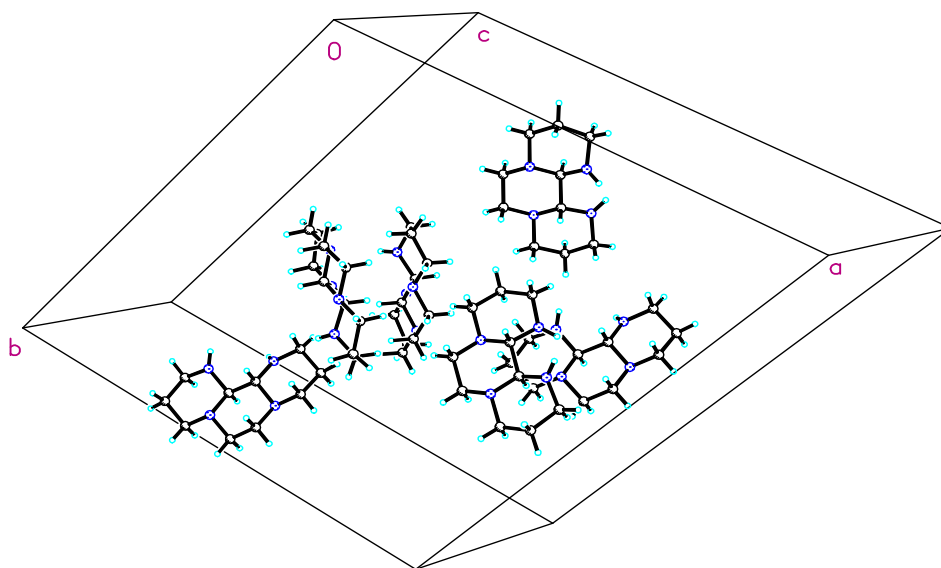


**Figure 2-21** The X-ray crystal packing diagram for the bisaminal 1,5,8,12-tetraazadodecane

## 2.2.4 The Amination Reaction

Once the secondary amines in the linear tetraamine had been protected, terminal addition to the 4'-(2-(bromomethyl)phenyl)-2,2':6',2''-terpyridine could take place. It was found that better results were achieved if the reaction mixture of solvent and the bisaminal were heated to reflux prior to the addition of the brominated tpy. Dried solvent was used in order to reduce the amount of degradation of 4'-(2-(bromomethyl)phenyl)-2,2':6',2''-terpyridine to its hydroxyl derivative. After overnight heating at reflux, the resulting mixture was then ready for purification.

The final challenge was with the purification of 4'-{2''-(12-amino-2,6,9-triazadodecyl)-phenyl}-2,2':6',2''-terpyridine. The sizes of the molecules in the final reaction mixture were vastly different. Based on this knowledge, column chromatography was chosen. Tests were carried out with thin layer chromatography to find the best stationary and mobile phases. Alumina was used in the column as the amine tended to “stick” when silica was used as the stationary phase. Two mobile phases were chosen, the first being chloroform to remove the two starting materials. A combination of acetonitrile, water and potassium nitrate saturated methanol formed the second eluent to pass through the column. This eluent has proved useful previously in the research group<sup>59</sup>. The final part of the purification was to remove the nitrate salts left from the second eluent. This was accomplished by a dichloromethane extraction, which also removed any remaining water.

The nomenclature of the basic 2,2':6',2''-terpyridine has been covered (Figure 1-2). For the assignment of protons and carbons on the tail from NMR spectra, the carbon atoms will be numbered 1 – 9 starting at the toluyl end and likewise for the protons attached to those carbon atoms (Figure 2-22).

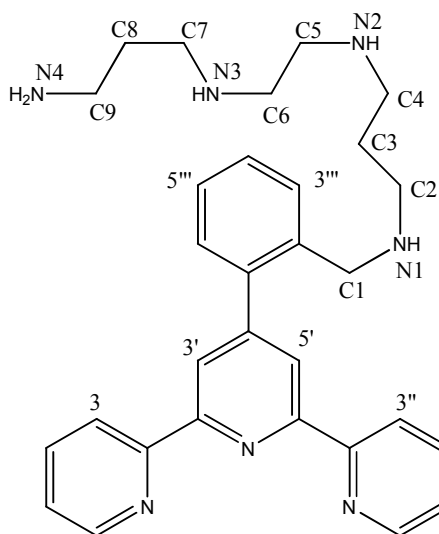


**Figure 2-22** The numbering of carbon atoms for the assignment of NMR spectral peaks on the tail region of 4'-{2'''-(12-amino-2,6,9-triazadodecyl)-phenyl}-2,2':6',2''-terpyridine

The terpyridine region of the  $^1\text{H}$  NMR spectrum (Figure 2-23) remains relatively unchanged from those in the terpyridine synthetic intermediates. The only major difference is the emergence of a doublet from the cluster of peaks between 7.27 to 7.36 ppm. This emergence of the doublet is similar to the change in the terpyridine region after the radical bromination. In the aliphatic region, a new singlet at 3.73 ppm most likely belonging to C1 protons and has an integral value of 2. Also in the aliphatic region, there is no peak at 4.47 ppm. This indicates that there is no 4'-(2-(bromomethyl)phenyl)-2,2':6',2''-terpyridine present. The next two sets of peaks are a multiplet and a triplet pair, each set in close proximity at 2.56 – 2.63 ppm and 2.79 – 2.87 ppm and both have an integral value of 6. The final peaks of interest are a pair of triplets at 1.55 ppm and 1.66 ppm, both with an integral value of 2. The total integral value for the aliphatic region is 18 and this value is expected. The total number of protons attached to carbon atoms in this molecule is 32 and integration of  $^1\text{H}$  NMR spectrum is consistent with this analysis.

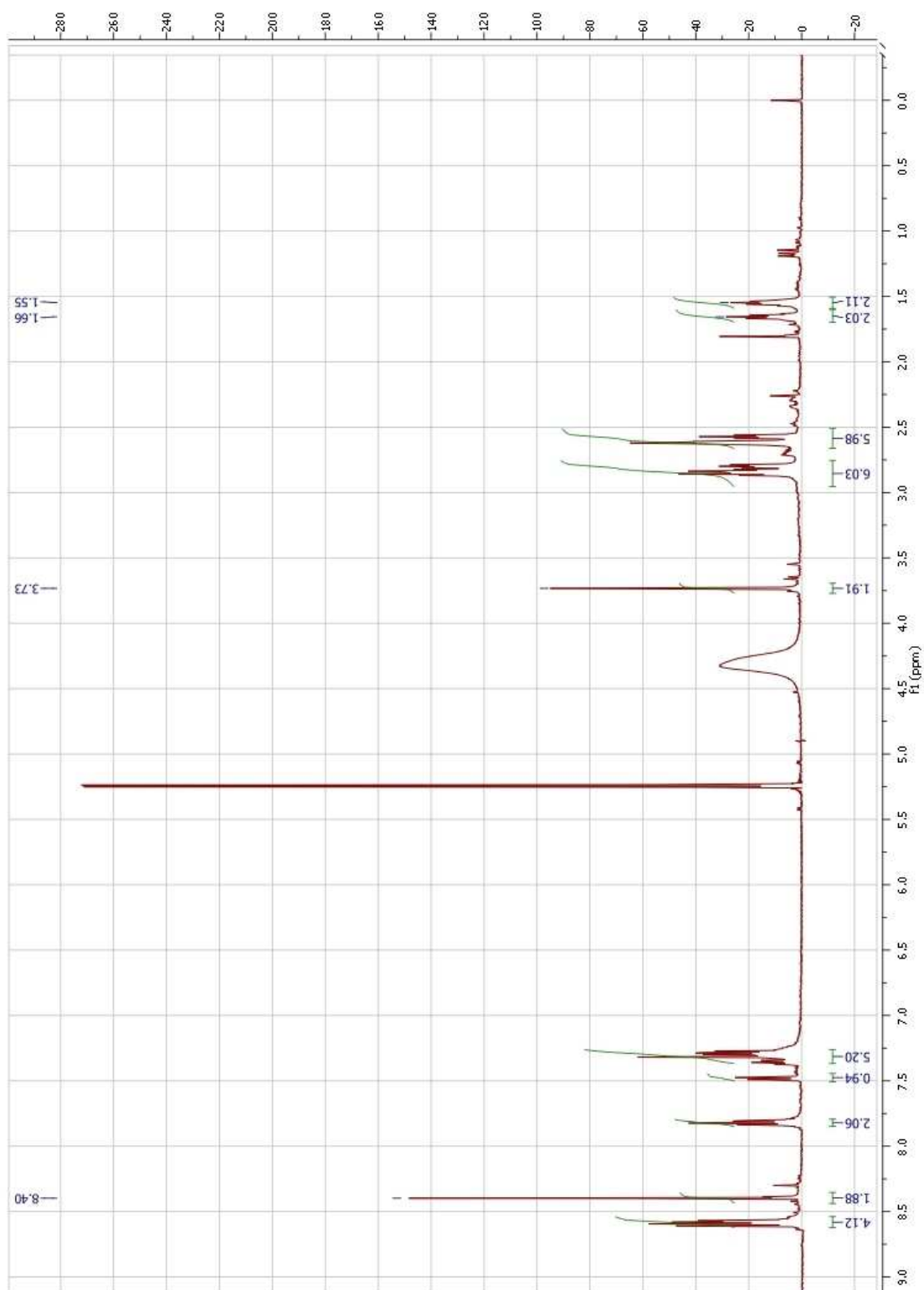
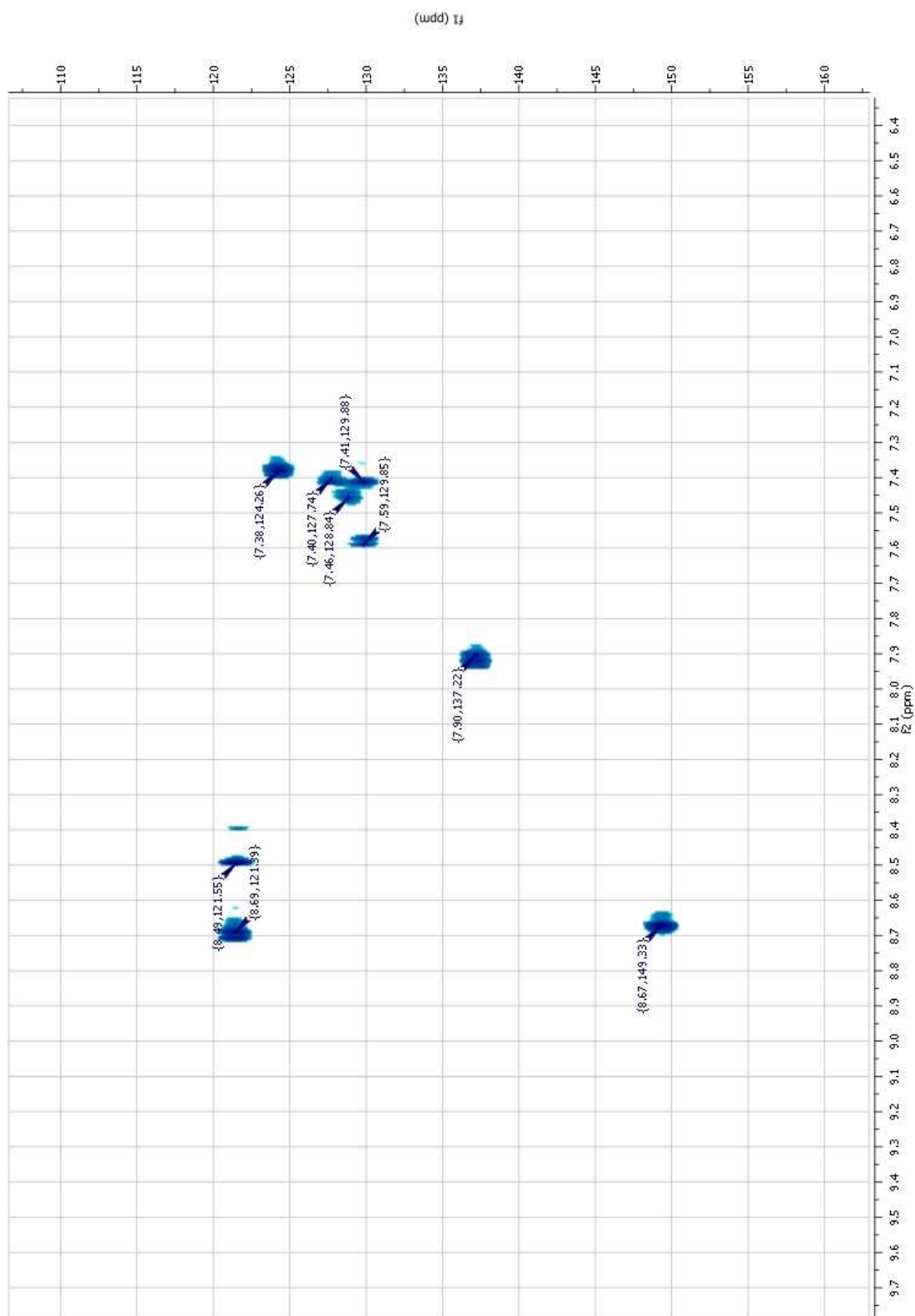


Figure 2-23 The <sup>1</sup>H NMR spectrum for 4'-{2'''-(12-amino-2,6,9-triazadodecyl)-phenyl}-2,2':6',2''-terpyridine

This molecule is expected to have 9 carbon atoms with protons attached in the aromatic regions. There are only 9 peaks in the aromatic region because of symmetry within the molecule. The aromatic section of the HSQC spectrum (Figure 2-24) confirms this.

The tail region of 4'-{2''-(12-amino-2,6,9-triazadodecyl)-phenyl}-2,2':6',2''-terpyridine is also expected to have 9 carbon atoms with protons attached. The HSQC spectrum for the aliphatic region (Figure 2-25) shows the C1 protons/carbon at the coordinates 3.83,50.83 ppm and confirms the presence of the remaining eight carbon atoms with protons attached. The HSQC spectrum shows a carbon atom peak at 40.5 ppm, protons at 2.94 ppm, which is appropriate for a carbon atom next to a primary amine. The tail region only has one carbon atom adjacent to a primary amine so this peak can be assigned to protons attached to C9.

The complete COSY spectrum for 4'-{2''-(12-amino-2,6,9-triazadodecyl)-phenyl}-2,2':6',2''-terpyridine (Figure 2-26) shows the couplings in the aromatic region to be similar to 4'-(2-(bromomethyl)phenyl)-2,2':6',2''-terpyridine. The peak at 8.49 ppm has no coupling and can be assigned to 3',5' protons. A peak at 7.59 ppm has coupling to a peak at 7.46 ppm but no coupling to any of the terpyridine protons at 8.69 ppm for H<sub>6,6''</sub>, 8.67 ppm for H<sub>3,3''</sub>, 8.49 ppm for H<sub>3,5'</sub>, 7.92 ppm for H<sub>4,4''</sub> and 7.39 ppm for H<sub>5,5''</sub>. From the <sup>1</sup>H NMR spectrum, this peak at 7.59 ppm is a doublet and has an integral value of 1 and therefore must be on the toluyl ring and represent the 3'' or 6'' proton.



**Figure 2-24** The aromatic section of the HSQC for 4'-{2'''-(12-amino-2,6,9-triazadodecyl)-phenyl}-2,2':6',2''-terpyridine

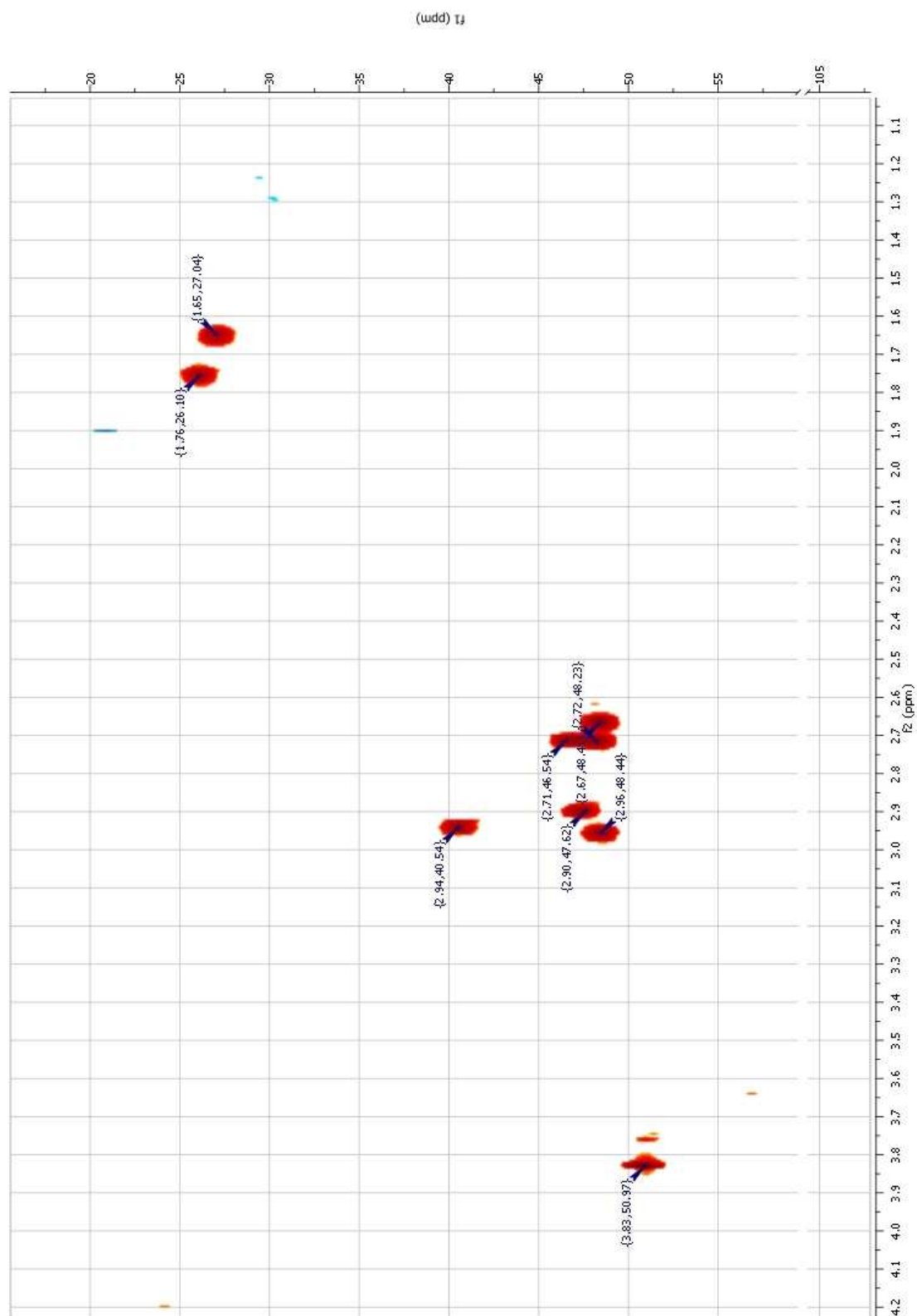


**Figure 2-25** The aliphatic section of the HSQC spectrum for 4'-{2''-(12-amino-2,6,9-triazadodecyl)-phenyl}-2,2':6',2''-terpyridine

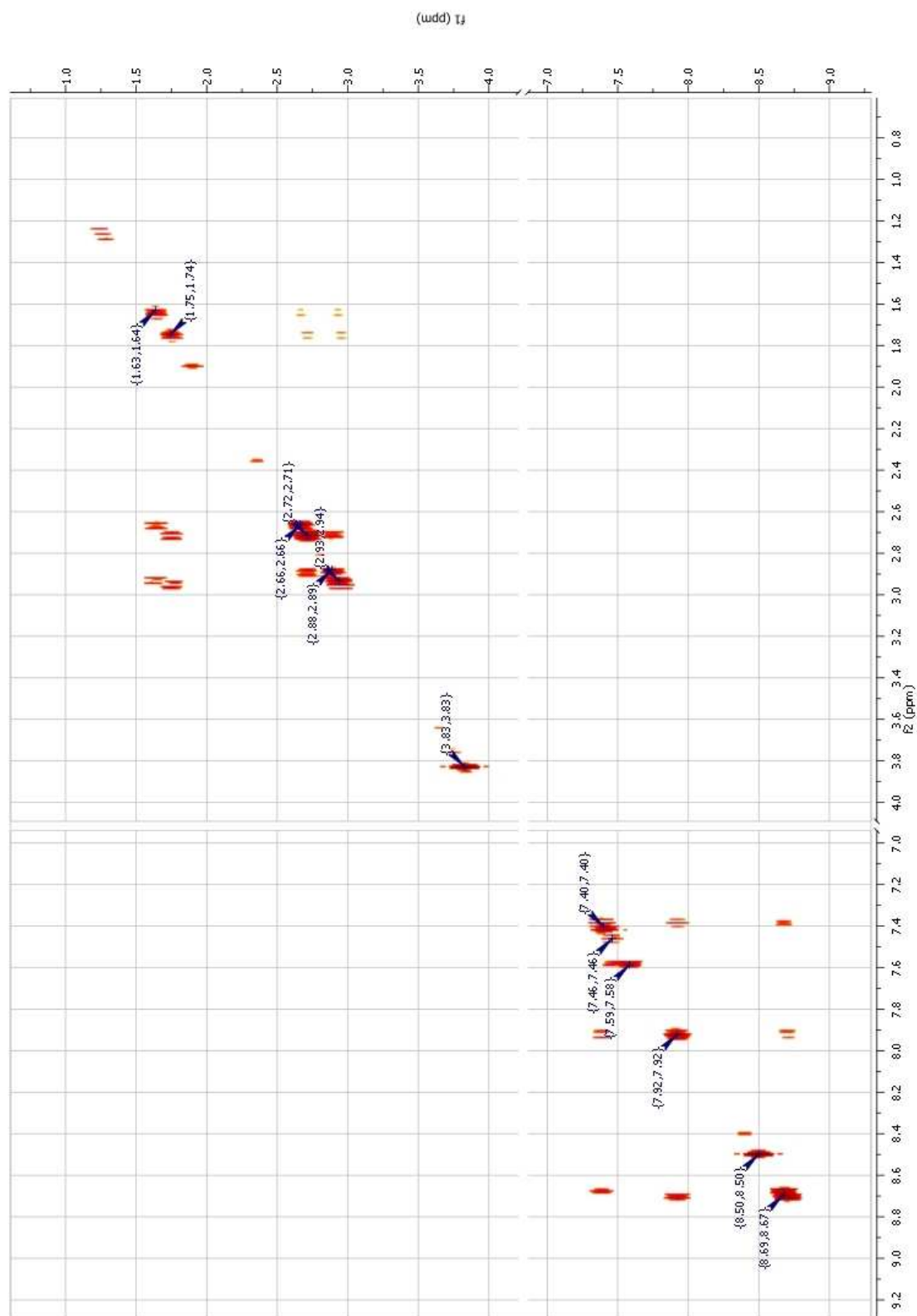


**Figure 2-26** The complete COSY spectrum for 4'-{2''-(12-amino-2,6,9-triazadodecyl)-phenyl}-2,2':6',2''-terpyridine

A close-up view of the COSY spectrum for the tail region (Figure 2-27) shows two peaks, 2.89 ppm and 2.71 ppm, coupled to each other but not to any of the other protons. These two peaks can be assigned to the four ethane-1,2-diyl section protons (pos<sup>n</sup> C5 and pos<sup>n</sup> C6). The peak at 2.89 ppm can be integrated, giving an expected value of 2. Integration of all peaks in the tail region, excluding the methylene protons at pos<sup>n</sup> C1 gives the expected value of 16. The two peaks at 1.75 ppm and at 1.64 ppm are both coupled to two other proton environments but not to each other. Both have an integral value of 2 and can be assigned to the central protons of the propane-1,3-diyl sections of the tail, pos<sup>n</sup> C3 and pos<sup>n</sup> C8. One of these peaks, at 1.75 ppm is coupled to a peak already assigned C9 at 2.94 ppm from the chemical shift due to a primary amine in the HSQC spectrum. Therefore, the peak at 1.75 ppm can be assigned protons on C8. These are coupled to another peak at 2.72 ppm, which can therefore be assigned to protons on C7

A NOESY 1D spectrum was obtained (Figure 2-28) to establish coupling between the methylene protons, pos<sup>n</sup> C1, and any other protons on the aromatic section of the molecule. A sample was irradiated at 3.74 ppm, the chemical shift predicted to be that for the methylene protons. The spectrum shows coupling to protons at 8.39 ppm, 7.47 ppm and 2.62 ppm. The peak at 8.39 ppm has already been assigned as the singlet peak for the 3', 5' protons. The peak at 7.47 ppm is the doublet that emerged from the cluster in 4'-*o*-toluyl 2,2':6',2'' terpyridine, at 7.30 – 7.34 ppm, after both the radical bromination and tail attachment reactions. The peak at 7.47 ppm can be assigned to the 3''' proton on the *o*-toluyl ring as there is no coupling in the COSY to the pyridine protons. The peak at 2.62 ppm can be assigned protons on C2.

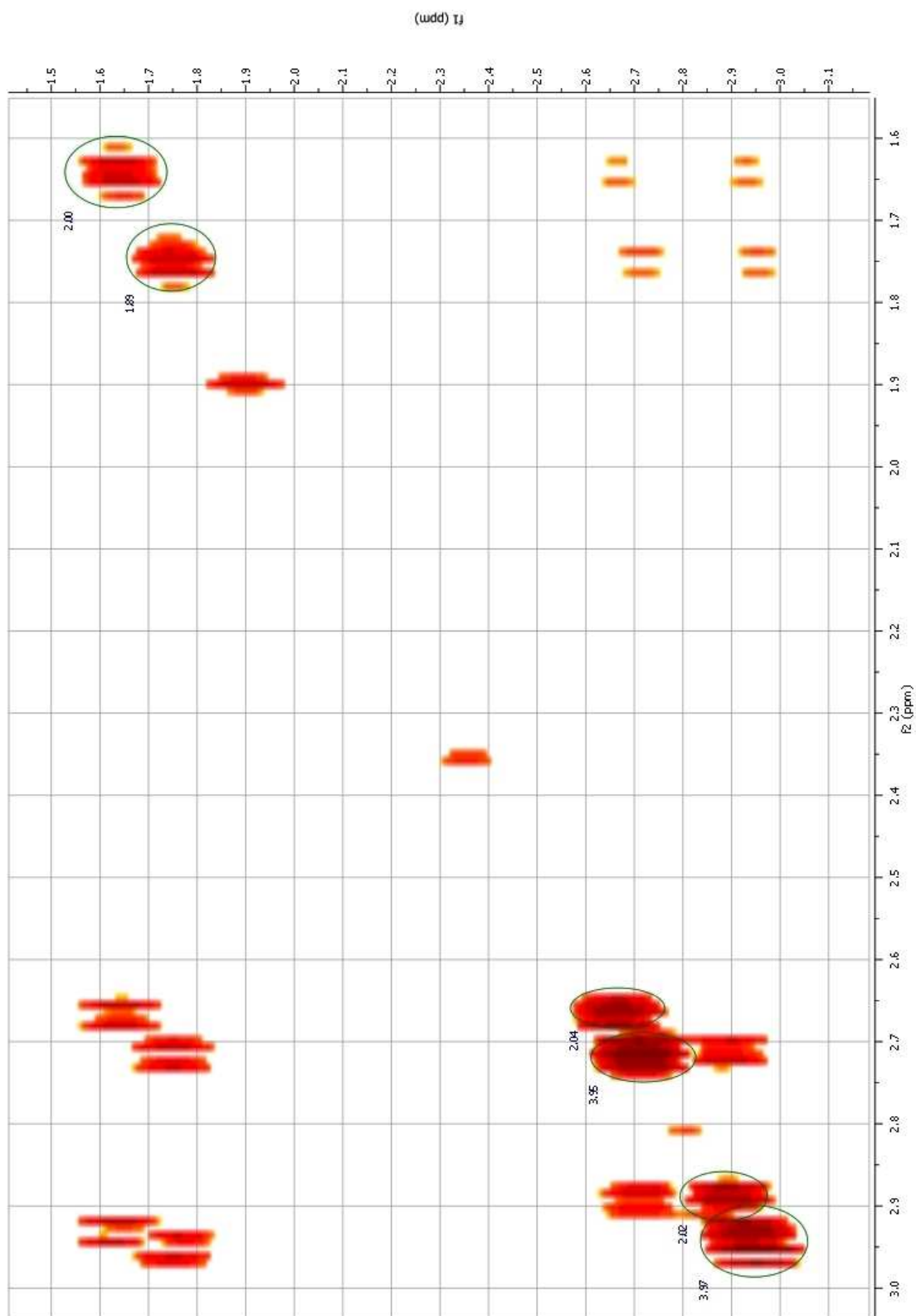


**Figure 2-27** The close-up view of the tail region of 4'-{2'''-(12-amino-2,6,9-triazadodecyl)-phenyl}-2,2':6',2''-terpyridine

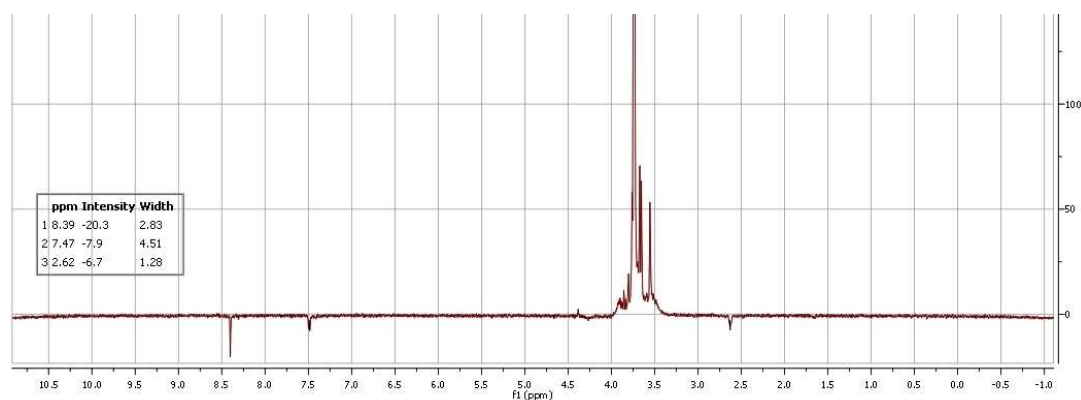


**Figure 2-28** The 1D NOESY spectrum for 4'-{2'''-(12-amino-2,6,9-triazadodecyl)-phenyl}-2,2':6',2''-terpyridine with irradiation at 3.74 ppm

From the close-up COSY spectrum (Figure 2-27) for the tail region, C2 at 2.62 ppm is coupled to the central propane-1,3-diyl protons on C3, at 1.63 ppm. These are coupled to protons on C4 at 2.93 ppm. The peak at 1.74 ppm can be assigned to the other central propane-1,3-diyl protons on C8. The peak assigned to protons on C8 is coupled to two other peaks at 2.72 ppm and 2.95 ppm. These are assigned to the protons on C7 and C9, but at this stage there is uncertainty which is which.

The mass spectrum of 4'-{2'''-(12-amino-2,6,9-triazadodecyl)-phenyl}-2,2':6',2''-terpyridine contains peaks that can be assigned to both the H<sup>+</sup> (Figure 2-29) and Na<sup>+</sup> (Figure 2-30) adducts, with major peaks at 496.3153 and 518.3011 respectively. The observed isotope patterns were in agreement with the calculated isotope patterns.

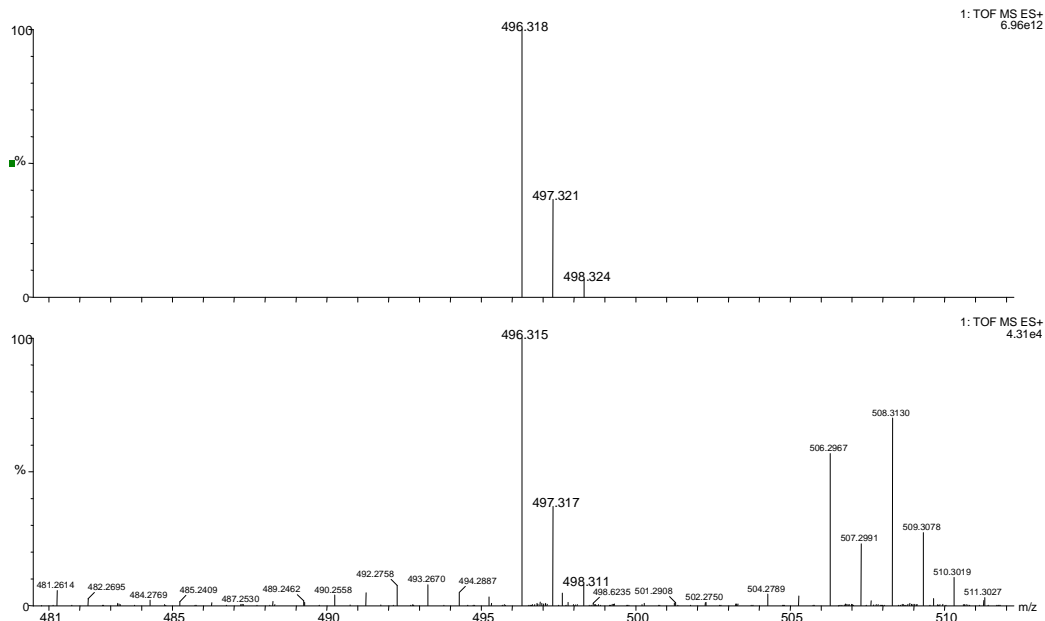


**Figure 2-29** 4'-{2'''-(12-amino-2,6,9-triazadodecyl)-phenyl}-2,2':6',2''-terpyridine (H<sup>+</sup>) Mass Spectrum (below) and calculated isotope pattern (above)

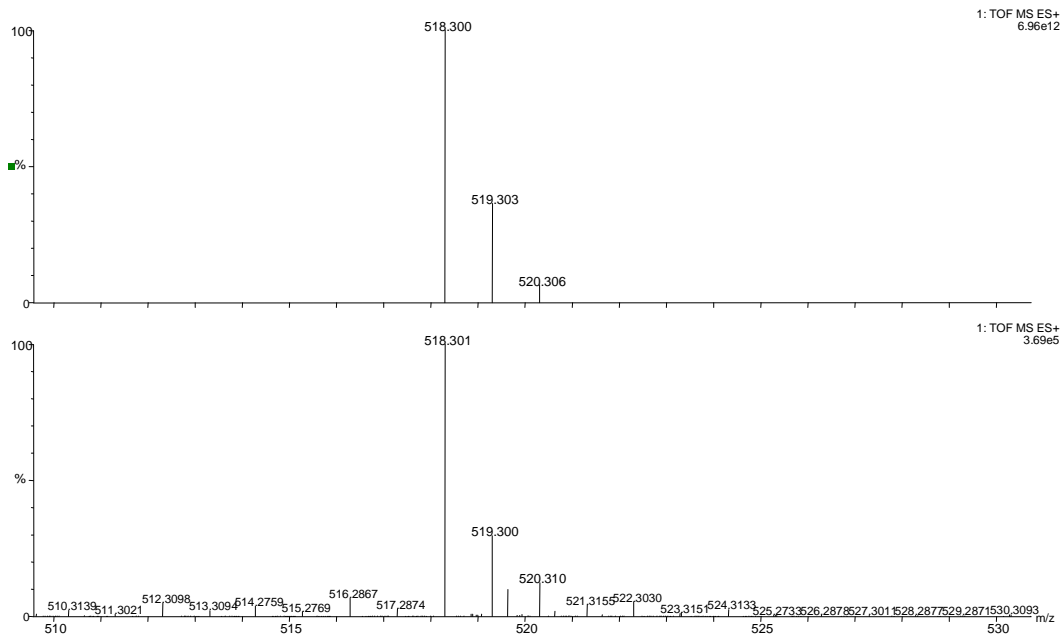


**Figure 2-30** 4'-{2'''-(12-amino-2,6,9-triazadodecyl)-phenyl}-2,2':6',2''-terpyridine (Na<sup>+</sup>) Mass Spectrum (below) with the calculated isotope pattern (above)

The original attempt to add the unprotected 3,2,3 tet to 4'-(2-(bromomethyl)phenyl)-2,2':6',2'' terpyridine was not particularly successful. The clue to this unsuccessful attempt was the <sup>1</sup>H NMR spectrum (Figure 2-31) of the aromatic region of a purified sample. In particular, the spectrum showed multiple peaks for the singlet of the 3',5' protons at 8.42 ppm. This indicated the presence of impurities. There were broad overlapping peaks in the tail region.

Now that a <sup>1</sup>H NMR spectrum of a purified successful addition is available (Figure 2-23), comparisons can be made to see if any 4'-{2''-(12-amino-2,6,9-triazadodecyl)-phenyl}-2,2':6',2''-terpyridine was present in the original sample. In Figure 2-31, the most notable peak is at 3.73 ppm and this is the same chemical shift for the peak assigned to C1 (Figure 2-23). It is not a clean singlet peak though, which could indicate either the presence of an impurity or the tail attaching through the secondary amine in some instances.

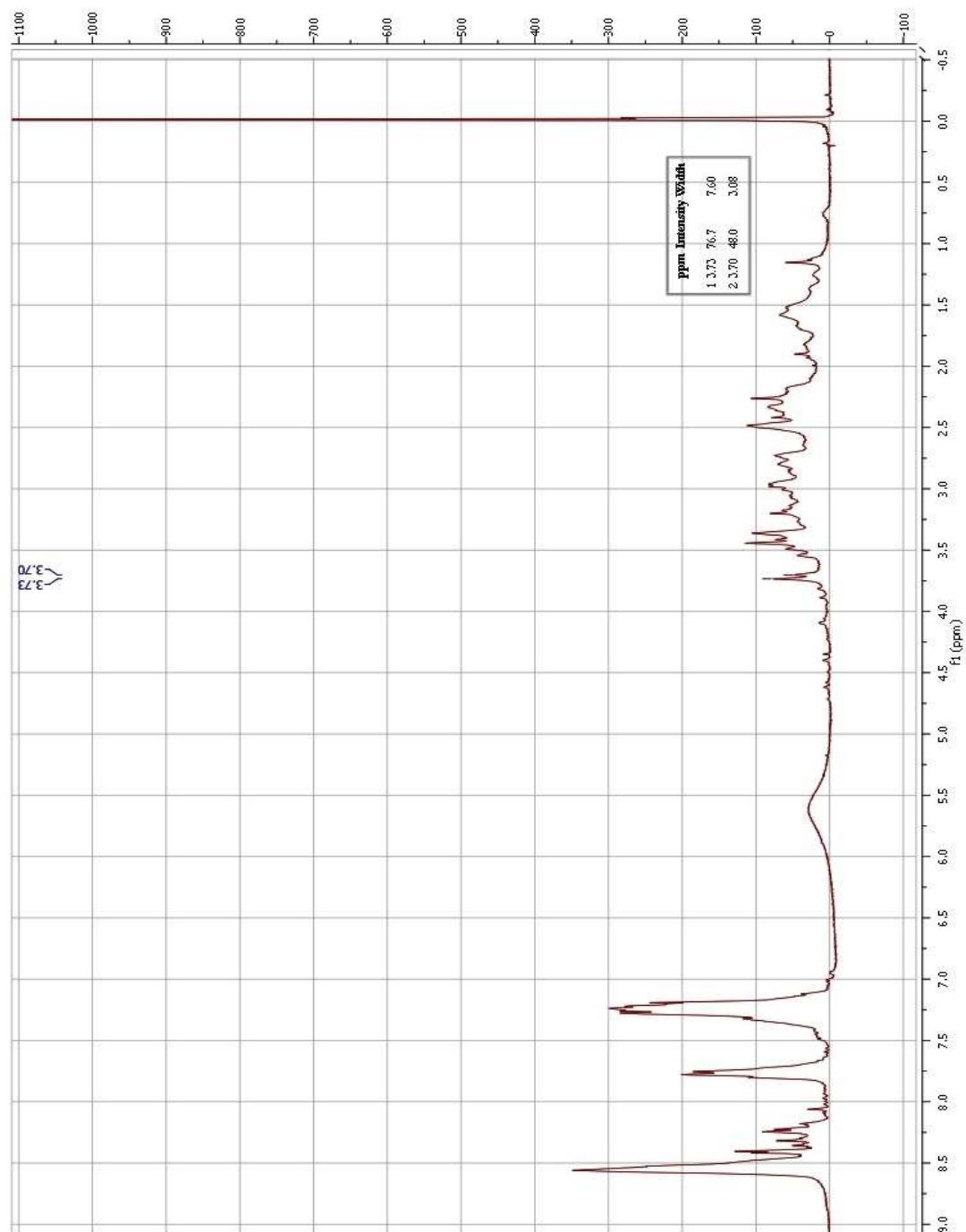


**Figure 2-31** The  $^1\text{H}$  NMR spectrum of the purified results from the original attempt at adding the unprotected 3,2,3 tet tail to 4'-(2-(bromomethyl)-phenyl) 2,2':6',2'' terpyridine.

## 2.3 Summary

The synthesis of this ligand brought about a few challenges. The more important of those challenges were the ones that required alterations to the reference experimental procedures. They also proved to be the most satisfying achievements.

The radical bromination reaction gave mediocre yields when performed in benzene as in the literature. The solvent was changed to carbon tetrachloride and the yields improved significantly. The protection of the polyamine tail, 3,2,3-tet, to ensure terminal addition proved another important step. Because of the reactivity of the secondary amines, terminal addition could not be guaranteed. The amine underwent a double condensation reaction to form three six-membered rings. The secondary amines were now tertiary amines and the primary amines were now secondary amines. For the addition of this molecule to the brominated 4'-(*o*-toluyl)-2,2':6',2''-terpyridine, the reaction conditions were altered from the literature conditions by applying heat to the system which increased the yield of 4'-(2''-(12-amino-2,6,9-triazadodecyl)-phenyl)-2,2':6',2''-terpyridine. The purification was the biggest breakthrough of this project. Without this, the reaction product mix was too complicated to decipher by NMR techniques. The aliphatic region peaks were broad and no definitive information could be obtained in this area other than there was no 4'-(2-(bromomethyl)-phenyl) 2,2':6',2'' terpyridine present. The aromatic region had a doubling of some peaks which was indicative of there being two 2,2':6',2''-terpyridine products present.

## Chapter 3: Metal Complexes & Characterisation

The previous chapter describes the synthesis and characterisation of a range of molecules, some of which are potential ligands. Attempts were made to prepare complexes and produce X-ray quality crystals from 4'-(*o*-toluyl)-2,2':6',2''-terpyridine and its derivatives with a range of metal ions such as iron(II), copper(II), cobalt(II), zinc(II), and silver(I). This chapter describes the synthesis and characterisation of the successful attempts.

### 3.1.1 [Cu(ottp)Cl<sub>2</sub>] $\cdot$ CH<sub>3</sub>OH

Copper(II) chloride was dissolved into methanol and added to a solution of 4'-(*o*-toluyl)-2,2':6',2''-terpyridine and chloroform. Ether was then diffused into the resulting blue solution. Initial attempts to achieve X-ray quality crystals of this copper-terpyridine complex proved difficult. The products formed using vapour diffusion methods were very fine needles, micro-crystals and precipitate. The diffusion rate was slowed, by capping the vial containing the sample with the cap having a 1 mm hole drilled through it, which resulted in blue, cubic X-ray quality crystals.

The X-ray crystal structure (Figure 3-1) shows the copper ion is bound to one 4'-(*o*-toluyl)-2,2':6',2''-terpyridine ligand and two chloride ions, to form a distorted trigonal bipyramidal complex. The crystal system is triclinic and the space group P-1. The *o*-toluyl ring is twisted to an angle of 46.1° because of steric clashes between its methyl group and the 3',5' protons.

In contrast, the X-ray crystal structure of the free ligand shows this twist to be  $77.2^\circ$ . Although not shown in this diagram, there is hydrogen bonding between the chloride ion (Cl1) and the methanol's hydroxyl hydrogen (O100) with a distance of  $2.381 \text{ \AA}$ .

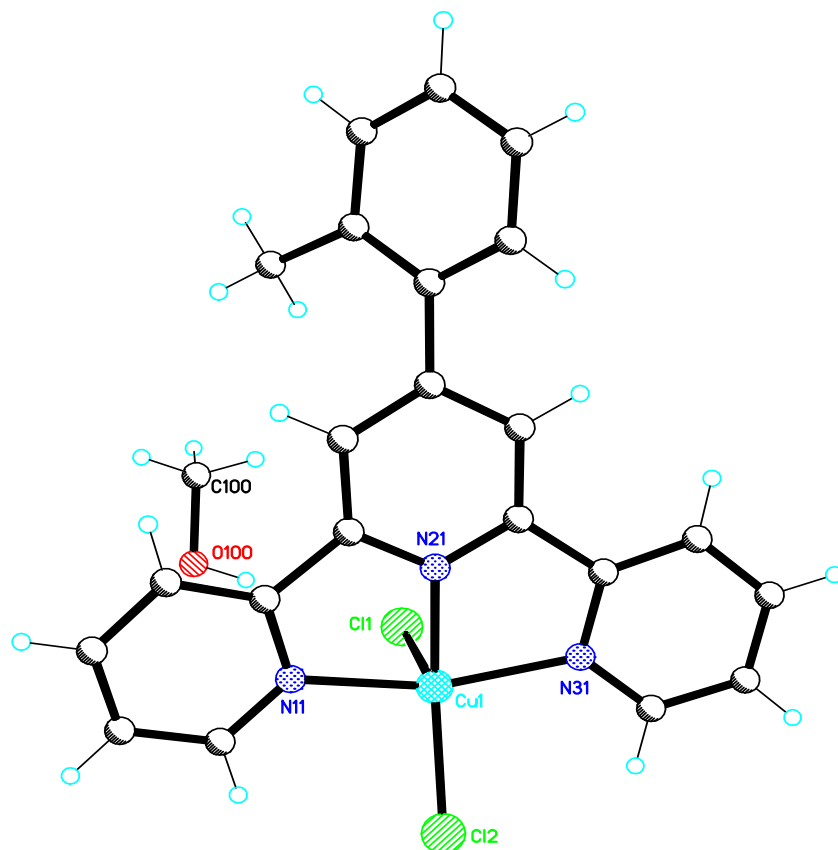


**Figure 3-1** The X-ray crystal structure for the (4'-(*o*-toluy)-2,2':6',2''-terpyridine)-copper complex

The packing diagrams for the (4'-(*o*-toluy)-2,2':6',2''-terpyridine)-copper complex shows interactions between the copper atom of one complex to the copper atom on the adjacent complex and also the chloride ion bonded to it. In Figure 3-2, the copper-copper distance is  $4.029 \text{ \AA}$  and at this distance, are unlikely to be interacting. The copper chloride bonds are

2.509 Å and the copper-chloride interaction to an adjacent complex is 3.772 Å. In Figure 3-3, there is hydrogen bonding holding pairs of complexes to other pairs of complexes. This involves hydrogen bonding between 3,3'' or 5,5'' positions hydrogen atoms and the chloride ions, Cl2A and Cl2F, and is 2.381 Å within the unit cell and 2.626 Å. to an adjacent unit cell.

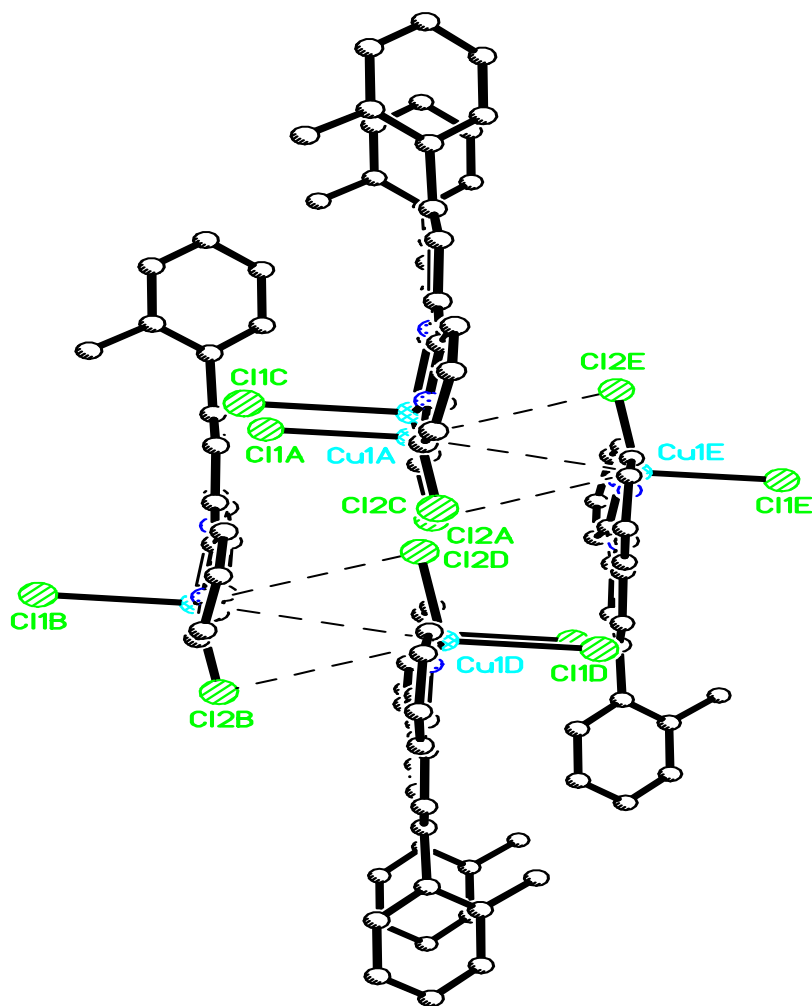


**Figure 3-2** The X-ray crystal structure packing diagram for the (4'-(*o*-toluyl)-2,2':6',2''-terpyridine)-copper complex with interactions between the metal center and chloride ligands

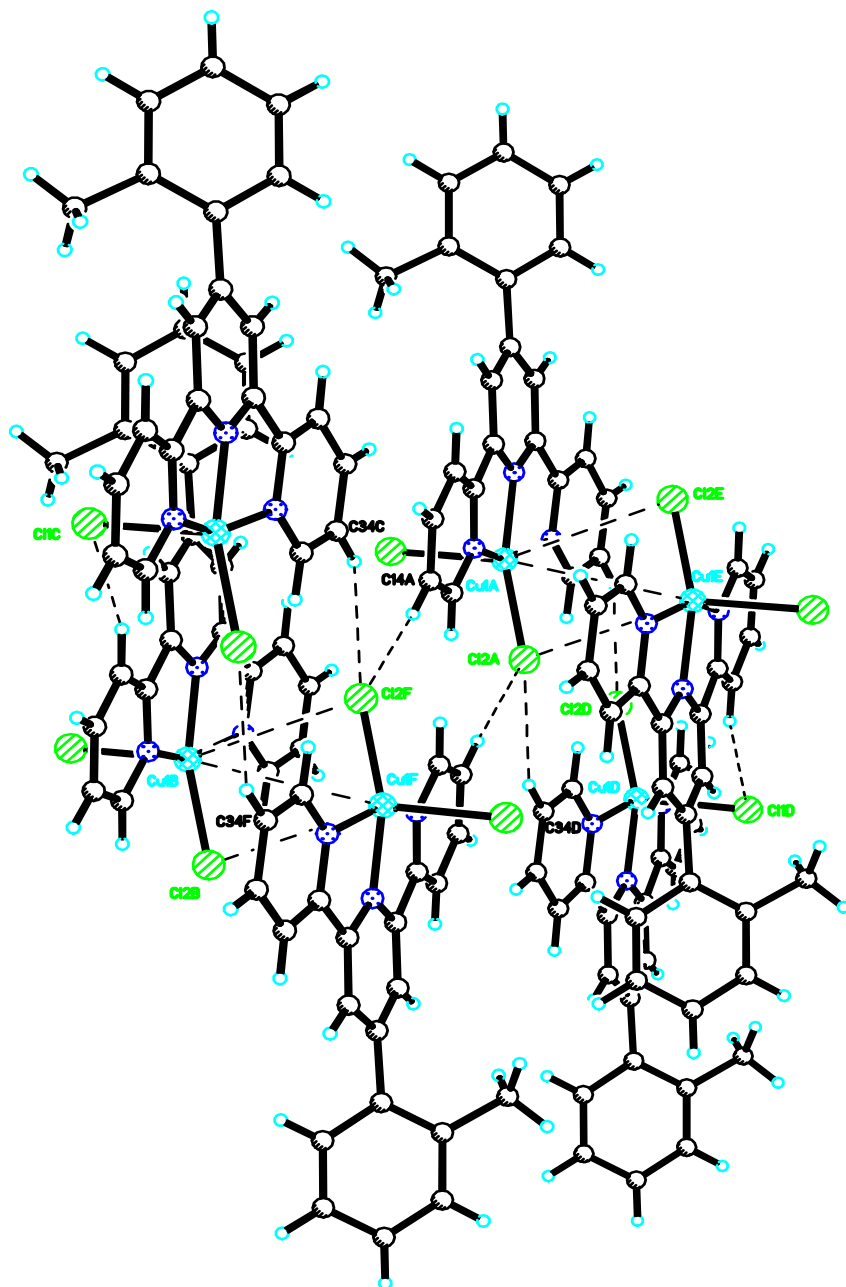


**Figure 3-3** The X-ray crystal structure packing diagram for the (4'-(*o*-toluyl)-2,2':6',2''-terpyridine)-copper complex with chloride atom/copper atom interactions and the chloride atom/hydrogen atom interactions.

### 3.1.2 [Co(ottp)<sub>2</sub>]Cl<sub>2</sub>·2.25CH<sub>3</sub>OH

The cobalt(II) chloride was dissolved in methanol and added, in a 1:2 molar ratio, to a solution of 4'-(*o*-toluyl)-2,2':6',2''-terpyridine and chloroform. Ether was diffused into the solution and red/brown X-ray quality crystals had formed after two days.

The presence of two chloride anions in the X-ray structure implies it is a cobalt(II) complex. Zhong Yu *et al*<sup>61</sup> describe two cobalt terpyridine complexes where each has the cobalt in either the 2<sup>+</sup> or 3<sup>+</sup> O.S. and coloured red and orange respectively. Table 3-1 lists the Co–N bond lengths and crystal colours for some cobalt terpyridine complexes with cobalt in a variety of oxidation and spin states and includes data from the complex [Co(ottp)<sub>2</sub>]Cl<sub>2</sub>·2.25CH<sub>3</sub>OH. Ana Galet *et al*<sup>62</sup> investigated the crystal structures of cobalt(II) complexes in low spin (L.S) and high spin (H.S) states and Brian N. Figgis *et al*<sup>63</sup> examined the crystal structure of a cobalt(III) terpyridine complex. From this information, the colour and bond length comparisons are consistent with the cobalt(II) formulation revealed by the X-ray structure solution: [Co(ottp)<sub>2</sub>]Cl<sub>2</sub>·2.25CH<sub>3</sub>OH.

**Table 3-1 The bond lengths and colours of cobalt terpyridine complexes with cobalt in different oxidation and spin states.**

N Atom N.o.	Co(II) L.S.	Co(II) H.S.	Co(III)	[Co(ottp) <sub>2</sub> .Cl <sub>2</sub> ]. 2.25CH <sub>3</sub> OH
1	1.950	2.083	1.930	2.003
2	1.856	1.904	1.863	1.869
3	1.955	2.089	1.926	2.001
4	1.944	2.093	1.937	2.182
5	1.862	1.906	1.853	1.939
6	1.948	2.096	1.921	2.162
Crystal Colour	Green	Brown	Pale Yellow	Red/Brown

As expected, the six coordinate cobalt atom coordinated with two 4'-(*o*-toluyl)-2,2':6',2''-terpyridine ligands and formed the distorted octahedral complex in Figure 3-4. The crystal system is monoclinic and the space group  $P2_1/n$ . The two central pyridine nitrogen-cobalt atom bond lengths at 1.867 Å (N21-Co1) and 1.93 Å (N61-Co1), are shorter than the four outer pyridine nitrogen-cobalt atom bond lengths, 2.001 – 2.182 Å. This is expected because of the rigidity of the ligand as the two outer terpyridine nitrogen atoms, on each ligand, hold the central terpyridine nitrogen atoms closer to the metal ion. One of the terpyridine units sits a little further away from the cobalt atom, approximately 0.15 Å, than the other terpyridine unit. One of the methanol solvent molecules, containing oxygen O101, only has  $\frac{1}{4}$  occupancy.

The packing diagram (Figure 3-5) show two complexes containing the atoms, Co1A and Co1B that have interactions between the chloride counter ions (Cl1A and Cl1B). The chloride ion, Cl1A is hydrogen bonding with one of the *o*-toluyl methyl hydrogen atoms in of complex A and with the 5'' hydrogen atom of one ligand in complex B. The bond lengths are 2.765 Å and 2.760 Å respectively. This chloride ion also hydrogen bonds with the hydroxyl hydrogen atom from one of the methanol solvent molecules, O20A, and has a bond length of 2.313 Å. The second chloride ion, Cl1B, has similar hydrogen bonding interactions with the 5'' hydrogen atom from the same ligand Cl1A interacts with in complex A, with the 3'' hydrogen atom, again, with the same ligand Cl1A interacts with in complex B and with the hydroxyl group of the other methanol solvent molecule O20B.

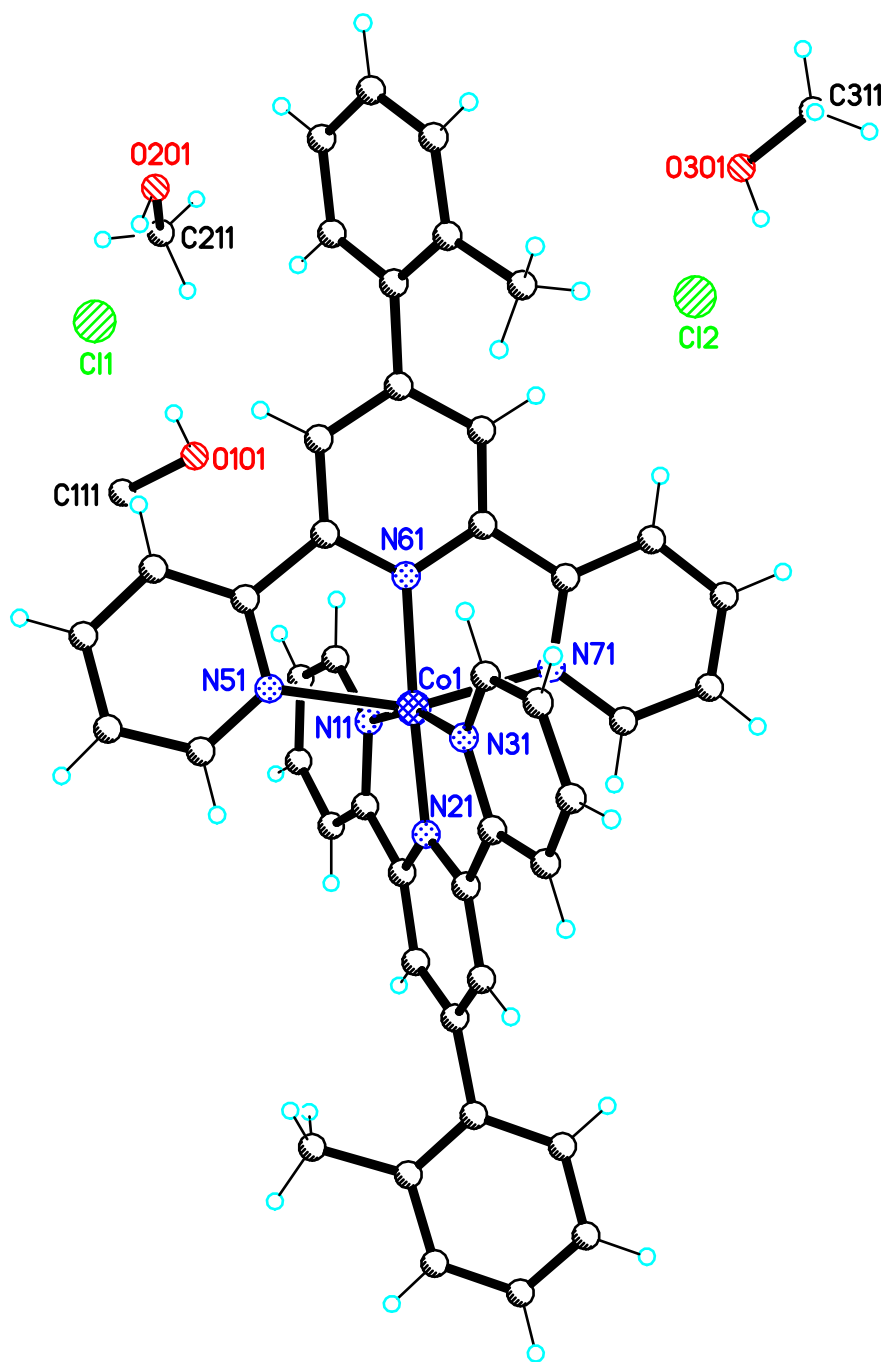
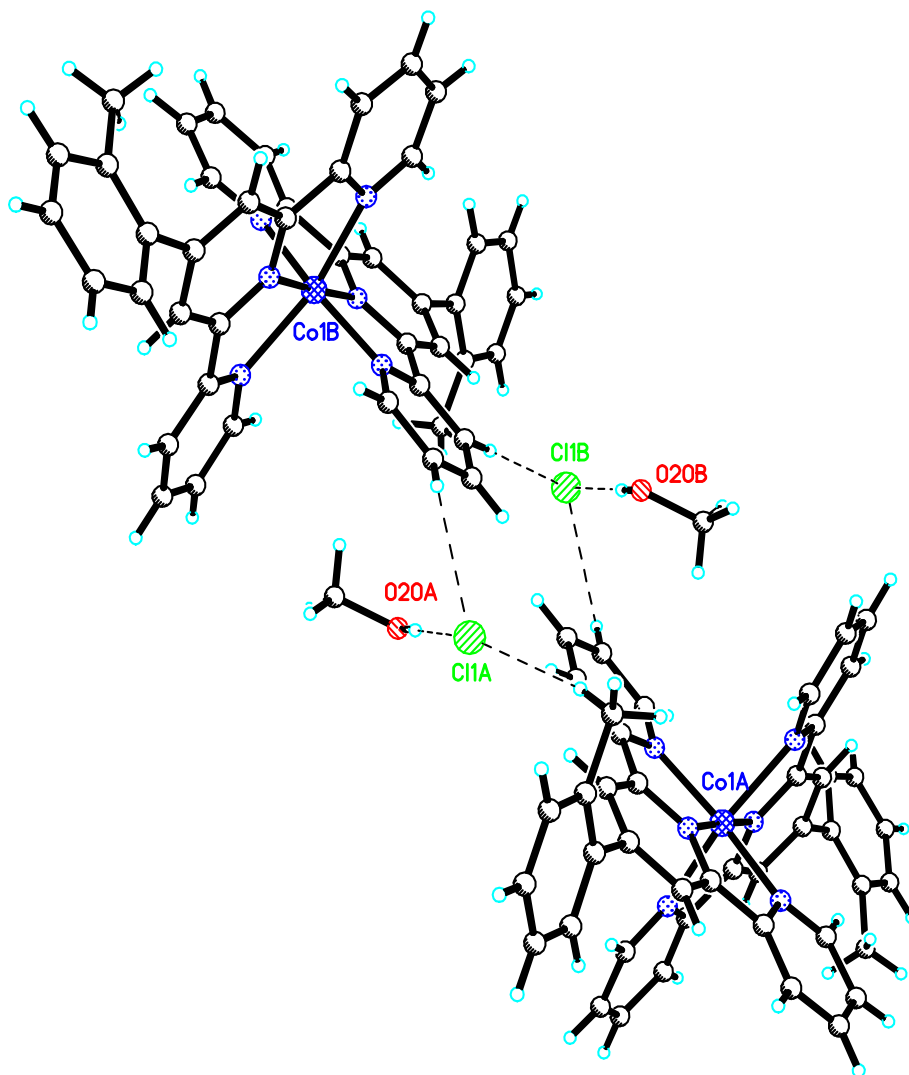


Figure 3-4 The X-ray crystal diagram of the bis(4'-(*o*-toluy)-2,2':6',2''-terpyridine)cobalt complex



**Figure 3-5** The X-ray crystal structure of the bis(4'-(*o*-toluyl)-2,2':6',2''-terpyridine)-cobalt complex with interactions of solvent molecules and counter ions

### 3.1.3 [Fe(ottp)<sub>2</sub>][PF<sub>6</sub>]<sub>2</sub>

Addition of iron(II) to two molar equivalents of 4'-(*o*-toluyl)-2,2':6',2''-terpyridine gave a purple solution. Solid material was obtained by addition of [PF<sub>6</sub>]<sup>-</sup> salts. We were unable to obtain X-ray quality crystals for this complex. Characterisation was undertaken using elemental analysis, UV/Visible and Mass spectrometry, <sup>1</sup>H NMR, COSY and HSQC.

The calculated elemental analysis was consistent with the actual elemental analysis found.

The UV/visible spectrum (Figure 3-6) was consistent with other literary examples<sup>64,74</sup>.

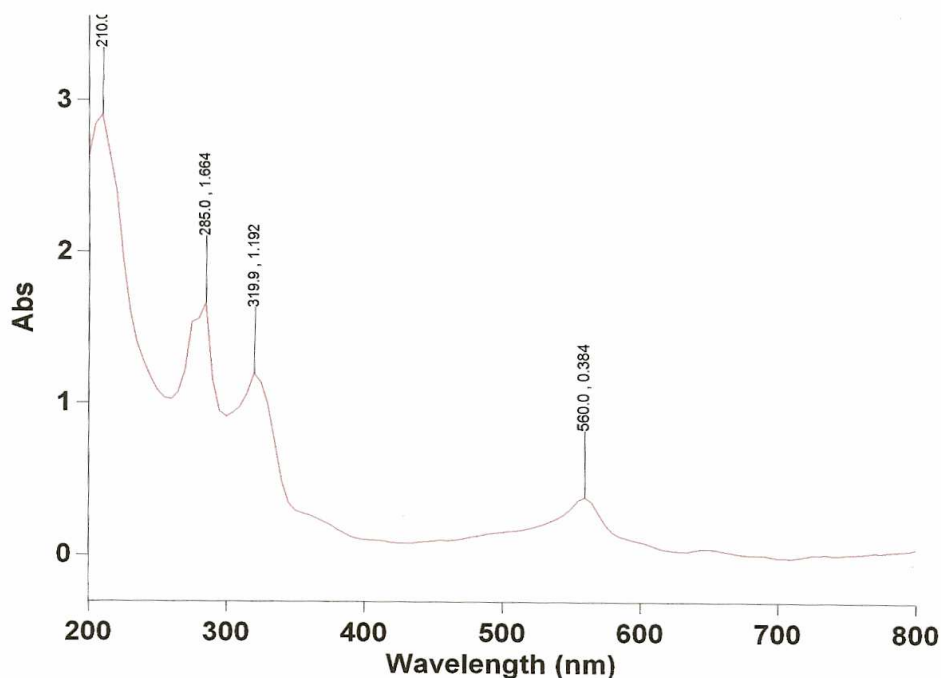


**Figure 3-6** UV/vis for (ottp)<sub>2</sub> Fe complex.  $\epsilon = 13492$ , (conc =  $2.8462 \times 10^{-5}$  mol L<sup>-1</sup>.)

Significant changes in chemical shifts in the  $^1\text{H}$  NMR spectrum (Figure 3-7) were observed on coordination of the two 4'-(*o*-toluyl)-2,2':6',2''-terpyridine ligands to an iron(II) ion compared to that of the uncoordinated ligand (Figure 2-7). There has been a general downfield shift for most of the peaks. The 3',5' proton singlet now appears at 9.29 ppm as opposed to 8.49 ppm in the  $^1\text{H}$  NMR spectrum of the uncoordinated ligand. The 3',5' proton peak now appears downfield from the 3,3'' proton doublet peak at 8.95 ppm. Two of the peaks, for the 5,5'' and 6,6'' protons, have moved upfield instead. The peak for the two 6,6'' protons have shifted from 8.72 ppm into the cluster of peaks at 7.57 – 7.61 ppm. The triplet 5,5'' proton peak which was originally in the cluster of peaks at 7.30 – 7.36 ppm has also shifted downfield to 7.27 ppm.

This upfield shift of the 5,5'' and 6,6'' proton peaks is commonly seen in bis(tpy)-complex  $^1\text{H}$  NMR spectra. The shift is brought about by the perpendicular geometry of the ligands on the metal. This means that these two pairs of protons, more so the 6,6'' protons, on one ligand, are now located above the ring plane of the aromatic ring of the other ligand<sup>64,65 & 66</sup>.

The COSY spectrum for the aromatic region of the bis(4'-(*o*-toluyl)-2,2':6',2''-terpyridine)-iron complex (Figure 3-8) shows the coupling of these shifted proton peaks. As expected, the 3',5' singlet is not coupled to any other protons. The 3,3'' doublet (8.95 ppm) is coupled to the 4,4'' triplet (8.06 ppm) which is coupled to the 5,5'' triplet (7.27 ppm) which is coupled to the 6,6'' doublet (7.58 ppm).

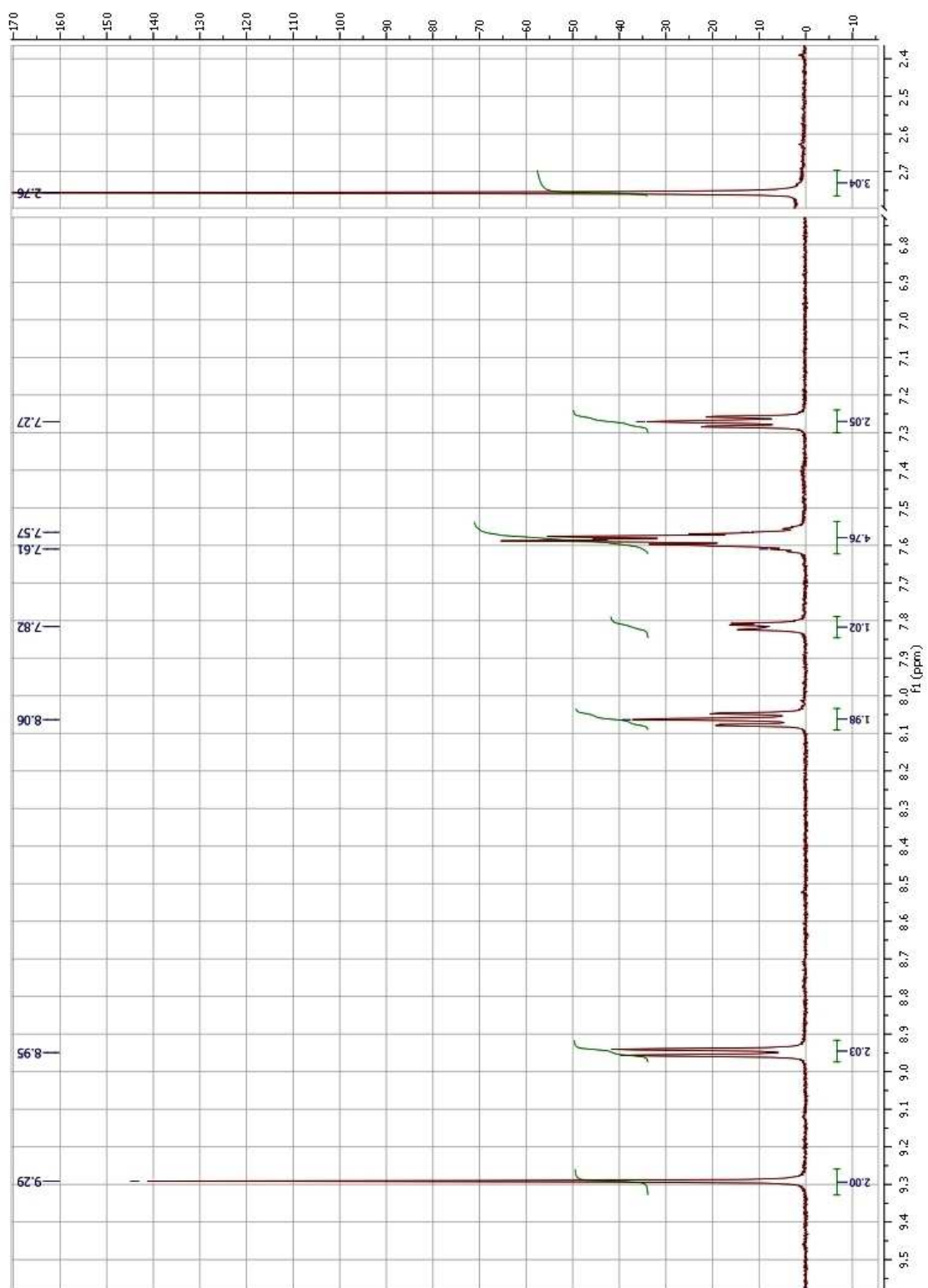
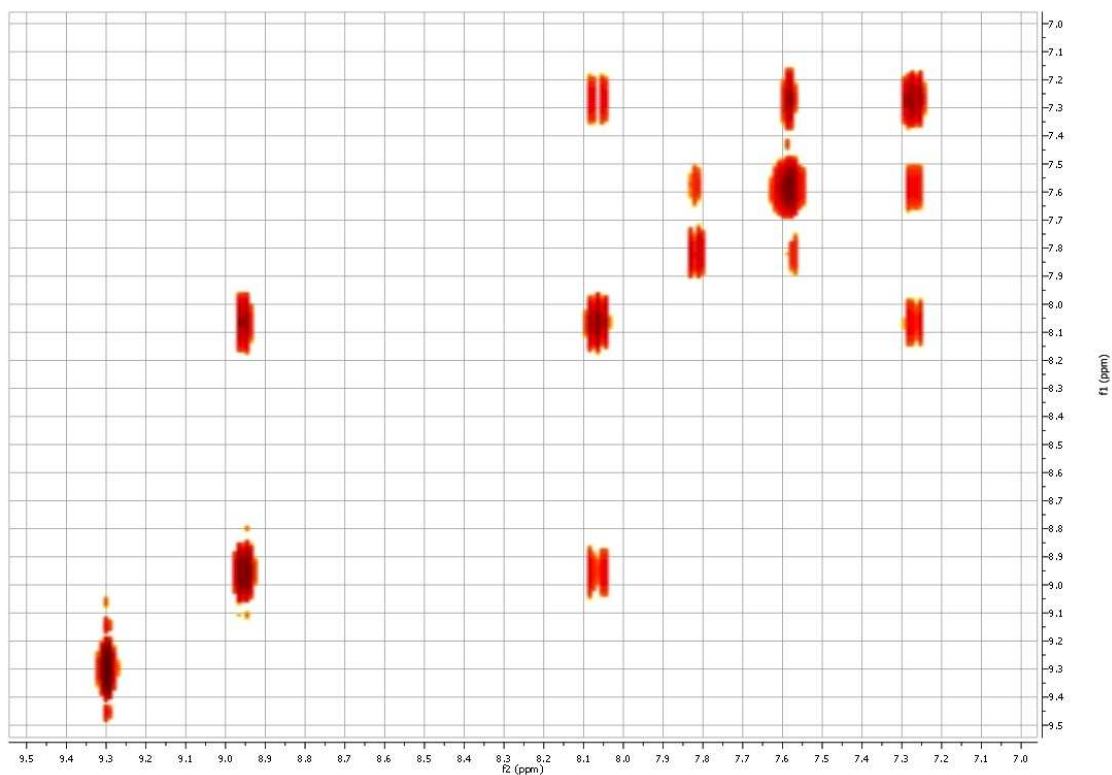
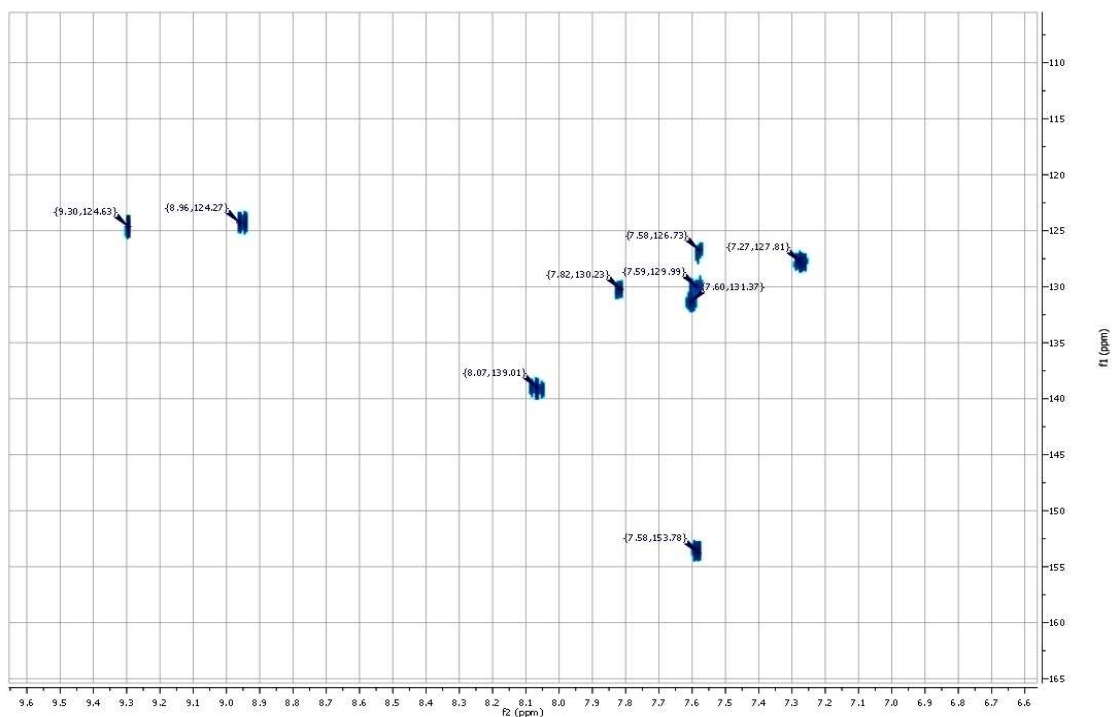


Figure 3-7 The  $^1\text{H}$  NMR spectrum of the bis(4'-(*o*-toluy)l)-2,2':6',2''-terpyridine-iron complex



**Figure 3-8** The COSY spectrum for the aromatic region of the bis(4'-(*o*-toluy)-2,2':6',2''-terpyridine)-iron complex



**Figure 3-9** The HSQC spectrum of the the bis(4'-(*o*-toluy)-2,2':6',2''-terpyridine)-iron complex

The HSQC spectrum for the bis(4'-(*o*-toluyl)-2,2':6',2''-terpyridine)-iron complex (Figure 3-9) also shows some minor chemical shifts in the carbon atoms when compared with the HSQC spectrum for the uncoordinated ligand (Figure 2-9).

### 3.1.4 [(Cl-ottp)Cu( $\mu$ -Cl)( $\mu$ -Br)Cu(Cl-ottp)][PF<sub>6</sub>]<sub>2</sub>

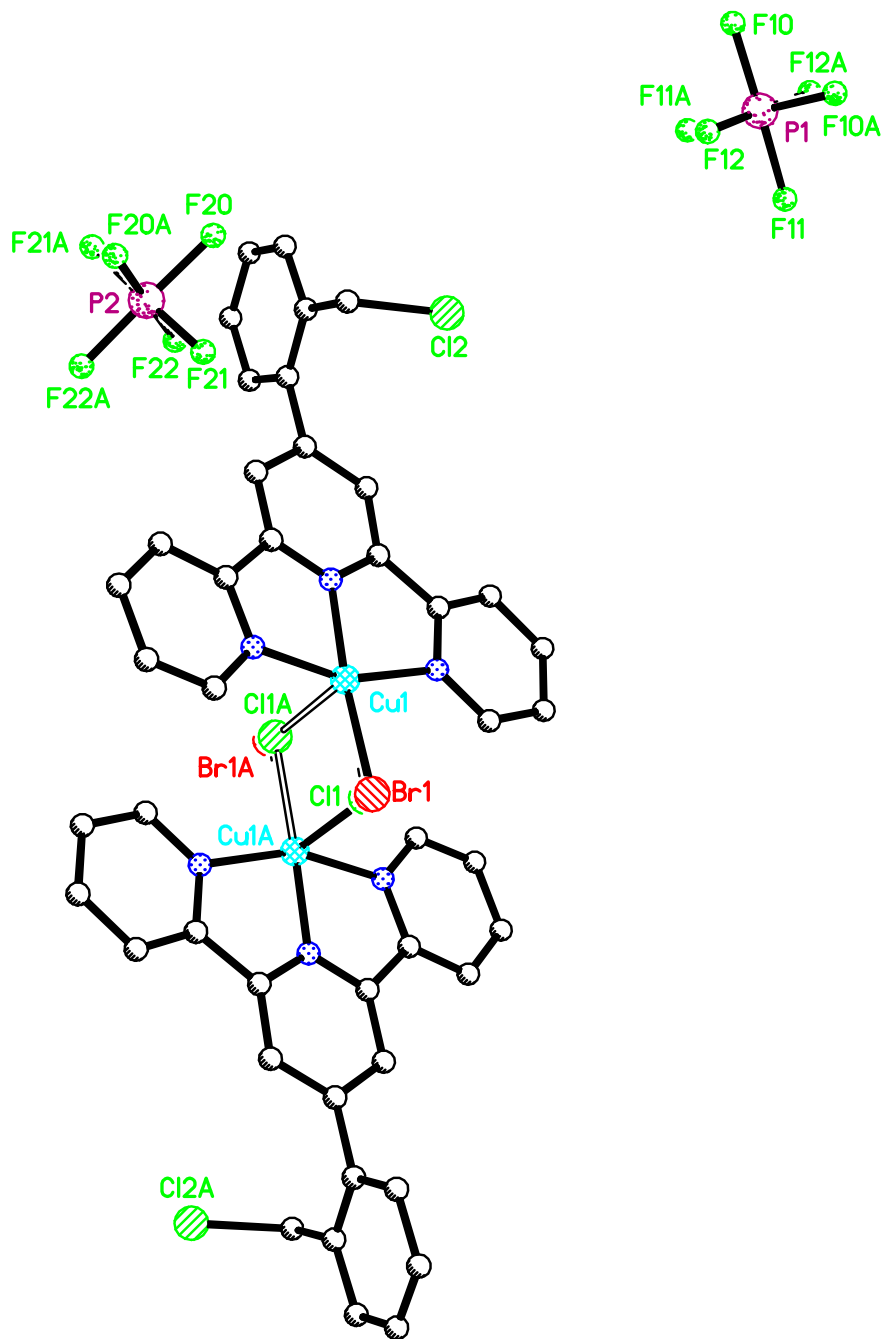
Copper(II) chloride was dissolved in water and added to a solution of 4'-(2-(bromomethyl)phenyl)-2,2':6',2''-terpyridine in ethanol resulting in a blue/green solution. The copper complex was precipitated out of the aqueous mixture by the addition of saturated ammonium hexafluorophosphate in methanol. The precipitate was filtered, washed with H<sub>2</sub>O and then CH<sub>2</sub>Cl<sub>2</sub>, dried and dissolved in CH<sub>3</sub>CN. Recrystallisation of the precipitate required a controlled diffusion rate as in the copper-(4'-(*o*-toluyl)-2,2':6',2''-terpyridine) crystal formation technique. Ether was diffused into the dissolved complex which afforded blue-green needles of X-ray quality.

The X-ray crystal structure (Figure 3-10) shows the complex has distorted trigonal bipyramidal geometry. The dimer is bridged by one chloride ion and one bromide ion. Each bridging halide atom has 50% occupancy which is shown more clearly in the asymmetric unit in Figure 3-11. The only source of bridging bromide ions is from the 4'-(2-(bromomethyl)phenyl)-2,2':6',2''-terpyridine starting material. The bromide ions have exchanged with the chloride ions from the copper salt. This appears to be a facile enthalpy driven process<sup>67</sup>. The preparation of heavier halides from lighter halides in early transition

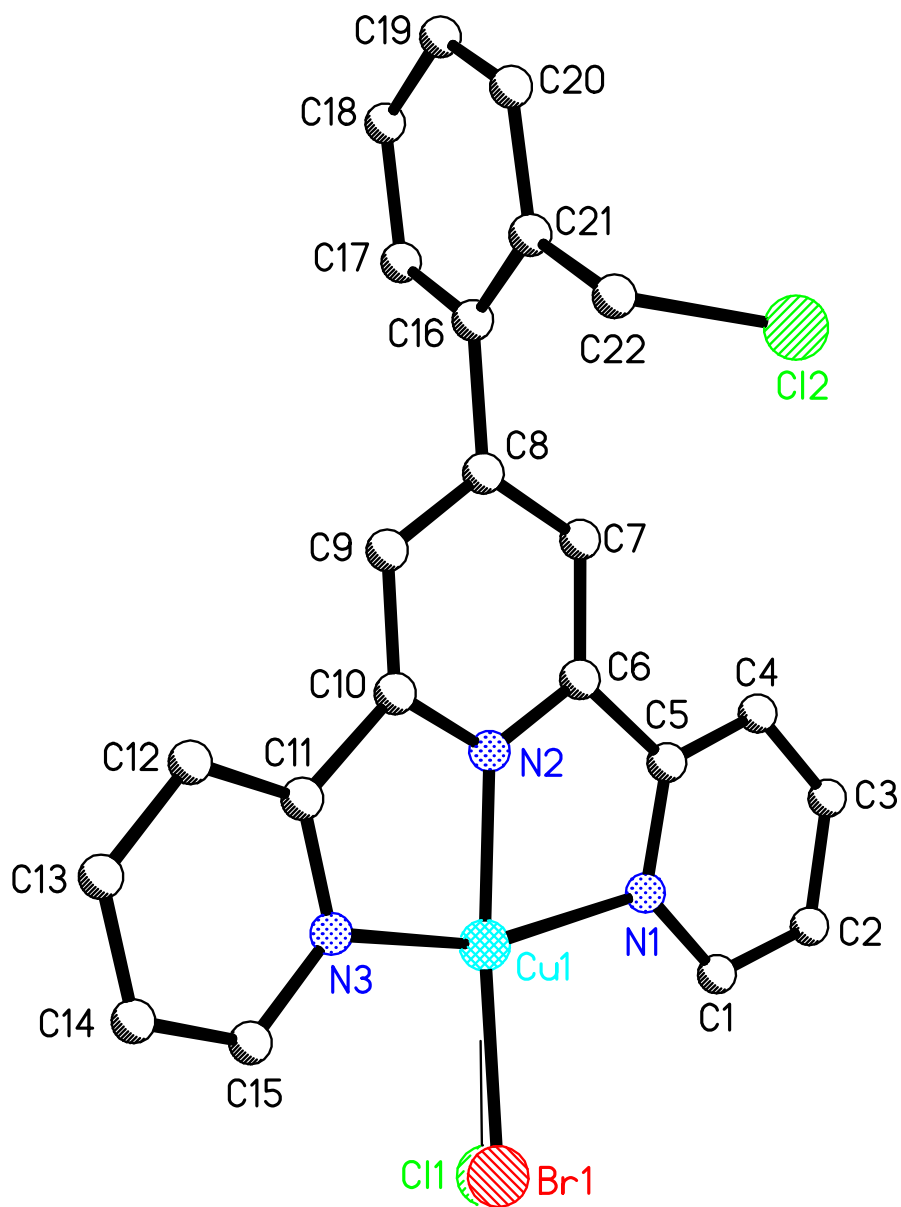
metals was first reported in 1925 by Biltz and Keunecke<sup>68</sup>. The bond enthalpy for carbon-bromine is 276 kJ mol<sup>-1</sup> and for copper-bromide, 331 kJ mol<sup>-1</sup><sup>69</sup>. The bond enthalpy for copper-chloride is 383 kJ mol<sup>-1</sup> and for carbon-chlorine, 397 kJ mol<sup>-1</sup><sup>70</sup>. It is therefore more thermodynamically favorable for the bromide ion to be bonded to the copper ion and the chlorine atom to be bonded to the carbon atom. The information gathered for the copper halide bond enthalpies did not stipulate the oxidation state of the copper ion only that the species was diatomic, but the bulk of the difference can be attributed to the relative strengths of the carbon halide bonds, and so the argument is probably still valid.

Figure 3-12 gives a view along the plane of the pyridine rings showing the bond angles of the bridging halide-copper more clearly. All the bridging halide-copper bond angles fall between 84.3° and 95.9°.

The X-ray crystal structure packing diagram, without counter ions (Figure 3-13), shows hydrogen bonding between the bridging halides and a hydrogen atom on the *o*-toluyl methyl group. The electron withdrawing effects of the chlorine atom attached to the *o*-toluyl methyl carbon atom has probably made this hydrogen atom more electron deficient in nature. The X-ray crystal structure packing diagram with counter ions (Figure 3-14) show another level of bonding. The [PF<sub>6</sub>]<sup>-</sup> ions are hydrogen bonding to some 6, 3'/5' and 6'' hydrogen atoms on the pyridine rings. These hydrogen bonding distances fall in the range 2.244 Å – 2.930 Å.



**Figure 3-10** The X-ray crystal structure of the dimeric  $[(\text{Cl-otp})\text{Cu}(\mu\text{-Cl})(\mu\text{-Br})\text{Cu}(\text{Cl-otp})]$  complex with the two  $\text{PF}_6$  counter ions shown



**Figure 3-11** The asymmetric unit of the X-ray crystal structure of the  $[(\text{Cl-ottp})\text{Cu}(\mu\text{-Cl})(\mu\text{-Br})\text{Cu}(\text{Cl-ottp})]$  complex with a view of the Br/Cl 50% occupancy

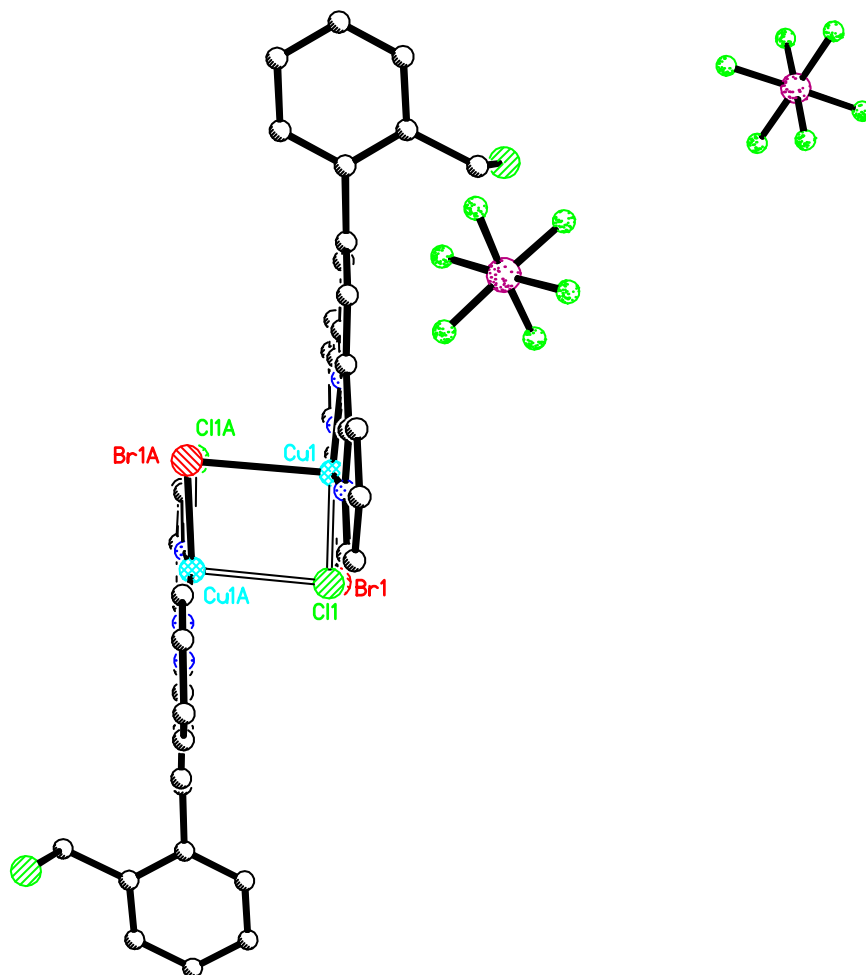


**Figure 3-12** A view of the X-ray crystal structure of the  $[(\text{Cl-ottp})\text{Cu}(\mu\text{-Cl})(\mu\text{-Br})\text{Cu}(\text{Cl-ottp})]$  complex looking along the plane of the pyridine rings.

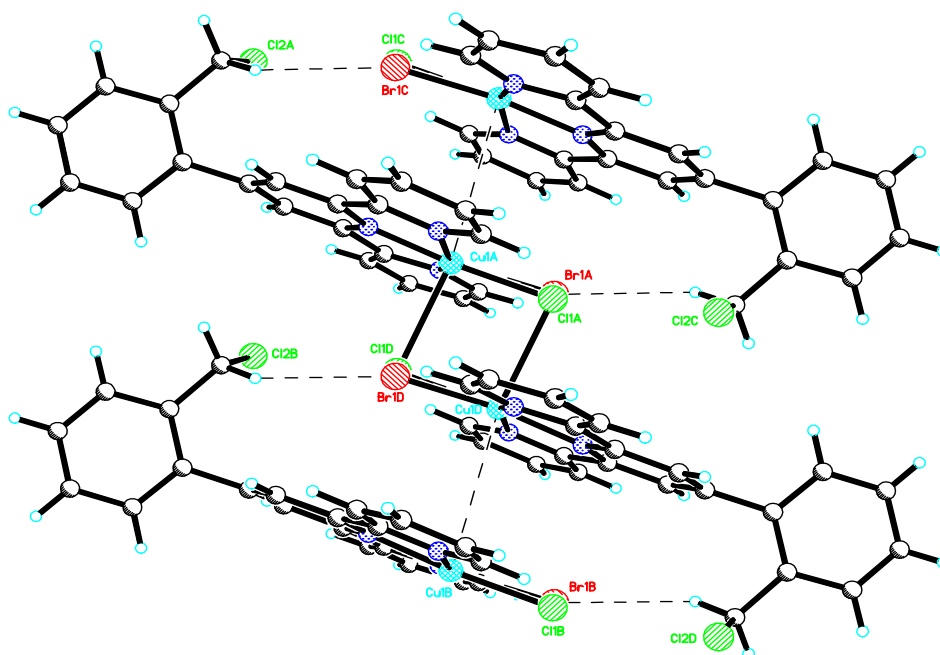


**Figure 3-13** The X-ray crystal structure packing diagram for the  $[(\text{Cl-ottp})\text{Cu}(\mu\text{-Cl})(\mu\text{-Br})\text{Cu}(\text{Cl-ottp})]$  complex without counter ions

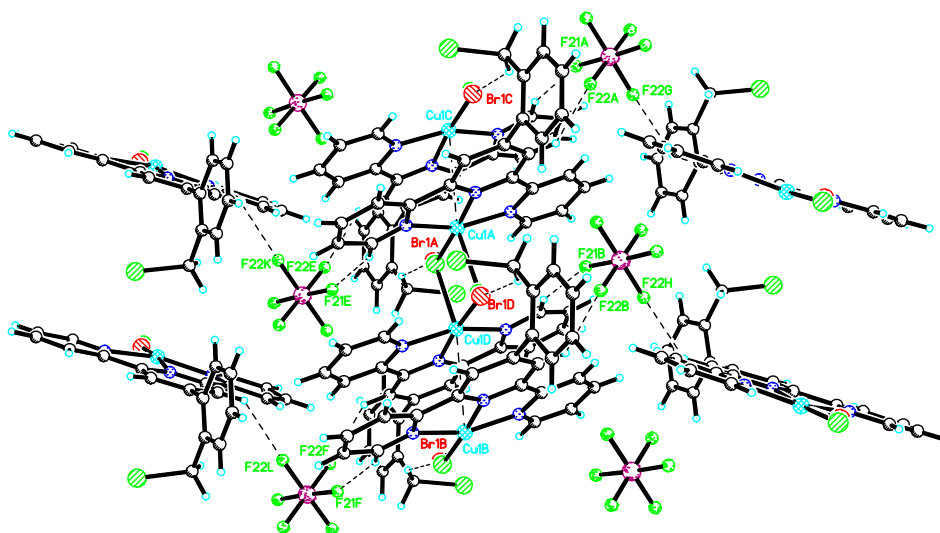


**Figure 3-14** The X-ray crystal structure packing diagram for the  $[(\text{Cl-ottp})\text{Cu}(\mu\text{-Cl})(\mu\text{-Br})\text{Cu}(\text{Cl-ottp})]$  complex with  $\text{PF}_6$  counter ions

### 3.1.5 The Iron(II) 2''-patottp Complex

Iron(II) chloride was dissolved in water and added to a solution of 4'-{2''-(12-amino-2,6,9-triazadodecyl)-phenyl}-2,2':6',2''-terpyridine in methanol, which resulted in an intense purple solution. Saturated ammonium hexafluorophosphate in methanol was added to the solution and a purple precipitate formed. The precipitate was filtered, washed with water, then with dichloromethane, dried and then dissolved in acetonitrile. No X-ray quality crystals resulted from numerous crystallisation attempts using a variety of techniques.

Although the iron(II) and 4'-{2''-(12-amino-2,6,9-triazadodecyl)-phenyl}-2,2':6',2''-terpyridine were added in a 1:1 stoichiometric ratio, there was no guarantee that they had coordinated in this fashion. A variety of analytical techniques were employed to try and determine the stoichiometric ratio.

<sup>1</sup>H NMR spectrometry was attempted for comparison with the characteristic chemical shifts described in section 3.1.3 for the bis(ottp)Fe complex. The <sup>1</sup>H NMR spectrum peaks had all broadened to a degree that it was hard to distinguish that the spectrum was of a 4'-{2''-(12-amino-2,6,9-triazadodecyl)-phenyl}-2,2':6',2''-terpyridine derivative. It was also not possible to distinguish a peak at approximately 9.3 ppm to determine if the complex contained one, two or a mixture of both terpyridine units. There could be two reasons for this phenomenon. Some of the iron(II) could have been oxidised to iron(III). The resulting material would be paramagnetic and degrade the spectrum. Alternatively the spin state of the iron could be approaching the point where it is about to cross-over. Spin crossover (S.C) behaviour in bis(2,2':6',2''-terpyridine)iron(II) complexes is sensitive to Fe-N bond length.

This behaviour can be enhanced by producing steric hindrance about the terminal rings<sup>71</sup>. Constable *et al*<sup>72</sup> investigated S.C. in bis(2,2':6',2''-terpyridine)Fe(II) complexes with steric bulk added to the 4,4'' and 6,6'' pos<sup>n</sup>. They found L.S. complexes were purple and H.S. complexes were orange, although some of the purple solutions contained both species. <sup>1</sup>H NMR data taken from these solutions found the peaks to have broadened considerably. Dong-Woo Yoo *et al*<sup>73</sup> investigate a novel mono (2,2':6',2''-terpyridine)Fe(II) derivative which is green. Of the information given above, comparison between the Constable *et al*<sup>74</sup> L.S. complex and the 4'-{2'''-(12-amino-2,6,9-triazadodecyl)-phenyl}-2,2':6',2''-terpyridine iron(II) complex in this thesis can be made with regards to the solution colour and <sup>1</sup>H NMR spectral characteristics. It is possible that the Fe(II) in the 4'-{2'''-(12-amino-2,6,9-triazadodecyl)-phenyl}-2,2':6',2''-terpyridine iron(II) complex solution is mainly L.S. and contains some iron(II) in the H.S. state. Further analysis such as Mössbauer spectroscopy and magnetic susceptibility measurements would confirm this. Temperature dependent NMR experiments may also be informative.

The results from elemental analysis did not allow us to determine the composition of the material, which means that we could not infer the oxidation state of the iron based on the number of counter ions. Calculations based on modelling of possible stoichiometric combinations pointed towards the complex being a 1:1 ratio but no models were close enough to be definite match.

A sample was run through mass spectrometry in positive ion mode. A major peak showed at 548 for a singly charged species which is just two mass units away from our complexes

calculated anisotropic mass, but again, not close enough to give a definitive stoichiometric ratio.

A UV/visible spectrum (Figure 3-15) was obtained and compared to that for the bis(ottp)Fe complex (Figure 3-6). Both spectra were remarkably similar and both had a peak at 560 nm. The extinction coefficients calculated for the bis(ottp)Fe and mono or bis 4'-{2''-(12-amino-2,6,9-triazadodecyl)-phenyl}-2,2':6',2''-terpyridine iron(II) complex combinations all indicated metal to ligand charge transfer (MLCT). The values were significantly lower for the 4'-{2''-(12-amino-2,6,9-triazadodecyl)-phenyl}-2,2':6',2''-terpyridine iron(II) complex than for the [Fe(ottp)<sub>2</sub>][PF<sub>6</sub>]<sub>2</sub> complex. The similar appearance of the spectra might lead to the inference that this species is a Fe(patottp)<sub>2</sub> complex, but the lower extinction coefficient, different NMR behaviour and elemental analysis results may be a better fit for a 1:1 complex. Overall it is not apparent at this time whether this complex contains one or two ligands per metal ion.

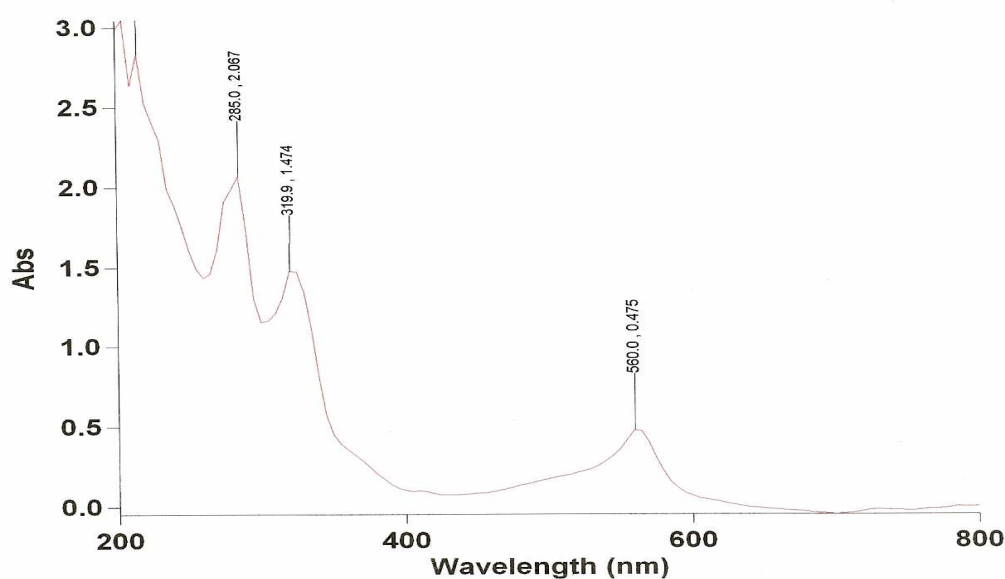


**Figure 3-15** UV/vis spectrum of (patottp)Fe complex.  $\epsilon = 2381.8$  (conc =  $1.9943 \times 10^{-4}$  mol L<sup>-1</sup>) or 4522.1 for bis complex (conc =  $1.0504 \times 10^{-4}$  mol L<sup>-1</sup>)

### 3.1.6 Miscellaneous 2''-patottp Complexes

Other attempts were made to made to form X-ray quality crystals with 4'-{2''-(12-amino-2,6,9-triazadodecyl)-phenyl}-2,2':6',2''-terpyridine and other metals. CuCl<sub>2</sub>, CoCl<sub>2</sub>, ZnCl<sub>2</sub> and AgCl were separately dissolved in water and added to separate solutions of 4'-{2''-(12-amino-2,6,9-triazadodecyl)-phenyl}-2,2':6',2''-terpyridine in methanol in a 1:1 stoichiometry. All solutions were then treated with PF<sub>6</sub><sup>-</sup> salts. None of the complexes yielded X-ray quality crystals from a variety of recrystallisation procedures. The copper and cobalt complexes formed blue/green and red/brown precipitates respectively. When the insoluble, brown complexes of zinc and silver were removed from the solvents, they were found to be of a thick oily consistency. This could be an indication that the zinc and silver complexes were polymeric in nature.

Mass spectrometry was performed on these complexes but the spectra of all samples were inconclusive due to the possibility of contamination.

## 3.2 Summary

4'-(*o*-Toluy)-2,2':6',2''-terpyridine and some of its derivatives were coordinated to metal ions to obtain X-ray quality crystals for characterisation. The complex, [(Cl-ottp)Cu(μ-Cl)(μ-Br)Cu(Cl-ottp)] gave an added bonus in that it displayed some interesting halide exchange chemistry. The bromine atom from 4'-(2-(bromomethyl)phenyl)-2,2':6',2''-terpyridine had

exchanged with one of the chloride atoms from the copper(II) chloride salt and formed a bridge, along with the remaining chloride, to another copper atom.

Unfortunately, X-ray quality crystals were not able to be produced from any of the complexes of 4'-{2''-(12-amino-2,6,9-triazadodecyl)-phenyl}-2,2':6',2''-terpyridine. There is obviously further investigation needed into the iron complex with regard to possible spin crossover and oxidation state properties.

## Chapter 4: Conclusions and Future Work

The research described in the second chapter of this thesis involved the synthesis and characterisation of the novel ligand 4'-{2'''-(12-amino-2,6,9-triazadodecyl)-phenyl}-2,2':6',2''-terpyridine.

The ligand synthesis was followed by NMR at each step to investigate purity and reaction completion. 4'-(*o*-Toluy)-2,2':6',2''-terpyridine was characterised by <sup>1</sup>H NMR, <sup>13</sup>C NMR, COSY and HSQC. The chemical shifts for the protons in the *o*-toluyl ring and 5,5'' protons were not assigned due to being in very close proximity but were consistent with the literature<sup>60</sup>.

Proof of a successful radical bromination came from <sup>1</sup>H NMR data and from the [(Cl-ottp)Cu(μ-Cl)(μ-Br)Cu(Cl-ottp)] complex (pg 66) which has a bridging bromine atom of 50% occupancy.

The protection of N,N'-bis(3-aminopropyl)ethane-1,2-diamine (3,2,3 tet) to give the bisaminal, 1,5,8,12-tetraazadodecane proved to be successful after comparison with NMR data in the literature.

The goal of this project was to synthesis and characterise the novel ligand, 4'-{2'''-(12-amino-2,6,9-triazadodecyl)-phenyl}-2,2':6',2''-terpyridine. This was achieved and proven by a variety of NMR techniques.

Future work on this project would involve analysing the properties of 4'-{2''-(12-amino-2,6,9-triazadodecyl)-phenyl}-2,2':6',2''-terpyridine and its complexes. Due to the lateness of the breakthrough with the purification, little data was obtained in this area. There was some doubt as to the oxidation state of the iron complex as it was possible it had undergone an oxidation process.

Other tails containing different donor atoms could be added to the 4'-(*o*-toluyl)-2,2':6',2''-terpyridine framework. Using hard/soft acid base knowledge and known preferences for coordination number, the ligand could be tuned to be selective for specific metal ions in solution. We only have to look at how metal ores are found in nature to find the best examples of their preferred ligands. The tail could also have other structural features such as some rigidity and/or an aromatic segment which could assist crystal formation, with added  $\pi$ - $\pi$  stacking, more so than the tail derived from N,N'-bis(3-aminopropyl)ethane-1,2-diamine.

## Chapter 5: Experimental

### 5.1 Materials

All reagents and solvents used were, of reagent grade or better, used unpurified unless otherwise stated. All deuterated NMR solvents were supplied by Cambridge Isotope Laboratories.

### 5.2 Nuclear Magnetic Resonance (NMR)

$^1\text{H}$ , COSY, NOESY and HSQC experiments were all recorded on a Varian INOVA 500 spectrometer at 23°C, operating at 500 MHz. The INOVA was equipped with a variable temperature and inverse-detection 5 mm probe or a triple-resonance indirect detection PFG. The  $^{13}\text{C}$  NMR spectra were recorded on either a Varian UNITY 300 NMR spectrometer equipped with a variable temperature direct broadband 5 mm probe, at 23°C, operating at 75 MHz or on a Varian INOVA 500 spectrometer at 23°C, operating at 125 MHz, using a 5mm variable temperature switchable PFG probe. Chemical shifts are expressed in parts per million (ppm) on the  $\delta$  scale, and were referenced to the appropriate solvent peaks:  $\text{CDCl}_3$  referenced to  $\text{CHCl}_3$  at  $\delta_{\text{H}}$  7.25 ( $^1\text{H}$ ) and  $\text{CHCl}_3$  at  $\delta_{\text{C}}$  77.0 ( $^{13}\text{C}$ );  $\text{CD}_3\text{OD}$  referenced to  $\text{CHD}_2\text{OD}$  at  $\delta_{\text{H}}$  3.31 ( $^1\text{H}$ ) and  $\text{CD}_3\text{OD}$  at  $\delta_{\text{C}}$  49.3 ( $^{13}\text{C}$ );  $\text{DMSO}-d_6$  referenced to  $\text{CD}_3(\text{CHD}_2)\text{SO}$  at  $\delta_{\text{H}}$  2.50 ( $^1\text{H}$ ) and  $(\text{CD}_3)_2\text{SO}$  at  $\delta_{\text{C}}$  39.6 ( $^{13}\text{C}$ ).

The peaks are described as singlets (s), doublets (d), triplets (t) or multiplets (m).

### 5.3 Synthesis of 4'-(*o*-Tolyl)-2,2':6',2''-terpyridine.

Two synthetic routes for 2,2':6',2'' terpyridine were investigated in this project. They both follow existing syntheses for *p*-toluyl 2,2':6',2'' terpyridine, both with modifications. Scheme 1 describes a “one pot” synthesis by Hanan and Wang<sup>75</sup>. Scheme 2 is a three step synthesis reported by Field *et al*<sup>6</sup> and Ballardini *et al*<sup>7</sup>.

#### Scheme 1. “One Pot” Method.

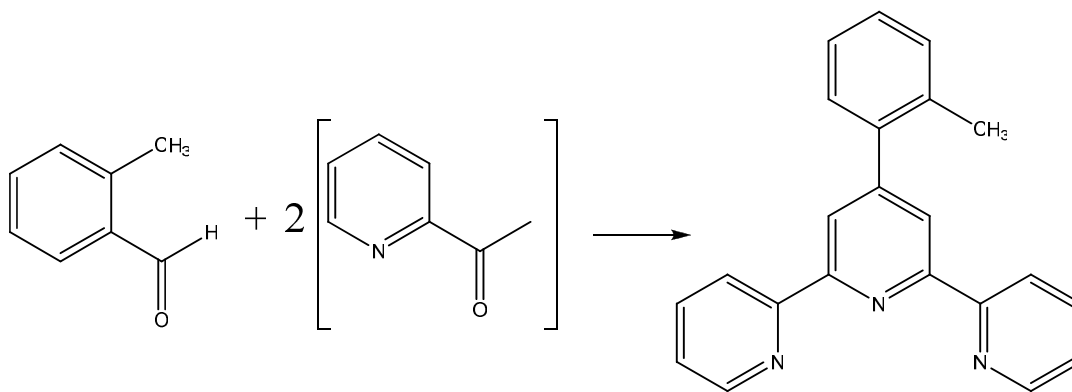


**Figure 5-1** Shows the “one pot” synthesis of 4'-(*o*-toluyl)-2,2':6',2''-terpyridine. The *o*-toluyl aldehyde is the source of the *ortho* methyl group on the 4'' benzyl ring.

*o*-Toluyaldehyde (2.4 g, 20 mmol) was added to *i*-propyl alcohol (100 mL) whilst stirring with a magnetic flea. To this solution, 2-acetylpyridine (4.84 g, 40 mmol), KOH pellets (3.08 g, 40 mmol) and concentrated ammonia solution (58 mL, 50 mmol) was added. The solution was heated at reflux for four hours during which time a white precipitate had formed. The solution was cooled to room temperature and then filtered under vacuum through a glass frit. The ppt. was washed with 50% ethanol and then recrystallised in ethanol.

Yield = 35358 g (51.2%). Mp (70 - 73°C). <sup>1</sup>H NMR (500 MHz CDCl<sub>3</sub>): δ = 8.72 (d, 2H, H<sub>6,6'</sub>), 8.71 (d, 2H, H<sub>3,3'</sub>), 8.49 (s, 2H, H<sub>3',5'</sub>) 7.90 (t, 2H, H<sub>4,4'</sub>) 7.30 – 7.36 (m, 6H, H<sub>5,5'</sub>,toluyl) 2.38 (s, 3H, CH<sub>3</sub>). <sup>13</sup>C NMR (75 MHz, CDCl<sub>3</sub>) 156.5, 155.6, 152.2, 149.4, 139.9, 137.1, 135.4, 130.7, 129.7, 128.5, 126.2, 124.1, 121.9, 121.6, 20.7 (CH<sub>3</sub>). MS(ES) *m/z*: 324.1383 ([M+H<sup>+</sup>], 100%)

### Scheme 2. Three Step Method.

Part 1. Synthesis of 2-methyl-1-[3-(2-pyridyl)-3-oxopropenyl]-benzene.

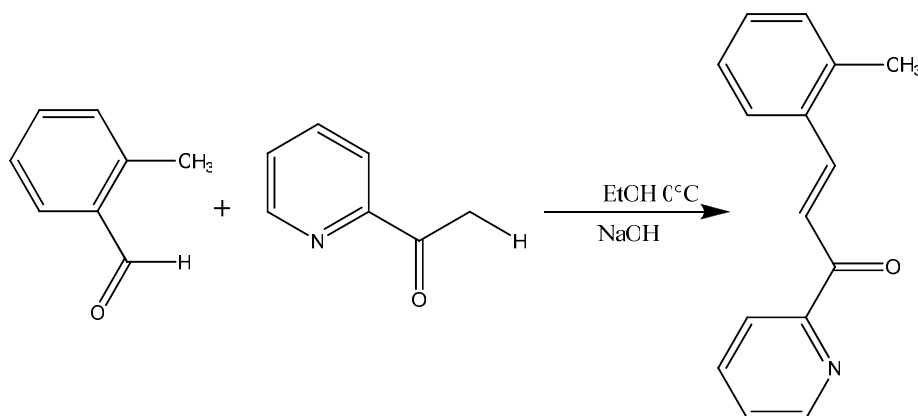


**Figure 5-2** the Field *et al* preparation was followed in the above synthesis of 2-methyl-1-[3-(2-pyridyl)-3-oxopropenyl]-benzene<sup>76</sup>.

A solution of *o*-toluyl aldehyde (2.402 g, 20 mmol) and ethanol (100 mL) was cooled to 0°C in an ice bath whilst stirring with a magnetic flea. 2-Acetylpyridine (2.422 g, 20 mmol) was added to the cooled solution and 1 M NaOH (20 mL, 20 mmol) was added drop wise. The

resulting mixture was stirred for another 3 hours at 0°C. The resulting ppt was vacuum filtered through a glass frit, washed with a small amount of ice cold ethanol and dried.

Yield = 2.75 g (33.9%). Mp (75 - 77°C). <sup>1</sup>H NMR (300 MHz CDCl<sub>3</sub>): δ = 8.75 (d, 1H), 8.21 – 8.29 (m, 3H), 7.90 (d, 1H), 7.84 (d, 1H), 7.51 (d, 1H), 7.31 (d, 1H), 7.24 – 7.29 (m, 2H), 2.52 (s, 3H, CH<sub>3</sub>)

## Part 2. Synthesis of (2-pyridacyl)-pyridinium Iodide

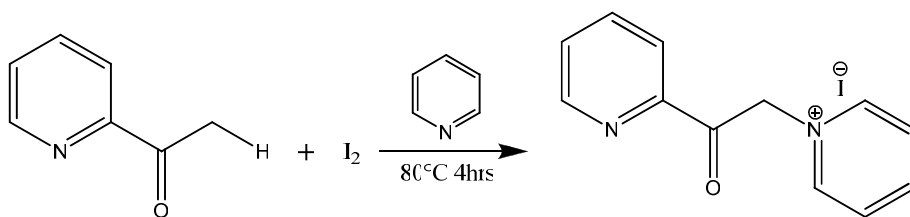


**Figure 5-3** the Ballardini *et al* preparation of (2-pyridacyl)pyridinium Iodide was followed<sup>77</sup>, scaled down.

Iodine (13.567 g, 50 mmol) was added to pyridine (47 mL) and warmed on a steam bath. The resulting mixture was added, under nitrogen, to 2-acetylpyridine (20 mL, 180 mmol) and the mixture stirred at reflux for 4 hours. The ppt was filtered under vacuum through a glass frit and washed with pyridine (20 mL). The ppt was then added to a boiling suspension of activated charcoal (1 spatula) and EtOH (660 mL). The mixture was filtered whilst still hot and allowed to cool where yellow/green crystals resulted.

Yield = 10.37 g (25.9%) Mp (212 - 213°C) <sup>1</sup>H NMR (500 MHz CD<sub>3</sub>OD) δ = 8.96 (d, 2H), 8.81 (d, 1H), 8.73 (t, 1H), 8.22 (t, 2H), 8.13 (d, 1H), 8.08 (d, 1H), 7.74 (t, 1H), 4.60 (s, 2H).

Part 3. Synthesis of 4'-*o*-toluyl 2,2':6',2'' Terpyridine.

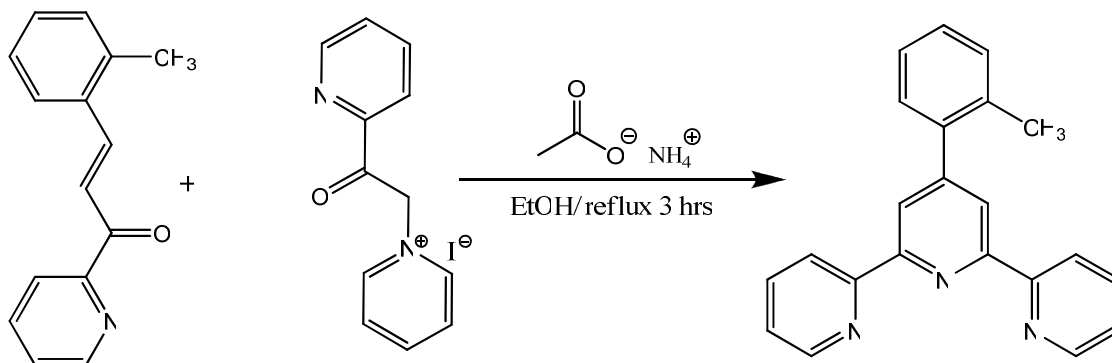


**Figure 5-4** the third and final step of a Field *et al* preparation<sup>76</sup> where a Michael addition followed by ring closure give 4'-*o*-toluyl 2,2':6',2'' terpyridine.

2-Methyl-1-[3-(2-pyridyl)3-oxopropenyl]benzene (0.445 g, 2 mmol) was added to EtOH (8 mL) and stirred with a magnetic flea until dissolved. (2-pyridacyl)pyridinium Iodide (0.68 g, 2 mmol) and ammonium acetate (10 g, 20 mmol) was added to the above solution and stirred at reflux for 3½ hours. The solution was cooled to room temperature and the resulting ppt filtered under vacuum through a glass frit. The ppt was washed with 50% EtOH (20 mL), dried and then recrystallised in EtOH..

Yield = 0.265 g (41.0%) (overall yield = 3.6%) <sup>1</sup>H NMR (500 MHz CDCl<sub>3</sub>) δ = 8.71 (d, 4H), 8.48 (s, 2H), 7.91 (t, 2H), 7.26 – 7.38 (m, 6H), 2.38 (s, 3H, CH<sub>3</sub>)

## 5.4 Bromination of 4'-(*o*-toluyl)-2,2':6',2''-terpyridine.

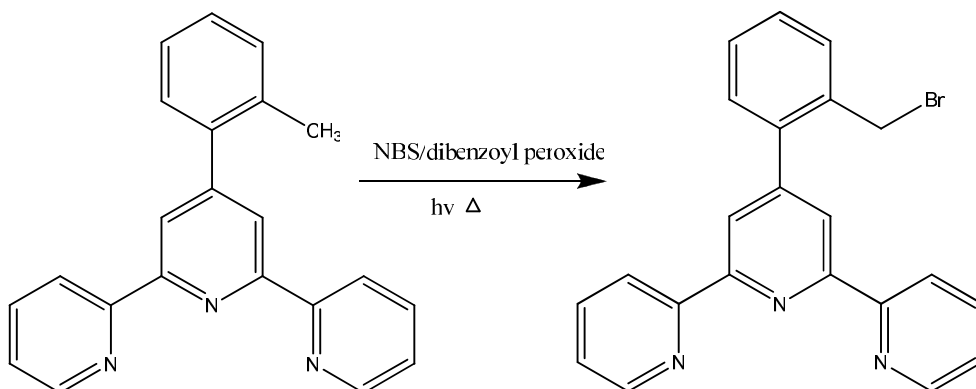


**Figure 5-5** The radical bromination of 4'-(*o*-toluyl)-2,2':6',2''-terpyridine to give 4'-(2-(bromomethyl)phenyl)-2,2':6',2''-terpyridine.

Carbon tetrachloride ( $\text{CCl}_4$ ) (~500 mL) was stored over phosphorus pentoxide ( $\text{P}_2\text{O}_5$ ) for initial drying for at least 4 days. Further drying was completed by heating at reflux under  $\text{N}_2$  for 4 hours.  $\text{CCl}_4$  (50 mL) was extracted using a syringe that had been dried in a  $70^\circ\text{C}$  oven and flushed with  $\text{N}_2$  and then transferred into a 250 mL 3-necked round bottom flask that had also been dried in a  $70^\circ\text{C}$  oven and flushed with  $\text{N}_2$ . Whilst stirring with a magnetic flea and flushing with  $\text{N}_2$ , 4'-(*o*-toluyl)-2,2':6',2''-terpyridine (0.84 g, 2.6 mmol), purified *N*-bromosuccinimide (NBS)<sup>78</sup> (0.46 g, 2.6 mmol) and a catalytic amount of purified dibenzoyl peroxide<sup>79</sup> was added to the 3-neck round bottom flask. The solution was irradiated with a tungsten lamp whilst at reflux, under  $\text{N}_2$ , for 4 hours. The solution was cooled to room temperature and filtered under vacuum through a glass frit where the filtrate contained the brominated 4'-(*o*-toluyl)-2,2':6',2''-terpyridine. The excess  $\text{CCl}_4$  was removed under vacuum and the dried product dissolved in a 2:1 mix of EtOH and acetone. This solution was heated on a steam bath and cooled to room temperature and then stored in a  $-18^\circ\text{C}$  freezer

overnight. The pale yellow ppt is filtered off through a glass frit and dried under vacuum. The ppt was stored in an airtight light excluding container.

Yield = 2.60 g (64%) Mp (138 - 140°C)  $^1\text{H}$  NMR (500 MHz  $\text{CDCl}_3$ )  $\delta$  = 8.72 (d, 2H), 8.71 (d, 2H), 8.58 (s, 2H), 7.91 (t, 2H), 7.58 (d, 1H), 7.35 – 7.44 (m, 5H), 4.45 (s, 2H,  $\text{CH}_2\text{Br}$ ).  $^{13}\text{C}$  NMR (75 MHz  $\text{CDCl}_3$ ) 156.2, 155.8, 150.5, 149.5, 140.1, 137.3, 135.3, 131.2, 130.4, 129.2, 129.0, 124.2, 121.8, 121.7, 31.8 ( $\text{CH}_2\text{Br}$ ). MS(ES)  $m/z$ : 402.0603, 403.0625 ( $[\text{M}+\text{H}^+]$ )

## 5.5 Protection Chemistry for N,N'-bis(3-aminopropyl)ethane-1,2-diamine (3,2,3 tet).

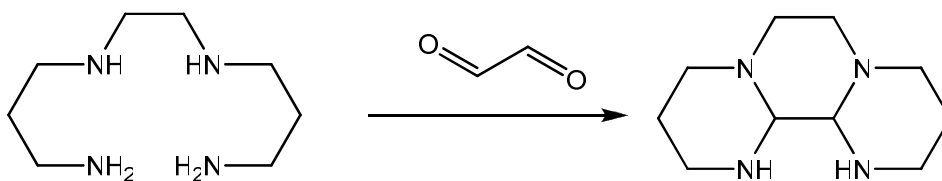


**Figure 5-6** A Claudon *et al* preparation gives protection of the 2° amines<sup>80</sup>. 3° Amines are formed *via* a condensation reaction between 3,2,3 tet and glyoxal to produce the bisaminal, 1,5,8,12-tetraazadodecane, on the right.

Glyoxal (726 mg, 5 mmol) was added to EtOH (10 mL). The mixture was added to N,N'-bis(3-aminopropyl)ethane-1,2-diamine (3,2,3 tet) (871 mg, 5 mmol) also in EtOH (10 mL). The resulting mixture was stirred for 2½ hours. Excess solvent was then removed under vacuum.  $\text{CH}_3\text{CN}$  (20 mL) and a few drops of water was then added to the residual oil and the solution heated at reflux overnight. The  $\text{CH}_3\text{CN}$  was removed under vacuum, the residue taken up in toluene and then filtered to remove the polymers. Excess solvent was removed

under vacuum which afforded an oily residue. Upon sitting for 3 days, the bisaminal, 1,5,8,12-tetraazadodecane, started to form crystals.

Yield = 3.96 g (81.5%)  $^1\text{H NMR } \delta = 3.12$  (2H), 2.93 (2H), 2.63 & 2.43 (4H,  $\text{H}_{6,7}$ ), 2.57 (2H,  $\text{H}_{13,14}$ ), 2.20 (2H), 1.79 (2H), 1.76 (2H), 1.54 (2H).  $^{13}\text{C NMR}$  (75 MHz  $\text{CDCl}_3$ ) 79.45, 54.84, 54.81, 52.68, 52.61, 43.05, 43.03, 26.65, 26.64.

## 5.6 Addition of Protected Tetraamine to Brominated Terpyridine and Deprotection

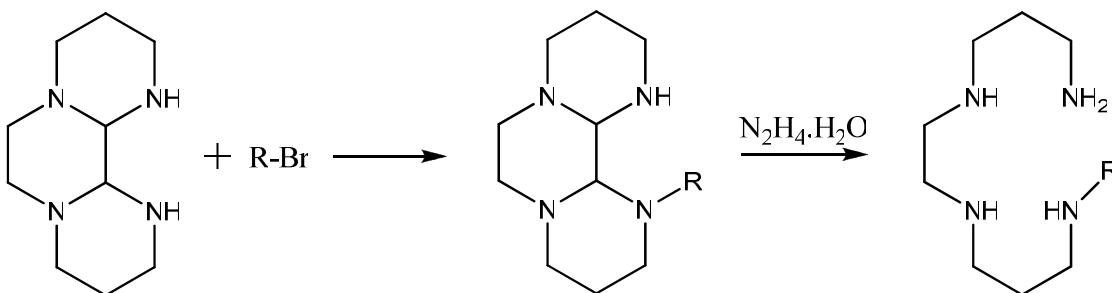


**Figure 5-7** after addition of a brominated “R” group to the protected tetraamine, “R” = 4’-(o-toluy)-2,2’:6’,2’’-terpyridine the “tail” can then undergo deprotection.

Bisaminal (0.9715 g, 5 mmol) was added to dry  $\text{CH}_3\text{CN}$  (20 mL) whilst stirring and heated to reflux. 4’-(2-(Bromomethyl)phenyl)-2,2’:6’,2’’-terpyridine (2.0114 g, 5 mmol) was added to the preheated mixture and stirred at reflux overnight. Excess solvent was removed under vacuum.

Hydrazine monohydrate (10 mL) was added to the residue and heated to reflux whilst stirring for 2 hours. The solution was allowed to cool to room temperature and the

hydrazine removed under vacuum. The residue was taken up in  $\text{CHCl}_3$  and insoluble polymers removed by filtering. Excess solvent was removed under reduced pressure to give an oily residue of crude aminated terpyridine product.

Yield (crude) = 1.67 g (64%)

## 5.7 Purification of 4'-{2''''-(12-amino-2,6,9-triazadodecyl)-phenyl}-2,2':6',2''-terpyridine.

An 25 mm x 230 mm column was  $\frac{1}{2}$  filled with an alumina and  $\text{CHCl}_3$  slurry and allowed to settle for 2 hours. The crude aminated terpyridine product was dissolved in a little  $\text{CHCl}_3$  and loaded onto the top of the column. The initial eluent was 100 mL  $\text{CHCl}_3$  which removed unreacted linear amine and the starting material, 4'-(o-toluy)-2,2':6',2''-terpyridine. The eluent was then changed to a blend of  $\text{CH}_3\text{CN}$ , water and methanol saturated with  $\text{KNO}_3$  (10:2:1 ratio) of which 100 mL was passed through the column to remove the aminated terpyridine. This solvent mixture was removed by reduced pressure and the aminated terpyridine removed from the resulting mixture with  $\text{CH}_2\text{Cl}_2$ . This solution then had the solvent removed under vacuum to give a purified sample of 4'-{2''''-(12-amino-2,6,9-triazadodecyl)-phenyl}-2,2':6',2''-terpyridine.

Yield = 162 mg (9.7%)  $^1\text{H}$  NMR (500 MHz  $\text{CD}_2\text{Cl}_2$ ):  $\delta$  = 8.70 (d, 2H,  $\text{H}_{6,6'}$ ), 8.68 (d, 2H,  $\text{H}_{3,3''}$ ), 8.50 (s, 2H,  $\text{H}_{3',5'}$ ), 7.92 (t, 2H,  $\text{H}_{5,5''}$ ), 7.58 (d, 1H,  $\text{H}_{3''}$ ), 7.45 (t, 1H,  $\text{H}_{4''}$ ), 7.37 – 7.43 (m, 4H,  $\text{H}_{4,4'',5'',6''}$ ), 3.73 (s, 2H,  $\text{H}_{\text{C}1}$ ), 2.94 (d, 2H,  $\text{H}_{\text{C}9}$ ), 2.93 (d, 2H,  $\text{H}_{\text{C}4}$ ), 2.89 & 2.71 (d, 4H,  $\text{H}_{\text{C}5}$  &  $\text{C}6$ ), 2.72 (d, 2H,  $\text{H}_{\text{C}7}$ ), 2.62 (d, 2H,  $\text{H}_{\text{C}2}$ ), 1.75 (t, 2H,  $\text{H}_{\text{C}8}$ ), 1.63 (t, 2H,  $\text{H}_{\text{C}3}$ ). MS(ES)  $m/z$ : 496.3153 ( $[\text{M}+\text{H}^+]$ ), 518.3011 ( $[\text{M}+\text{Na}^+]$ ).

## 5.8 Metal Complexes of 4'-(*o*-Toluy1)-2,2':6',2''-terpyridine (ottp) and Derivatives

### 5.8.1 Cu(ottp)Cl<sub>2</sub>·CH<sub>3</sub>OH

Copper(II) chloride (11.3 mg,  $6.648 \times 10^{-4}$  mol) was dissolved in methanol (5 mL) and added to a solution of 4'-(*o*-toluy1)2,2':6',2''-terpyridine (21.5 mg,  $6.648 \times 10^{-4}$  mol) in CHCl<sub>3</sub> (2 mL). The resulting solution turned blue. An NMR vial was 1/3 filled with the solution and a cap with a 1 mm hole drilled in it secured onto the vial. Vapour diffusion of ether into the ethanol/CHCl<sub>3</sub> solution resulted in the formation of small blue cubic crystals after a week.

### 5.8.2 [Co(ottp)<sub>2</sub>]Cl<sub>2</sub>·2.25CH<sub>3</sub>OH

Cobalt(II) chloride (30.7 mg,  $1.29 \times 10^{-4}$  mol) was dissolved in a solution of methanol (5 mL) and added to a solution of 4'-(*o*-toluy1)2,2':6',2''-terpyridine (83.4 mg,  $2.58 \times 10^{-4}$  mol) in CHCl<sub>3</sub> (2 mL). The resulting solution turned red/brown. An NMR vial was 1/3 filled with the solution and vapour diffusion of ether into the ethanol/ CHCl<sub>3</sub> solution resulted in the formation of medium red/brown cubic crystals after 2 days.

### 5.8.3 [Fe(ottp)<sub>2</sub>][PF<sub>6</sub>]<sub>2</sub>

Iron(II) chloride (13.2 mg,  $6.64 \times 10^{-5}$  mol) was dissolved in water (3 mL) and added to a solution of 4'-(*o*-toluy1)2,2':6',2''-terpyridine (42.9 mg,  $1.33 \times 10^{-4}$  mol) in ethanol (3 mL) and the resulting solution turned intense purple. Two drops of ammonium hexafluorophosphate saturated methanol was added and the complex fell out of solution as a precipitate. The

precipitate was washed with water and then with CH<sub>2</sub>Cl<sub>2</sub> to remove uncoordinated ligand and metal salts. The complex was then analysed by <sup>1</sup>H NMR, COSY, HSQC and elemental analysis.

Absorption spectra in CH<sub>3</sub>CN ( $\lambda_{\max}$ ,  $\epsilon_{\max}$ ): 560 nm, 13492 M<sup>-1</sup>cm<sup>-1</sup>. Anal. Calcd. for C<sub>44</sub>H<sub>34</sub>ClF<sub>6</sub>FeN<sub>6</sub>P: C, 59.85; H, 3.88; N, 9.52. Found: C 59.53; H 3.91; N 9.64. <sup>1</sup>H NMR (500 MHz CDCl<sub>3</sub>):  $\delta$  = 9.29 (s, 2H, H<sub>3',5'</sub>), 8.95 (d, 2H, H<sub>3,3''</sub>), 8.06 (t, 2H, H<sub>4,4''</sub>), 7.82 (d, 1H, H<sub>3'''</sub>), 7.57 – 7.61 (m, 5H, H<sub>6,6'',4''',5''',6'''</sub>), 2.76 (s, 3H, CH<sub>3</sub>).

#### 5.8.4 [(Cl-ottp)Cu( $\mu$ -Cl)( $\mu$ -Br)Co(Cl-ottp)][PF<sub>6</sub>]<sub>2</sub>

Copper(II) chloride (15.6 mg, 9.15 x 10<sup>-5</sup> mol) was dissolved in water (5 mL) and added to a solution of 4'-(2-(bromomethyl)phenyl)-2,2':6',2''-terpyridine (36.8 mg, 9.15 x 10<sup>-5</sup> mol) dissolved in ethanol (5 mL). The resulting solution turned blue/green to which two drops of ammonium hexafluorophosphate saturated methanol was added. A pale blue/green precipitate resulted. The solution was filtered and the precipitate washed with water. To remove any excess metal salts, and then with CH<sub>2</sub>Cl<sub>2</sub>, to remove any excess 4'-(2-(bromomethyl)phenyl)-2,2':6',2''-terpyridine. The precipitate was dissolved in CH<sub>3</sub>CN (1 mL) and vapour diffusion of pet ether into the CH<sub>3</sub>CN solution resulted in blue/green needle-like crystals over one week.

### 5.8.5 The Iron(II) 2''-patottp Complex

Iron(II)chloride (7.9 mg,  $3.983 \times 10^{-5}$  mol) was dissolve in water and added to a solution of 4'-{2''-(12-amino-2,6,9-triazadodecyl)-phenyl}-2,2':6',2''-terpyridine (19.7 mg,  $3.983 \times 10^{-5}$  mol) in methanol (1 mL). Two drops of saturated ammonium hexafluorophosphate in methanol was added to the resulting purple solution and a precipitate resulted. The purple precipitate was filtered and washed with water and then with  $\text{CH}_2\text{Cl}_2$  and dried. The precipitate was then dissolved in  $\text{CH}_3\text{CN}$  and pet ether was diffused into this solution. No X-ray quality crystals resulted.

Absorption spectra in  $\text{CH}_3\text{CN}$  ( $\lambda_{\text{max}}$ ,  $\epsilon_{\text{max}}$ ): 560 nm,  $2381.8 \text{ M}^{-1}\text{cm}^{-1}$  (ML) or  $4522.1 \text{ M}^{-1}\text{cm}^{-1}$  (ML<sub>2</sub>). Anal. Calcd. for  $\text{C}_{30}\text{H}_{36}\text{ClF}_{12}\text{FeN}_7\text{P}_2$ : C, 41.14; H, 4.14; N, 11.19. Found: C 41.44; H 3.65; N 9.71. MS(ES)  $m/z$ : 548.0375 ([M+H<sup>+</sup>])

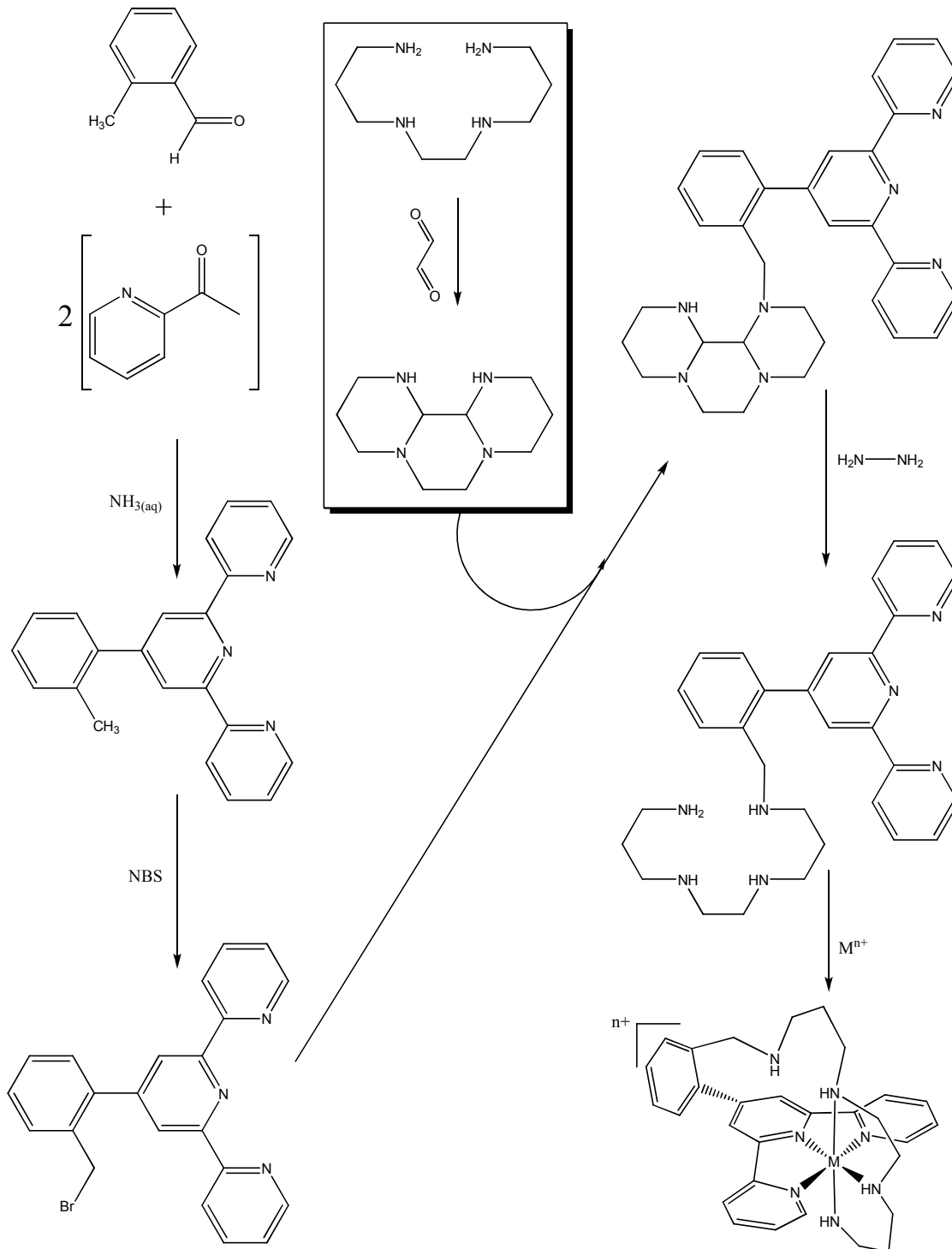


**Figure 5-8** Shows the general overall reaction scheme from start to finish and includes the coordination of the ligand to a central metal ion.

## References

- <sup>1</sup> J. G. Dick. *Analytical Chemistry*. McGraw Hill Inc. U.S.A., **1973**, p 161 – 169.
- <sup>2</sup> Donald C. Bowman. *J. Chem. Ed.* Vol. 83, No. 8, **2006**, p 1158 – 1160.
- <sup>3</sup> Ulrich S Schubert, Harald Hofmeier, George R. Newkome. *Modern Terpyridine Chemistry*. Wiley-VCH, Germany, **2006**, p 37.
- <sup>4</sup> Douglas A. Skoog, Donald M. West, F. James Holler. *Analytical Chemistry. An Introduction*. Saunders College Publishing, U.S.A. **1994**, p 238 – 239.
- <sup>5</sup> Douglas A. Skoog, Donald M. West, F. James Holler. *Analytical Chemistry. An Introduction*. Saunders College Publishing, U.S.A. **1994**, p 250.
- <sup>6</sup> M. G. Mellon. *Colorimetry for Chemists*. The Frederick Smith Chemical Co. Ohio, **1945**, p 2.
- <sup>7</sup> Li Xiang-Hong, Liu Zhi-Qiang, Li Fu-You, Duan Xin-Fang, Huang Chun-Hui. *Chin. J. Chem.*, **2007**, 25, p 186 – 189.
- <sup>8</sup> Malcolm H. Chisholm, Christopher M. Hadad, Katja Heinze, Klaus Hempel, Namrata Singh, Shubham Vyas. *J. Clust. Sci.* **2008**, 19, p 209–218.
- <sup>9</sup> Zuo-Qin Liang, Cai-Xia Wang, Jia-Xiang Yang, Hong-Wen Gao, Yu-Peng Tian, Xu-Tang Tao, Min-Hua Jiang. *New J. Chem.*, **2007**, 31, p 906 – 910.
- <sup>10</sup> E. C. Constable, J. M. Holmes and R. C. S. McQueen, *J. Chem. Soc., Dalton Trans.*, **1987**, p 5.
- <sup>11</sup> E. C. Constable, G. Baum, E. Bill, R. Dyson, R. Eldik, D. Fenske, S. Kaderli, M. Zehnder, A. D. Zuberbühler. *Chem. Eur. J.*, **1999**, 5, p 498 – 508.
- <sup>12</sup> U. S. Schubert, C. Eschbaumer, G. Hochwimmer. *Synthesis*, **1999**, p 779 – 782.
- <sup>13</sup> E. C. Constable, T. Kulke, M. Neuburger, M. Zehnder. *Chem. Commun.*, **1997**, p 489 – 490.
- <sup>14</sup> Ulrich S Schubert, Harald Hofmeier, George R. Newkome. *Modern Terpyridine Chemistry*. Wiley-VCH, Germany, **2006**, pg 11, 13.
- <sup>15</sup> S. Trofimenko. *Chem. Rev.* **1993**, 93, 943-980.
- <sup>16</sup> Pier Sandro Pallavicini, Angelo Perotti, Antonio Poggi, Barbara Seghi and Luigi Fabbrizzi. *J. Am. Chem. Soc.* **1987**, 109, p 5139 – 5144.
- <sup>17</sup> S. G. Morgan, F. H. Burstall. *J. Chem. Soc.* **1932**, p 20 – 30.
- <sup>18</sup> Harald Hofmeier and Ulrich S. Schubert. *Chem. Soc. Rev.*, **2004**, 33, p 374.
- <sup>19</sup> J. K. Stille. *Angew. Chem. Int. Ed. Engl.*, **1986**, 25, p 508 – 524.
- <sup>20</sup> Arturo L. Casado, Pablo Espinet and Ana M. Gallego. *J. Am. Chem. Soc.* **2000**, 122, p 11771 – 11782.
- <sup>21</sup> Pablo Espinet and Antonio M. Echavarren. *Angew. Chem. Int. Ed.* **2004**, 43, p 4704 – 4734.
- <sup>22</sup> Ulrich S. Schubert and Christian Eschbaumer. *Org. Lett.* **1999**, 1, p 1027 – 1029.
- <sup>23</sup> T. W. Graham Solomons. *Organic Chemistry*, 6<sup>th</sup> Ed., John Wiley & Sons, Inc., U.S.A., **1996**, p 1029
- <sup>24</sup> Fritz Kröhnke. *Synthesis*. **1976**, p 1 – 24.
- <sup>25</sup> Yang Hao, Liu Dong, Wang Defen, Hu Hongwen. *Hecheng Huaxue*, **1996**, 4, p 1 – 4.
- <sup>26</sup> George R. Newkome, David C. Hager and Garry E. Kiefer. *J. Org. Chem.*, **1986**, 51, p 850 – 853.
- <sup>27</sup> Charles Mikel, Pierre G. Potvin. *Inorganica Chimica Acta*, **2001**, 325, p 1– 8
- <sup>28</sup> Kimberly Hutchison, James C. Morris, Terence A. Nile, Jerry L. Walsh, David W. Thompson, John D. Petersen and Jon R. Schoonover. *Inorg. Chem.*, **1999**, 38, p 2516 – 2523.
- <sup>29</sup> Ibrahim Eryazici, Charles N. Moorefield, Semih Durmus, and George R. Newkome. *J. Org. Chem.*, **2006**, 71, p 1009 – 1014.
- <sup>30</sup> I. Sasaki, J. C. Daran, G. G. A. Balavoine. *Synthesis*. **1999**, p 815 – 820.
- <sup>31</sup> Jianhua Wang, Garry S. Hanan. *Synlett*. **2005**, 8, p 1251 – 1254.
- <sup>32</sup> Gareth W. V. Cave, Colin L. Raston. *Chem. Commun.* **2000**, p 2199 – 2200.
- <sup>33</sup> Gareth W. V. Cave, Colin L. Raston. *J. Chem. Soc., Perkin Trans. 1*, **2001**, p 3258–3264.
- <sup>34</sup> Ulrich S Schubert, Harald Hofmeier, George R. Newkome. *Modern Terpyridine Chemistry*. Wiley-VCH, Germany, **2006**, p 2

- 
- <sup>35</sup> Carla Bazzicalupi, Andrea Bencini, Antonio Bianchi, Andrea Danesi, Enrico Faggi, Claudia Giorgi, Samuele Santarelli, Barbara Valtancoli. *Coordination Chemistry Reviews*, **2008**, 252, p 1052 – 1068. (Refs. 30 – 86).
- <sup>36</sup> Kai Wing Cheng, Chris S. C. Mak, Wai Kin Chan, Alan Man Ching Ng, Aleksandra B. Djurišić. *J. of Polymer Science: Part A: Polymer Chemistry*, **2008**, 46, p 1305–1317.
- <sup>37</sup> Chao Li, Wendy Fan, Daniel A. Straus, Bo Lei, Sylvia Asano, Daihua Zhang, Jie Han, M. Meyyappan and Chongwu Zhou. *J. Am. Chem. Soc.* **2004**, 126, p 7750–7751.
- <sup>38</sup> R. H. Friend. *Pure Appl. Chem.*, Vol. 73, No. 3, **2001**, p 425–430.
- <sup>39</sup> Christoph J. Brabec, N. Serdar Sariciftci and Jan C. Hummelen. *Adv. Funct. Mater.* **1**, **2001**, p 11
- <sup>40</sup> Luigi Fabbrizzi, Maurizio Licchelli, Giuliano Rabaioli, Angelo Taglietti. *Coord. Chem. Rev.*, **2000**, 205, p 85–108.
- <sup>41</sup> Rajeev Kumar, Udai P. Singh. *Journal of Molecular Structure*, **2008**, 875, p 427–434.
- <sup>42</sup> Chao-Feng Zhang, Hong-Xiang Huang, Bing Liu, Meng Chen, Dong-Jin Qian. *Journal of Luminescence*, **2008**, 128, p 469 – 475.
- <sup>43</sup> Chao Li, Wendy Fan, Daniel A. Straus, Bo Lei, Sylvia Asano, Daihua Zhang, Jie Han, M. Meyyappan and Chongwu Zhou. *J. Am. Chem. Soc.* **2004**, 126, p 7750 – 7751.
- <sup>44</sup> Christoph J. Brabec, N. Serdar Sariciftci and Jan C. Hummelen. *Adv. Funct. Mater.* **2001**, 11, p 15 – 26.
- <sup>45</sup> Mai Zhou, J. Mickey Laux, Kimberly D. Edwards, John C. Hemminger and Bo Hong. *Chem. Commun.*, **1997**, 20, p 1977.
- <sup>46</sup> Coralie Houarner-Rassin, Errol Blart, Pierrick Buvat, Fabrice Odobel. *J. Photochemistry and Photobiology A: Chemistry*, 186, **2007**, p 135 – 142.
- <sup>47</sup> Jon A. McCleverty, Thomas J. Meyer. *Comprehensive Coordination Chemistry II*, Vol. 9, Elsevier Ltd., United Kingdom, **2004**, p 720
- <sup>48</sup> Andrew C. Benniston. *Chem. Soc. Rev.*, **2004**, 33, p 573 – 578.
- <sup>49</sup> David W. Pipes, Thomas J. Meyer. *J. Am. Chem. Soc.* **1984**, 106, p 7653 – 7654.
- <sup>50</sup> John H. Yoe. *Photometric Chemical Analysis*, Vol. 1, Colorimetry, John Wiley & Sons, Inc., **1928**, p 1 – 9.
- <sup>51</sup> Fritz Kröhnke. *Synthesis*. **1976**, p14.
- <sup>52</sup> Zuo-Qin Liang, Cai-Xia Wang, Jia-Xiang Yang, Hong-Wen Gao, Yu-Peng Tian, Xu-Tang Tao, Min-Hua Jiang. *New J. Chem.* **2007**, 31, p 906 – 910.
- <sup>53</sup> Eugenio Coronado, José R. Galán-Mascarós, Carlos Martí-Gastaldo, Emilio Palomares, James R. Durrant, Ramón Vilar, M. Gratzel and Md. K. Nazeeruddin. *J. Am. Chem. Soc.* **2005**, 127, p 12351 – 12356.
- <sup>54</sup> Raja Shunmugam, Gregory J. Gabriel, Cartney E. Smith, Khaled A. Aamer and Gregory N. Tew. *Chem. Eur. J.* **2008**, 14, p 3904 – 3907.
- <sup>55</sup> Douglas A. Skoog, Donald M. West, F. James Holler. *Analytical Chemistry. An Introduction*. Saunders College Publishing, U.S.A. **1994**, p 239.
- <sup>56</sup> J. G. Dick. *Analytical Chemistry*, McGraw-Hill, Inc., **1973**, Sect 4.10 & Chpt. 8
- <sup>57</sup> *CCLA Carbon tetrachloride*. (2003 – 2009, 5<sup>th</sup> March 2009 – last update). [online]. Available <http://www.nationmaster.com/encyclopedia/CCLA> [5<sup>th</sup> March 2009].
- <sup>58</sup> Jarosław Jazwiński and Ryszard A. Koliński. *Tet. Lett.*, **1981**, 22, p 1711 – 1714.
- <sup>59</sup> Zibaseresht, R., Approaches to Photo-activated Cytotoxins. PhD Thesis, University of Canterbury, **2006**.
- <sup>60</sup> Jocelyn M. Starkey. Synthesis of Polyamine-Substituted Terpyridine Ligands, BSc Honors Research Project Report, Department of Chemistry, University of Canterbury, **2004**.
- <sup>61</sup> Zhong Yu, Atsuhiko Nabei, Takafumi Izumi, Takashi Okubo and Takayoshi Kuroda-Sowa. *Acta Cryst.*, **2008**, C64, p m209 – m212.
- <sup>62</sup> Ana Galet, Ana Belén Gaspar, M. Carmen Muñoz and José Antonio Real. *Inorganic Chemistry*, **2006**, 45, p 4413 – 4422.
- <sup>63</sup> Brian N. Figgis, Edward S. Kucharski and Allan H. White. *Aust. J. Chem.*, **1983**, 36, p 1563 - 1571
- <sup>64</sup> Ulrich S Schubert, Harald Hofmeier, George R. Newkome. *Modern Terpyridine Chemistry*. Wiley-VCH, Germany, **2006**, p 40 – 43.
- <sup>65</sup> Zibaseresht, R., PhD Thesis, University of Canterbury, **2006**, p 151
- <sup>66</sup> James R. Jeitler, Mark M. Turnbull, Jan L. Wikaira. *Inorganica Chimica Acta*, **2003**, 351, p 331 – 344.
- <sup>67</sup> Daniela Belli Dell'Amico, Fausto Calderazzo, Guido Pampaloni. *Inorganica Chimica Acta*, **2008**, 361, p 2997–3003.

- 
- <sup>68</sup> W. Biltz, E. Keunecke, *Z. Anorg. Allg. Chem.*, **1925**, 147, p 171.
- <sup>69</sup> Peter Atkins and Julio de Paula. *Elements of Physical Chemistry* 4<sup>th</sup> Ed., *Oxford University Press*, **2005**, p 71
- <sup>70</sup> Mark Winter. *Copper: bond enthalpies in gaseous diatomic species*. (2003 – 2009, 5<sup>th</sup> March 2009 – last update). [online]. Available [http://www.webelements.com/copper/bond\\_enthalpies.html](http://www.webelements.com/copper/bond_enthalpies.html) [5<sup>th</sup> March 2009].
- <sup>71</sup> Philipp Gütlich, Yann Garcia and Harold A. Goodwin. *Chem. Soc. Rev.*, **2000**, 29, p 419 – 427.
- <sup>72</sup> Edwin C. Constable, Gerhard Baum, Eckhard Bill, Raylene Dyson, Rudi van Eldik, Dieter Fenske, Susan Kaderli, Darrell Morris, Anton Neubrand, Markus Neuburger, Diane R. Smith, Karl Wieghardt, Margareta Zehnder and Andreas D. Zuberbühler. *Chem. Eur. J.* **1999**, 5, p 498 – 508.
- <sup>73</sup> Dong-Woo Yoo, Sang-Kun Yoo, Cheal Kim and Jin-Kyu Lee. *J. Chem. Soc., Dalton Trans.*, **2002**, p 3931 – 3932.
- <sup>74</sup> Edwin C. Constable, Gerhard Baum, Eckhard Bill, Raylene Dyson, Rudi van Eldik, Dieter Fenske, Susan Kaderli, Darrell Morris, Anton Neubrand, Markus Neuburger, Diane R. Smith, Karl Wieghardt, Margareta Zehnder and Andreas D. Zuberbühler. *Chem. Eur. J.* **1999**, 5, p 498 – 508.
- <sup>75</sup> Jianhua Wang, Garry S. Hanan. *Synlett*. **2005**, 8, p 1251–1254
- <sup>76</sup> Field, J. S. Haines, R. J. McMillan, D. R. Summerton, G. C. J. *Chem. Soc., Dalton Trans.*, **2002**, p 1369 – 1376.
- <sup>77</sup> Ballardini, R. Balzani, V. Clemente-Leon, M. Credi, A. Gandolfi, M. Ishow, E. Perkins, J. Stoddart, J. F. Tseng, H. Wenger, *S. J. Am. Chem. Soc.* **2002**, 124, p 12786 – 12795.
- <sup>78</sup> D. D. Perrin and W. L. F. Armarego. *Purification of Laboratory Chemicals*, 3<sup>RD</sup> Ed., p105
- <sup>79</sup> D. D. Perrin and W. L. F. Armarego. *Purification of Laboratory Chemicals*, 3<sup>RD</sup> Ed., p 95
- <sup>80</sup> Géraldine Claudon, Nathalie Le Bris, Hélène Bernard and Henri Handel. *Eur. J. Org. Chem.* **2004**, p 5027 – 5030.

# Appendix

## X-ray Crystallography Tables

Crystals were mounted on a glass fibre using perfluorinated oil. Data were collected at low temperature using a APEX II CCD area detector. The crystals were mounted 37.5 mm from the detector and irradiated with graphite monochromised Mo K $\alpha$  ( $\gamma = 0.71073 \text{ \AA}$ ) radiation. The data reduction was performed using SAINTPLUS<sup>1</sup>. Intensities were corrected for Lorentzian polarization effects and for absorption effects using multi-scan methods. Space groups were determined from systematic absences and checked for higher symmetry. Structures were solved by direct methods using SHELXS-97<sup>2</sup> and refined with full-matrix least squares on  $F^2$  using SHELXL-97<sup>3</sup> or with SHELXTL<sup>4</sup>. All non-hydrogen atoms were refined anisotropically, unless specified otherwise. Hydrogen atom positions were placed at ideal positions and refined with a riding model.

### 1.1 Table 1. 1,5,8,12-Tetraazadodecane

Identification code	PATBA
Empirical formula	C <sub>10</sub> H <sub>20</sub> N <sub>4</sub>
Formula weight	196.30
Temperature	119(2) K
Wavelength	0.71073 Å
Crystal system, space group	rhombohedral, R3c
Crystal size	0.83 x 0.15 x 0.10 mm
Crystal colour	colourless
Crystal form	needle

Unit cell dimensions	a = 23.9469(9) Å    alpha = 90 deg. b = 23.9469(9) Å    beta = 90 deg. c = 9.7831(5) Å    gamma = 120 deg.
Volume	4858.5(4) Å <sup>3</sup>
Z, Calculated density	18, 1.208 Mg/m <sup>3</sup>
Absorption coefficient	0.076 mm <sup>-1</sup>
Absorption Correction	multiscan
F(000)	1944
Theta range for data collection	1.70 to 25.04 deg.
Limiting indices	-28<=h<=28, -28<=k<=28, -11<=l<=11
Reflections collected / unique	7266 / 1914 [R(int) = 0.0374]
Completeness to theta = 25.04	100.0 %
Max. and min. transmission	0.9924 and 0.9394
Refinement method	Full-matrix least-squares on F <sup>2</sup>
Data / restraints / parameters	1914 / 1 / 127
Goodness-of-fit on F <sup>2</sup>	1.031
Final R indices [I>2sigma(I)]	R1 = 0.0368, wR2 = 0.1000
R indices (all data)	R1 = 0.0433, wR2 = 0.1075
Absolute structure parameter	2(3)
Largest diff. peak and hole	0.310 and -0.305 e.Å <sup>-3</sup>

## 1.2 Table 2.

Atomic coordinates ( $\times 10^4$ ) and equivalent isotropic displacement parameters ( $\text{Å}^2 \times 10^3$ ) for PATBA.

U(eq) is defined as one third of the trace of the orthogonalized U<sub>ij</sub> tensor.

---

	x	y	z	U(eq)
N(3)	4063(1)	2018(1)	1185(2)	25(1)
N(2)	4690(1)	1452(1)	2651(2)	28(1)
C(10)	4962(1)	2152(1)	2638(2)	25(1)
N(1)	5290(1)	2443(1)	3909(2)	32(1)
N(4)	4740(1)	3015(1)	2254(2)	31(1)
C(9)	4441(1)	2323(1)	2413(2)	24(1)
C(7)	3828(1)	2903(1)	986(2)	34(1)
C(2)	5561(1)	1580(1)	4150(2)	38(1)
C(3)	5207(1)	1300(1)	2814(2)	35(1)
C(5)	3793(1)	1322(1)	1262(2)	33(1)
C(6)	3553(1)	2181(1)	1036(2)	32(1)
C(4)	4328(1)	1166(1)	1401(2)	34(1)
C(8)	4264(1)	3222(1)	2201(2)	36(1)
C(1)	5805(1)	2299(1)	4200(2)	41(1)

---

### 1.3 Table 3.

Bond lengths [Å] and angles [deg] for PATBA.

---

N(3)-C(5)	1.459(3)
N(3)-C(6)	1.462(3)
N(3)-C(9)	1.460(2)

N(2)-C(10)	1.464(3)
N(2)-C(4)	1.456(3)
N(2)-C(3)	1.463(3)
C(10)-N(1)	1.449(3)
C(10)-C(9)	1.512(3)
C(10)-H(10A)	1.0000
N(1)-C(1)	1.466(3)
N(1)-H(1A)	0.8800
N(4)-C(9)	1.450(3)
N(4)-C(8)	1.455(3)
N(4)-H(4A)	0.8800
C(9)-H(9A)	1.0000
C(7)-C(6)	1.513(3)
C(7)-C(8)	1.512(3)
C(7)-H(7A)	0.9900
C(7)-H(7B)	0.9900
C(2)-C(3)	1.520(3)
C(2)-C(1)	1.518(4)
C(2)-H(2A)	0.9900
C(2)-H(2B)	0.9900
C(3)-H(3A)	0.9900
C(3)-H(3B)	0.9900
C(5)-C(4)	1.509(3)
C(5)-H(5A)	0.9900
C(5)-H(5B)	0.9900
C(6)-H(6A)	0.9900
C(6)-H(6B)	0.9900
C(4)-H(4B)	0.9900
C(4)-H(4C)	0.9900
C(8)-H(8A)	0.9900
C(8)-H(8B)	0.9900
C(1)-H(1B)	0.9900

C(1)-H(1C)	0.9900
C(5)-N(3)-C(6)	110.93(16)
C(5)-N(3)-C(9)	109.72(15)
C(6)-N(3)-C(9)	109.89(15)
C(10)-N(2)-C(4)	110.52(16)
C(10)-N(2)-C(3)	109.77(17)
C(4)-N(2)-C(3)	110.72(17)
N(1)-C(10)-N(2)	111.56(15)
N(1)-C(10)-C(9)	108.47(16)
N(2)-C(10)-C(9)	110.86(16)
N(1)-C(10)-H(10A)	108.6
N(2)-C(10)-H(10A)	108.6
C(9)-C(10)-H(10A)	108.6
C(10)-N(1)-C(1)	111.77(17)
C(10)-N(1)-H(1A)	124.1
C(1)-N(1)-H(1A)	124.1
C(9)-N(4)-C(8)	111.72(18)
C(9)-N(4)-H(4A)	124.1
C(8)-N(4)-H(4A)	124.1
N(4)-C(9)-N(3)	108.13(15)
N(4)-C(9)-C(10)	108.76(16)
N(3)-C(9)-C(10)	111.96(15)
N(4)-C(9)-H(9A)	109.3
N(3)-C(9)-H(9A)	109.3
C(10)-C(9)-H(9A)	109.3
C(6)-C(7)-C(8)	110.36(17)
C(6)-C(7)-H(7A)	109.6
C(8)-C(7)-H(7A)	109.6
C(6)-C(7)-H(7B)	109.6
C(8)-C(7)-H(7B)	109.6
H(7A)-C(7)-H(7B)	108.1
C(3)-C(2)-C(1)	110.00(18)

C(3)-C(2)-H(2A)	109.7
C(1)-C(2)-H(2A)	109.7
C(3)-C(2)-H(2B)	109.7
C(1)-C(2)-H(2B)	109.7
H(2A)-C(2)-H(2B)	108.2
N(2)-C(3)-C(2)	109.80(18)
N(2)-C(3)-H(3A)	109.7
C(2)-C(3)-H(3A)	109.7
N(2)-C(3)-H(3B)	109.7
C(2)-C(3)-H(3B)	109.7
H(3A)-C(3)-H(3B)	108.2
N(3)-C(5)-C(4)	109.95(18)
N(3)-C(5)-H(5A)	109.7
C(4)-C(5)-H(5A)	109.7
N(3)-C(5)-H(5B)	109.7
C(4)-C(5)-H(5B)	109.7
H(5A)-C(5)-H(5B)	108.2
N(3)-C(6)-C(7)	111.32(18)
N(3)-C(6)-H(6A)	109.4
C(7)-C(6)-H(6A)	109.4
N(3)-C(6)-H(6B)	109.4
C(7)-C(6)-H(6B)	109.4
H(6A)-C(6)-H(6B)	108.0
N(2)-C(4)-C(5)	109.81(17)
N(2)-C(4)-H(4B)	109.7
C(5)-C(4)-H(4B)	109.7
N(2)-C(4)-H(4C)	109.7
C(5)-C(4)-H(4C)	109.7
H(4B)-C(4)-H(4C)	108.2
N(4)-C(8)-C(7)	108.45(17)
N(4)-C(8)-H(8A)	110.0
C(7)-C(8)-H(8A)	110.0

N(4)-C(8)-H(8B)	110.0
C(7)-C(8)-H(8B)	110.0
H(8A)-C(8)-H(8B)	108.4
N(1)-C(1)-C(2)	111.60(19)
N(1)-C(1)-H(1B)	109.3
C(2)-C(1)-H(1B)	109.3
N(1)-C(1)-H(1C)	109.3
C(2)-C(1)-H(1C)	109.3
H(1B)-C(1)-H(1C)	108.0

---

Symmetry transformations used to generate equivalent atoms:

'x, y, z'  
 '-y, x-y, z'  
 '-x+y, -x, z'  
 '-y, -x, z+1/2'  
 '-x+y, y, z+1/2'  
 'x, x-y, z+1/2'  
 'x+2/3, y+1/3, z+1/3'  
 '-y+2/3, x-y+1/3, z+1/3'  
 '-x+y+2/3, -x+1/3, z+1/3'  
 '-y+2/3, -x+1/3, z+5/6'  
 '-x+y+2/3, y+1/3, z+5/6'  
 'x+2/3, x-y+1/3, z+5/6'  
 'x+1/3, y+2/3, z+2/3'  
 '-y+1/3, x-y+2/3, z+2/3'  
 '-x+y+1/3, -x+2/3, z+2/3'  
 '-y+1/3, -x+2/3, z+7/6'  
 '-x+y+1/3, y+2/3, z+7/6'  
 'x+1/3, x-y+2/3, z+7/6'

#### 1.4 Table 4.

Anisotropic displacement parameters ( $\text{\AA}^2 \times 10^3$ ) for PATBA.

The anisotropic displacement factor exponent takes the form:

$$-2 \pi^2 [ h^2 a^{*2} U_{11} + \dots + 2 h k a^* b^* U_{12} ]$$

---

	U11	U22	U33	U23	U13	U12
N(3)	26(1)	26(1)	23(1)	-2(1)	-3(1)	13(1)
N(2)	33(1)	30(1)	25(1)	2(1)	1(1)	19(1)
C(10)	24(1)	28(1)	20(1)	2(1)	3(1)	11(1)
N(1)	32(1)	38(1)	28(1)	-6(1)	-7(1)	19(1)
N(4)	27(1)	25(1)	38(1)	0(1)	-3(1)	12(1)
C(9)	24(1)	26(1)	20(1)	-1(1)	1(1)	12(1)
C(7)	36(1)	40(1)	34(1)	3(1)	0(1)	25(1)
C(2)	36(1)	58(2)	33(1)	13(1)	5(1)	33(1)
C(3)	41(1)	44(1)	33(1)	8(1)	6(1)	31(1)
C(5)	33(1)	28(1)	33(1)	-6(1)	-4(1)	13(1)
C(6)	26(1)	37(1)	35(1)	-2(1)	-5(1)	16(1)
C(4)	41(1)	31(1)	32(1)	-6(1)	-3(1)	21(1)
C(8)	45(1)	32(1)	40(1)	-1(1)	-2(1)	25(1)
C(1)	31(1)	57(2)	36(1)	3(1)	-4(1)	23(1)

---

### 1.5 Table 5.

Hydrogen coordinates ( $\times 10^4$ ) and isotropic displacement parameters ( $\text{\AA}^2 \times 10^3$ ) for PATBA.

	x	y	z	U(eq)
H(10A)	5280	2338	1873	30
H(1A)	5191	2677	4441	38
H(4A)	5159	3279	2197	37
H(9A)	4148	2183	3225	28
H(7A)	3472	3000	991	40
H(7B)	4076	3077	130	40
H(2A)	5929	1502	4229	46
H(2B)	5266	1365	4928	46
H(3A)	5513	1483	2040	42
H(3B)	5023	827	2812	42
H(5A)	3540	1116	427	39
H(5B)	3500	1148	2059	39
H(6A)	3251	1999	1816	39
H(6B)	3309	1984	187	39
H(4B)	4144	693	1426	40
H(4C)	4620	1337	602	40
H(8A)	4481	3697	2107	43
H(8B)	4007	3098	3053	43
H(1B)	5986	2466	5118	49
H(1C)	6156	2522	3522	49

## 2.1 Table 1. [Cu(ottp)]Cl<sub>2</sub>·CH<sub>3</sub>OH

Crystal data and structure refinement for [Cu(ottp)]Cl<sub>2</sub>·CH<sub>3</sub>OH

Identification code	L1CuA	
Empirical formula	C <sub>23</sub> H <sub>21</sub> Cl <sub>2</sub> Cu N <sub>3</sub> O	
Formula weight	489.87	
Temperature	110(2) K	
Wavelength	0.71073 Å	
Crystal system, space group	Triclinic, P-1	
Crystal size	0.42 x 0.36 x 0.20 mm	
Crystal colour	blue	
Crystal form	block	
Unit cell dimensions	a = 8.0345(11) Å b = 9.0879(14) Å c = 15.404(2) Å	alpha = 74.437(4) deg. beta = 76.838(4) deg. gamma = 82.023(4) deg.
Volume	1051.4(3) Å <sup>3</sup>	
Z, Calculated density	2, 1.547 Mg/m <sup>3</sup>	
Absorption coefficient	1.313 mm <sup>-1</sup>	
Absorption correction	Multi-scan	
F(000)	502	
Theta range for data collection	2.33 to 25.05 deg.	
Limiting indices	-9<=h<=5, -10<=k<=10, -18<=l<=18	
Reflections collected / unique	6994 / 3664 [R(int) = 0.0432]	
Completeness to theta = 25.00	98.0 %	
Max. and min. transmission	0.769 and 0.367	
Refinement method	Full-matrix least-squares on F <sup>2</sup>	

Data / restraints / parameters	3664 / 0 / 274
Goodness-of-fit on $F^2$	1.122
Final R indices [ $I > 2\sigma(I)$ ]	R1 = 0.0401, wR2 = 0.1164
R indices (all data)	R1 = 0.0429, wR2 = 0.1188
Largest diff. peak and hole	0.442 and -0.801 e.Å <sup>-3</sup>

## 2.2 Table 2.

Atomic coordinates ( $\times 10^4$ ) and equivalent isotropic displacement parameters ( $\text{Å}^2 \times 10^3$ ) for [Cu(ottp)]Cl<sub>2</sub>·CH<sub>3</sub>OH. U(eq) is defined as one third of the trace of the orthogonalized U<sub>ij</sub> tensor.

	x	y	z	U(eq)
Cu(1)	4760(1)	1300(1)	3743(1)	19(1)
Cl(1)	3938(1)	2973(1)	2295(1)	32(1)
Cl(2)	2683(1)	1891(1)	4867(1)	27(1)
N(11)	6568(3)	2640(3)	3788(2)	20(1)
C(11)	8174(4)	2279(3)	3352(2)	21(1)
C(12)	9544(4)	3056(4)	3333(2)	27(1)
C(13)	9240(4)	4274(4)	3745(2)	30(1)
C(14)	7597(4)	4693(4)	4150(2)	29(1)
C(15)	6288(4)	3832(4)	4167(2)	25(1)
N(21)	6813(3)	369(3)	3086(2)	18(1)
C(21)	8293(4)	1012(3)	2900(2)	19(1)
C(22)	9728(4)	502(3)	2329(2)	21(1)
C(23)	9599(4)	-687(3)	1937(2)	21(1)
C(24)	8058(4)	-1393(3)	2190(2)	22(1)
C(25)	6690(4)	-825(3)	2767(2)	20(1)
N(31)	3845(3)	-613(3)	3630(2)	21(1)
C(31)	4970(4)	-1421(3)	3099(2)	20(1)
C(32)	4565(4)	-2710(4)	2910(2)	26(1)
C(33)	2931(4)	-3199(4)	3286(2)	28(1)
C(34)	1775(4)	-2373(4)	3819(2)	28(1)
C(35)	2265(4)	-1085(4)	3974(2)	24(1)
C(41)	11050(4)	-1251(4)	1282(2)	22(1)
C(42)	12012(4)	-248(4)	536(2)	24(1)
C(43)	13299(4)	-890(4)	-61(2)	30(1)

C(44)	13672(4)	-2452(4)	75(2)	33(1)
C(45)	12733(5)	-3431(4)	813(2)	33(1)
C(46)	11430(4)	-2826(4)	1402(2)	26(1)
C(47)	11681(5)	1469(4)	332(2)	33(1)
O(100)	7007(4)	5138(3)	1737(2)	42(1)
C(100)	8287(6)	4604(4)	1076(3)	43(1)

---

### 2.3 Table 3.

Bond lengths [Å] and angles [deg] for [Cu(ottp)]Cl<sub>2</sub>·CH<sub>3</sub>OH

---

Cu(1)-N(21)	1.942(2)
Cu(1)-N(31)	2.042(3)
Cu(1)-N(11)	2.044(3)
Cu(1)-Cl(2)	2.2375(8)
Cu(1)-Cl(1)	2.5093(9)
N(11)-C(15)	1.333(4)
N(11)-C(11)	1.352(4)
C(11)-C(12)	1.378(4)
C(11)-C(21)	1.480(4)
C(12)-C(13)	1.386(5)
C(12)-H(12)	0.9500
C(13)-C(14)	1.375(5)
C(13)-H(13)	0.9500
C(14)-C(15)	1.387(5)
C(14)-H(14)	0.9500
C(15)-H(15)	0.9500
N(21)-C(25)	1.329(4)
N(21)-C(21)	1.336(4)
C(21)-C(22)	1.388(4)
C(22)-C(23)	1.397(4)
C(22)-H(0MA)	0.9500
C(23)-C(24)	1.401(4)
C(23)-C(41)	1.488(4)
C(24)-C(25)	1.381(4)
C(24)-H(7TA)	0.9500
C(25)-C(31)	1.485(4)
N(31)-C(35)	1.341(4)
N(31)-C(31)	1.351(4)
C(31)-C(32)	1.376(4)
C(32)-C(33)	1.391(4)
C(32)-H(32)	0.9500

C(33)-C(34)	1.375(5)
C(33)-H(33)	0.9500
C(34)-C(35)	1.379(5)
C(34)-H(34)	0.9500
C(35)-H(35)	0.9500
C(41)-C(46)	1.392(4)
C(41)-C(42)	1.407(4)
C(42)-C(43)	1.394(5)
C(42)-C(47)	1.505(5)
C(43)-C(44)	1.378(5)
C(43)-H(43)	0.9500
C(44)-C(45)	1.380(5)
C(44)-H(44)	0.9500
C(45)-C(46)	1.377(5)
C(45)-H(45)	0.9500
C(46)-H(46)	0.9500
C(47)-H(8TA)	0.9800
C(47)-H(8TB)	0.9800
C(47)-H(8TC)	0.9800
O(100)-C(100)	1.408(4)
O(100)-H(100)	0.8400
C(100)-H(10A)	0.9800
C(100)-H(10B)	0.9800
C(100)-H(10C)	0.9800
N(21)-Cu(1)-N(31)	79.26(10)
N(21)-Cu(1)-N(11)	79.11(10)
N(31)-Cu(1)-N(11)	156.56(10)
N(21)-Cu(1)-Cl(2)	162.50(8)
N(31)-Cu(1)-Cl(2)	99.06(7)
N(11)-Cu(1)-Cl(2)	98.83(7)
N(21)-Cu(1)-Cl(1)	93.36(7)
N(31)-Cu(1)-Cl(1)	94.40(7)
N(11)-Cu(1)-Cl(1)	95.77(7)
Cl(2)-Cu(1)-Cl(1)	104.15(3)
C(15)-N(11)-C(11)	119.0(3)
C(15)-N(11)-Cu(1)	126.3(2)
C(11)-N(11)-Cu(1)	114.7(2)
N(11)-C(11)-C(12)	121.8(3)
N(11)-C(11)-C(21)	113.8(3)
C(12)-C(11)-C(21)	124.4(3)
C(11)-C(12)-C(13)	118.5(3)
C(11)-C(12)-H(12)	120.7
C(13)-C(12)-H(12)	120.7
C(14)-C(13)-C(12)	119.8(3)
C(14)-C(13)-H(13)	120.1
C(12)-C(13)-H(13)	120.1
C(13)-C(14)-C(15)	118.5(3)
C(13)-C(14)-H(14)	120.8

C(15)-C(14)-H(14)	120.8
N(11)-C(15)-C(14)	122.2(3)
N(11)-C(15)-H(15)	118.9
C(14)-C(15)-H(15)	118.9
C(25)-N(21)-C(21)	121.1(3)
C(25)-N(21)-Cu(1)	119.2(2)
C(21)-N(21)-Cu(1)	119.5(2)
N(21)-C(21)-C(22)	120.9(3)
N(21)-C(21)-C(11)	112.5(3)
C(22)-C(21)-C(11)	126.5(3)
C(21)-C(22)-C(23)	118.9(3)
C(21)-C(22)-H(0MA)	120.5
C(23)-C(22)-H(0MA)	120.5
C(22)-C(23)-C(24)	118.5(3)
C(22)-C(23)-C(41)	122.4(3)
C(24)-C(23)-C(41)	119.1(3)
C(25)-C(24)-C(23)	119.0(3)
C(25)-C(24)-H(7TA)	120.5
C(23)-C(24)-H(7TA)	120.5
N(21)-C(25)-C(24)	121.3(3)
N(21)-C(25)-C(31)	112.5(3)
C(24)-C(25)-C(31)	126.2(3)
C(35)-N(31)-C(31)	118.1(3)
C(35)-N(31)-Cu(1)	127.6(2)
C(31)-N(31)-Cu(1)	114.16(19)
N(31)-C(31)-C(32)	122.7(3)
N(31)-C(31)-C(25)	114.0(3)
C(32)-C(31)-C(25)	123.2(3)
C(31)-C(32)-C(33)	118.3(3)
C(31)-C(32)-H(32)	120.8
C(33)-C(32)-H(32)	120.8
C(34)-C(33)-C(32)	119.2(3)
C(34)-C(33)-H(33)	120.4
C(32)-C(33)-H(33)	120.4
C(33)-C(34)-C(35)	119.3(3)
C(33)-C(34)-H(34)	120.3
C(35)-C(34)-H(34)	120.3
N(31)-C(35)-C(34)	122.3(3)
N(31)-C(35)-H(35)	118.9
C(34)-C(35)-H(35)	118.9
C(46)-C(41)-C(42)	119.2(3)
C(46)-C(41)-C(23)	118.6(3)
C(42)-C(41)-C(23)	122.2(3)
C(43)-C(42)-C(41)	117.8(3)
C(43)-C(42)-C(47)	118.7(3)
C(41)-C(42)-C(47)	123.5(3)
C(44)-C(43)-C(42)	122.1(3)
C(44)-C(43)-H(43)	118.9

C(42)-C(43)-H(43)	118.9
C(43)-C(44)-C(45)	119.8(3)
C(43)-C(44)-H(44)	120.1
C(45)-C(44)-H(44)	120.1
C(46)-C(45)-C(44)	119.2(3)
C(46)-C(45)-H(45)	120.4
C(44)-C(45)-H(45)	120.4
C(45)-C(46)-C(41)	121.8(3)
C(45)-C(46)-H(46)	119.1
C(41)-C(46)-H(46)	119.1
C(42)-C(47)-H(8TA)	109.5
C(42)-C(47)-H(8TB)	109.5
H(8TA)-C(47)-H(8TB)	109.5
C(42)-C(47)-H(8TC)	109.5
H(8TA)-C(47)-H(8TC)	109.5
H(8TB)-C(47)-H(8TC)	109.5
C(100)-O(100)-H(100)	109.5
O(100)-C(100)-H(10A)	109.5
O(100)-C(100)-H(10B)	109.5
H(10A)-C(100)-H(10B)	109.5
O(100)-C(100)-H(10C)	109.5
H(10A)-C(100)-H(10C)	109.5
H(10B)-C(100)-H(10C)	109.5

---

Symmetry transformations used to generate equivalent atoms:

x, y, z            -x, -y, -z

## 2.4 Table 4.

Anisotropic displacement parameters ( $\text{\AA}^2 \times 10^3$ ) for  $[\text{Cu}(\text{ottp})]\text{Cl}_2 \cdot \text{CH}_3\text{OH}$  The anisotropic displacement factor exponent takes the form:

$$-2 \pi^2 [h^2 a^{*2} U_{11} + \dots + 2 h k a^* b^* U_{12}]$$

---

	U11	U22	U33	U23	U13	U12
Cu(1)	17(1)	23(1)	18(1)	-9(1)	1(1)	-4(1)
Cl(1)	25(1)	40(1)	22(1)	1(1)	-1(1)	-1(1)

---

Cl(2)	25(1)	36(1)	22(1)	-15(1)	5(1)	-6(1)
N(11)	18(1)	25(1)	18(1)	-7(1)	0(1)	-4(1)
C(11)	23(2)	22(2)	16(1)	-4(1)	0(1)	-5(1)
C(12)	23(2)	32(2)	26(2)	-11(1)	1(1)	-6(1)
C(13)	29(2)	35(2)	29(2)	-14(1)	1(1)	-14(1)
C(14)	33(2)	31(2)	28(2)	-16(1)	0(1)	-9(1)
C(15)	24(2)	28(2)	23(2)	-13(1)	1(1)	-2(1)
N(21)	16(1)	22(1)	17(1)	-5(1)	-3(1)	-5(1)
C(21)	19(1)	22(2)	16(1)	-3(1)	-3(1)	-2(1)
C(22)	22(2)	24(2)	18(2)	-4(1)	-1(1)	-7(1)
C(23)	22(2)	24(2)	14(1)	-4(1)	-2(1)	-1(1)
C(24)	24(2)	23(2)	19(2)	-7(1)	-2(1)	-6(1)
C(25)	23(2)	21(2)	16(1)	-4(1)	0(1)	-4(1)
N(31)	18(1)	24(1)	18(1)	-4(1)	-1(1)	-6(1)
C(31)	20(2)	25(2)	16(1)	-5(1)	-3(1)	-6(1)
C(32)	25(2)	30(2)	24(2)	-12(1)	1(1)	-4(1)
C(33)	28(2)	31(2)	31(2)	-13(1)	-4(1)	-10(1)
C(34)	21(2)	37(2)	25(2)	-7(1)	0(1)	-10(1)
C(35)	18(2)	30(2)	21(2)	-6(1)	0(1)	-2(1)
C(41)	23(2)	27(2)	18(2)	-9(1)	-4(1)	-4(1)
C(42)	24(2)	30(2)	20(2)	-9(1)	-2(1)	-3(1)
C(43)	27(2)	40(2)	22(2)	-12(1)	0(1)	-5(1)
C(44)	24(2)	49(2)	28(2)	-24(2)	0(1)	4(2)
C(45)	41(2)	30(2)	29(2)	-14(1)	-8(2)	8(2)
C(46)	30(2)	27(2)	21(2)	-7(1)	-2(1)	-1(1)
C(47)	39(2)	30(2)	24(2)	-5(1)	7(2)	-6(1)
O(100)	42(2)	41(2)	44(2)	-27(1)	7(1)	-5(1)
C(100)	57(3)	37(2)	32(2)	-15(2)	5(2)	-7(2)

## 2.5 Table 5.

Hydrogen coordinates ( $\times 10^4$ ) and isotropic displacement parameters ( $\text{\AA}^2 \times 10^3$ ) for  $[\text{Cu}(\text{ottp})]\text{Cl}_2 \cdot \text{CH}_3\text{OH}$

	x	y	z	U(eq)
H(12)	10671	2763	3043	32
H(13)	10165	4819	3748	36
H(14)	7363	5552	4412	35

H(15)	5154	4101	4458	30
H(OMA)	10781	953	2207	26
H(7TA)	7956	-2249	1968	26
H(32)	5382	-3252	2532	31
H(33)	2617	-4093	3176	34
H(34)	651	-2686	4079	33
H(35)	1455	-512	4336	28
H(43)	13939	-230	-579	35
H(44)	14572	-2854	-338	39
H(45)	12984	-4509	914	39
H(46)	10772	-3502	1903	32
H(8TA)	10444	1750	398	49
H(8TB)	12259	1921	-298	49
H(8TC)	12124	1855	764	49
H(100)	6093	4739	1796	63
H(10A)	9414	4821	1131	64
H(10B)	8084	5123	459	64
H(10C)	8254	3496	1176	64

---

### 3.1 Table 1. $[\text{Co}(\text{ottp})_2 \cdot \text{Cl}_2] \cdot 2.25\text{CH}_3\text{OH}$

Crystal data and structure refinement for  $[\text{Co}(\text{ottp})_2 \cdot \text{Cl}_2] \cdot 2.25\text{CH}_3\text{OH}$

Identification code	L1CoA
Empirical formula	C <sub>46.25</sub> H <sub>42.50</sub> Cl <sub>2</sub> Co N <sub>6</sub> O <sub>2.50</sub>
Formula weight	852.19
Temperature	114(2) K
Wavelength	0.71073 Å
Crystal system, space group	monoclinic, P2 <sub>1</sub> /n
Crystal size	0.34 x 0.11 x 0.08 mm
Crystal colour	red-brown
Crystal form	block

Unit cell dimensions	a = 9.0517(10) Å b = 41.431(5) Å c = 11.7073(15) Å	alpha = 90 deg. beta = 107.147(7) deg. gamma = 90 deg.
Volume	4195.3(9) Å <sup>3</sup>	
Z, Calculated density	4, 1.349 Mg/m <sup>3</sup>	
Absorption coefficient	0.584 mm <sup>-1</sup>	
F(000)	1772	
Theta range for data collection	0.98 to 25.02 deg.	
Limiting indices	-10 ≤ h ≤ 10, -49 ≤ k ≤ 49, -13 ≤ l ≤ 13	
Reflections collected / unique	55339 / 7394 [R(int) = 0.1164]	
Completeness to theta = 25.00	99.9 %	
Max. and min. transmission	1.000000 0.673456	
Refinement method	Full-matrix least-squares on F <sup>2</sup>	
Data / restraints / parameters	7394 / 0 / 506	
Goodness-of-fit on F <sup>2</sup>	1.072	
Final R indices [I > 2σ(I)]	R1 = 0.0648, wR2 = 0.1813	
R indices (all data)	R1 = 0.1074, wR2 = 0.2109	
Largest diff. peak and hole	529 and -0.690 e.Å <sup>-3</sup>	

### 3.2 Table 2.

Atomic coordinates ( $\times 10^4$ ) and equivalent isotropic displacement parameters ( $\text{Å}^2 \times 10^3$ ) for  $[\text{Co}(\text{ottp})_2 \cdot \text{Cl}_2] \cdot 2.25\text{CH}_3\text{OH}$ .

U(eq) is defined as one third of the trace of the orthogonalized Uij tensor.

	x	y	z	U(eq)
Co(1)	4721(1)	1226(1)	1777(1)	15(1)
N(11)	3132(5)	880(1)	1626(4)	18(1)

C(11)	2351(6)	802(1)	477(5)	18(1)
C(12)	1305(6)	551(1)	204(5)	20(1)
C(13)	1064(6)	368(1)	1113(5)	26(1)
C(14)	1866(6)	445(1)	2278(5)	27(1)
C(15)	2889(6)	701(1)	2499(5)	21(1)
N(21)	3905(4)	1219(1)	113(4)	16(1)
C(21)	4406(5)	1437(1)	-553(5)	18(1)
C(22)	3758(6)	1450(1)	-1770(5)	20(1)
C(23)	2568(5)	1234(1)	-2339(4)	18(1)
C(24)	2063(6)	1014(1)	-1630(5)	20(1)
C(25)	2745(6)	1010(1)	-417(4)	17(1)
N(31)	6059(5)	1566(1)	1378(4)	18(1)
C(31)	5621(5)	1648(1)	187(5)	18(1)
C(32)	6224(6)	1912(1)	-234(5)	25(1)
C(33)	7333(6)	2099(1)	579(5)	30(1)
C(34)	7809(6)	2010(1)	1765(5)	28(1)
C(35)	7147(6)	1746(1)	2136(5)	24(1)
C(41)	1841(6)	1256(1)	-3652(5)	20(1)
C(42)	1337(6)	1561(1)	-4124(5)	26(1)
C(43)	619(7)	1601(2)	-5339(5)	34(2)
C(44)	438(7)	1338(2)	-6078(5)	37(2)
C(45)	940(6)	1040(2)	-5635(5)	32(1)
C(46)	1663(6)	990(1)	-4413(5)	24(1)
C(47)	2239(7)	657(2)	-3978(6)	37(2)
N(51)	6426(5)	838(1)	2180(4)	20(1)
C(51)	6973(6)	782(1)	3359(5)	18(1)
C(52)	7842(6)	510(1)	3834(5)	24(1)
C(53)	8142(6)	285(1)	3041(5)	26(1)
C(54)	7576(6)	341(1)	1822(5)	26(1)
C(55)	6726(6)	617(1)	1439(5)	24(1)
N(61)	5515(4)	1251(1)	3504(4)	17(1)
C(61)	5047(6)	1494(1)	4093(5)	19(1)
C(62)	5686(6)	1534(1)	5313(5)	20(1)
C(63)	6819(6)	1318(1)	5949(5)	22(1)
C(64)	7250(6)	1065(1)	5340(5)	20(1)
C(65)	6580(5)	1038(1)	4121(5)	17(1)
N(71)	3435(5)	1631(1)	2160(4)	19(1)
C(71)	3891(6)	1714(1)	3327(4)	18(1)
C(72)	3348(6)	1990(1)	3741(5)	23(1)
C(73)	2293(6)	2186(1)	2928(5)	28(1)
C(74)	1844(6)	2104(1)	1743(5)	26(1)
C(75)	2439(6)	1829(1)	1387(5)	25(1)
C(81)	7602(6)	1361(1)	7248(5)	21(1)
C(82)	7569(7)	1100(1)	8018(5)	27(1)
C(83)	8337(6)	1122(2)	9222(5)	29(1)
C(84)	9157(7)	1396(2)	9668(5)	36(2)
C(85)	9200(7)	1652(2)	8925(5)	33(1)
C(86)	8400(6)	1641(1)	7711(5)	25(1)

C(87)	8434(7)	1937(2)	6953(6)	36(2)
Cl(1)	9027(2)	344(1)	7102(1)	25(1)
Cl(2)	4360(2)	2211(1)	6859(1)	25(1)
C(111)	5000	0	5000	19(3)
O(101)	5462(12)	353(3)	5380(10)	63(3)
O(201)	7181(5)	317(1)	9002(4)	47(1)
C(211)	5725(8)	172(2)	8526(7)	53(2)
O(301)	2415(7)	2204(2)	8721(6)	73(2)
C(311)	2819(19)	2510(4)	9342(14)	166(6)

---

### 3.3 Table 3.

Bond lengths [Å] and angles [deg] for [Co(ottp)<sub>2</sub>Cl<sub>2</sub>]. 2.25CH<sub>3</sub>OH

---

Co(1)-N(21)	1.869(4)
Co(1)-N(61)	1.939(4)
Co(1)-N(31)	2.001(4)
Co(1)-N(11)	2.003(4)
Co(1)-N(71)	2.162(4)
Co(1)-N(51)	2.182(4)
N(11)-C(15)	1.332(7)
N(11)-C(11)	1.361(6)
C(11)-C(12)	1.378(7)
C(11)-C(25)	1.479(7)
C(12)-C(13)	1.376(7)
C(12)-H(12)	0.9500
C(13)-C(14)	1.381(8)
C(13)-H(13)	0.9500
C(14)-C(15)	1.379(8)
C(14)-H(14)	0.9500
C(15)-H(15)	0.9500
N(21)-C(21)	1.357(6)
N(21)-C(25)	1.359(6)
C(21)-C(22)	1.373(7)
C(21)-C(31)	1.471(7)
C(22)-C(23)	1.407(7)
C(22)-H(22)	0.9500
C(23)-C(24)	1.399(7)
C(23)-C(41)	1.486(7)
C(24)-C(25)	1.372(7)
C(24)-H(24)	0.9500
N(31)-C(35)	1.341(6)

N(31)-C(31)	1.374(6)
C(31)-C(32)	1.377(7)
C(32)-C(33)	1.397(8)
C(32)-H(32)	0.9500
C(33)-C(34)	1.377(8)
C(33)-H(33)	0.9500
C(34)-C(35)	1.378(8)
C(34)-H(34)	0.9500
C(35)-H(35)	0.9500
C(41)-C(46)	1.398(7)
C(41)-C(42)	1.400(7)
C(42)-C(43)	1.388(8)
C(42)-H(42)	0.9500
C(43)-C(44)	1.373(9)
C(43)-H(43)	0.9500
C(44)-C(45)	1.362(9)
C(44)-H(44)	0.9500
C(45)-C(46)	1.402(8)
C(45)-H(45)	0.9500
C(46)-C(47)	1.510(8)
C(47)-H(47A)	0.9800
C(47)-H(47B)	0.9800
C(47)-H(47C)	0.9800
N(51)-C(51)	1.342(6)
N(51)-C(55)	1.343(7)
C(51)-C(52)	1.394(7)
C(51)-C(65)	1.492(7)
C(52)-C(53)	1.399(8)
C(52)-H(52)	0.9500
C(53)-C(54)	1.387(8)
C(53)-H(53)	0.9500
C(54)-C(55)	1.377(8)
C(54)-H(54)	0.9500
C(55)-H(55)	0.9500
N(61)-C(65)	1.350(6)
N(61)-C(61)	1.355(6)
C(61)-C(62)	1.384(7)
C(61)-C(71)	1.476(7)
C(62)-C(63)	1.398(7)
C(62)-H(62)	0.9500
C(63)-C(64)	1.389(7)
C(63)-C(81)	1.487(7)
C(64)-C(65)	1.381(7)
C(64)-H(64)	0.9500
N(71)-C(75)	1.349(6)
N(71)-C(71)	1.350(6)
C(71)-C(72)	1.389(7)
C(72)-C(73)	1.393(7)

C(72)-H(72)	0.9500
C(73)-C(74)	1.369(8)
C(73)-H(73)	0.9500
C(74)-C(75)	1.377(8)
C(74)-H(74)	0.9500
C(75)-H(75)	0.9500
C(81)-C(86)	1.391(8)
C(81)-C(82)	1.412(8)
C(82)-C(83)	1.379(8)
C(82)-H(82)	0.9500
C(83)-C(84)	1.371(9)
C(83)-H(83)	0.9500
C(84)-C(85)	1.378(9)
C(84)-H(84)	0.9500
C(85)-C(86)	1.393(8)
C(85)-H(85)	0.9500
C(86)-C(87)	1.517(8)
C(87)-H(87A)	0.9800
C(87)-H(87B)	0.9800
C(87)-H(87C)	0.9800
C(111)-O(101)#1	1.550(11)
C(111)-O(101)	1.550(11)
O(101)-H(11A)	0.8400
O(201)-C(211)	1.405(8)
O(201)-H(201)	0.8400
C(211)-H(21A)	0.9800
C(211)-H(21B)	0.9800
C(211)-H(21C)	0.9800
O(301)-C(311)	1.451(15)
O(301)-H(301)	0.8400
C(311)-H(31A)	0.9800
C(311)-H(31B)	0.9800
C(311)-H(31C)	0.9800
N(21)-Co(1)-N(61)	177.51(18)
N(21)-Co(1)-N(31)	81.29(17)
N(61)-Co(1)-N(31)	98.20(17)
N(21)-Co(1)-N(11)	80.97(17)
N(61)-Co(1)-N(11)	99.56(17)
N(31)-Co(1)-N(11)	162.24(17)
N(21)-Co(1)-N(71)	99.08(17)
N(61)-Co(1)-N(71)	78.44(16)
N(31)-Co(1)-N(71)	84.40(17)
N(11)-Co(1)-N(71)	99.12(16)
N(21)-Co(1)-N(51)	104.45(17)
N(61)-Co(1)-N(51)	78.03(16)
N(31)-Co(1)-N(51)	97.50(16)
N(11)-Co(1)-N(51)	86.23(16)
N(71)-Co(1)-N(51)	156.42(16)

C(15)-N(11)-C(11)	118.1(4)
C(15)-N(11)-Co(1)	127.5(3)
C(11)-N(11)-Co(1)	114.0(3)
N(11)-C(11)-C(12)	121.9(5)
N(11)-C(11)-C(25)	113.5(4)
C(12)-C(11)-C(25)	124.6(5)
C(13)-C(12)-C(11)	119.4(5)
C(13)-C(12)-H(12)	120.3
C(11)-C(12)-H(12)	120.3
C(12)-C(13)-C(14)	118.7(5)
C(12)-C(13)-H(13)	120.7
C(14)-C(13)-H(13)	120.7
C(15)-C(14)-C(13)	119.4(5)
C(15)-C(14)-H(14)	120.3
C(13)-C(14)-H(14)	120.3
N(11)-C(15)-C(14)	122.5(5)
N(11)-C(15)-H(15)	118.7
C(14)-C(15)-H(15)	118.7
C(21)-N(21)-C(25)	120.4(4)
C(21)-N(21)-Co(1)	119.4(3)
C(25)-N(21)-Co(1)	120.1(3)
N(21)-C(21)-C(22)	120.6(4)
N(21)-C(21)-C(31)	112.1(4)
C(22)-C(21)-C(31)	127.2(5)
C(21)-C(22)-C(23)	120.0(5)
C(21)-C(22)-H(22)	120.0
C(23)-C(22)-H(22)	120.0
C(24)-C(23)-C(22)	118.2(5)
C(24)-C(23)-C(41)	122.1(4)
C(22)-C(23)-C(41)	119.6(5)
C(25)-C(24)-C(23)	119.6(5)
C(25)-C(24)-H(24)	120.2
C(23)-C(24)-H(24)	120.2
N(21)-C(25)-C(24)	121.2(5)
N(21)-C(25)-C(11)	111.3(4)
C(24)-C(25)-C(11)	127.5(5)
C(35)-N(31)-C(31)	118.0(4)
C(35)-N(31)-Co(1)	127.8(4)
C(31)-N(31)-Co(1)	113.4(3)
N(31)-C(31)-C(32)	122.2(5)
N(31)-C(31)-C(21)	113.1(4)
C(32)-C(31)-C(21)	124.6(5)
C(31)-C(32)-C(33)	118.5(5)
C(31)-C(32)-H(32)	120.8
C(33)-C(32)-H(32)	120.8
C(34)-C(33)-C(32)	119.2(5)
C(34)-C(33)-H(33)	120.4
C(32)-C(33)-H(33)	120.4

C(33)-C(34)-C(35)	119.6(5)
C(33)-C(34)-H(34)	120.2
C(35)-C(34)-H(34)	120.2
N(31)-C(35)-C(34)	122.4(5)
N(31)-C(35)-H(35)	118.8
C(34)-C(35)-H(35)	118.8
C(46)-C(41)-C(42)	119.8(5)
C(46)-C(41)-C(23)	122.9(5)
C(42)-C(41)-C(23)	117.2(5)
C(43)-C(42)-C(41)	120.8(5)
C(43)-C(42)-H(42)	119.6
C(41)-C(42)-H(42)	119.6
C(44)-C(43)-C(42)	118.9(6)
C(44)-C(43)-H(43)	120.6
C(42)-C(43)-H(43)	120.6
C(45)-C(44)-C(43)	121.0(6)
C(45)-C(44)-H(44)	119.5
C(43)-C(44)-H(44)	119.5
C(44)-C(45)-C(46)	121.7(6)
C(44)-C(45)-H(45)	119.1
C(46)-C(45)-H(45)	119.1
C(41)-C(46)-C(45)	117.7(5)
C(41)-C(46)-C(47)	122.9(5)
C(45)-C(46)-C(47)	119.4(5)
C(46)-C(47)-H(47A)	109.5
C(46)-C(47)-H(47B)	109.5
H(47A)-C(47)-H(47B)	109.5
C(46)-C(47)-H(47C)	109.5
H(47A)-C(47)-H(47C)	109.5
H(47B)-C(47)-H(47C)	109.5
C(51)-N(51)-C(55)	117.6(5)
C(51)-N(51)-Co(1)	111.8(3)
C(55)-N(51)-Co(1)	128.9(4)
N(51)-C(51)-C(52)	122.9(5)
N(51)-C(51)-C(65)	114.3(4)
C(52)-C(51)-C(65)	122.7(5)
C(51)-C(52)-C(53)	118.2(5)
C(51)-C(52)-H(52)	120.9
C(53)-C(52)-H(52)	120.9
C(54)-C(53)-C(52)	119.0(5)
C(54)-C(53)-H(53)	120.5
C(52)-C(53)-H(53)	120.5
C(55)-C(54)-C(53)	118.5(5)
C(55)-C(54)-H(54)	120.7
C(53)-C(54)-H(54)	120.7
N(51)-C(55)-C(54)	123.7(5)
N(51)-C(55)-H(55)	118.1
C(54)-C(55)-H(55)	118.1

C(65)-N(61)-C(61)	119.7(4)
C(65)-N(61)-Co(1)	120.6(3)
C(61)-N(61)-Co(1)	119.6(3)
N(61)-C(61)-C(62)	121.1(5)
N(61)-C(61)-C(71)	114.9(4)
C(62)-C(61)-C(71)	123.9(5)
C(61)-C(62)-C(63)	119.4(5)
C(61)-C(62)-H(62)	120.3
C(63)-C(62)-H(62)	120.3
C(64)-C(63)-C(62)	118.9(5)
C(64)-C(63)-C(81)	119.6(5)
C(62)-C(63)-C(81)	121.5(5)
C(65)-C(64)-C(63)	119.2(5)
C(65)-C(64)-H(64)	120.4
C(63)-C(64)-H(64)	120.4
N(61)-C(65)-C(64)	121.8(5)
N(61)-C(65)-C(51)	113.8(4)
C(64)-C(65)-C(51)	124.5(4)
C(75)-N(71)-C(71)	118.0(4)
C(75)-N(71)-Co(1)	128.7(4)
C(71)-N(71)-Co(1)	112.6(3)
N(71)-C(71)-C(72)	121.9(5)
N(71)-C(71)-C(61)	114.1(4)
C(72)-C(71)-C(61)	123.9(5)
C(71)-C(72)-C(73)	118.9(5)
C(71)-C(72)-H(72)	120.5
C(73)-C(72)-H(72)	120.5
C(74)-C(73)-C(72)	119.0(5)
C(74)-C(73)-H(73)	120.5
C(72)-C(73)-H(73)	120.5
C(73)-C(74)-C(75)	119.2(5)
C(73)-C(74)-H(74)	120.4
C(75)-C(74)-H(74)	120.4
N(71)-C(75)-C(74)	122.9(5)
N(71)-C(75)-H(75)	118.6
C(74)-C(75)-H(75)	118.6
C(86)-C(81)-C(82)	119.8(5)
C(86)-C(81)-C(63)	122.2(5)
C(82)-C(81)-C(63)	118.0(5)
C(83)-C(82)-C(81)	120.2(5)
C(83)-C(82)-H(82)	119.9
C(81)-C(82)-H(82)	119.9
C(84)-C(83)-C(82)	119.8(6)
C(84)-C(83)-H(83)	120.1
C(82)-C(83)-H(83)	120.1
C(83)-C(84)-C(85)	120.5(5)
C(83)-C(84)-H(84)	119.7
C(85)-C(84)-H(84)	119.7

C(84)-C(85)-C(86)	121.2(6)
C(84)-C(85)-H(85)	119.4
C(86)-C(85)-H(85)	119.4
C(81)-C(86)-C(85)	118.5(5)
C(81)-C(86)-C(87)	123.0(5)
C(85)-C(86)-C(87)	118.6(5)
C(86)-C(87)-H(87A)	109.5
C(86)-C(87)-H(87B)	109.5
H(87A)-C(87)-H(87B)	109.5
C(86)-C(87)-H(87C)	109.5
H(87A)-C(87)-H(87C)	109.5
H(87B)-C(87)-H(87C)	109.5
O(101)#1-C(111)-O(101)	180.0(3)
C(111)-O(101)-H(11A)	109.5
C(211)-O(201)-H(201)	109.5
O(201)-C(211)-H(21A)	109.5
O(201)-C(211)-H(21B)	109.5
H(21A)-C(211)-H(21B)	109.5
O(201)-C(211)-H(21C)	109.5
H(21A)-C(211)-H(21C)	109.5
H(21B)-C(211)-H(21C)	109.5
C(311)-O(301)-H(301)	109.5
O(301)-C(311)-H(31A)	109.5
O(301)-C(311)-H(31B)	109.5
H(31A)-C(311)-H(31B)	109.5
O(301)-C(311)-H(31C)	109.5
H(31A)-C(311)-H(31C)	109.5
H(31B)-C(311)-H(31C)	109.5

Symmetry transformations used to generate equivalent atoms:

#1 -x+1,-y,-z+1

### 3.4 Table 4.

Anisotropic displacement parameters ( $\text{Å}^2 \times 10^3$ ) for  $[\text{Co}(\text{ottp})_2\text{Cl}_2] \cdot 2.25\text{CH}_3\text{OH}$

The anisotropic displacement factor exponent takes the form:

$$-2 \pi^2 [ h^2 a^{*2} U_{11} + \dots + 2 h k a^* b^* U_{12} ]$$

U11	U22	U33	U23	U13	U12
-----	-----	-----	-----	-----	-----

Co(1)	16(1)	15(1)	13(1)	0(1)	0(1)	-1(1)
N(11)	18(2)	20(2)	16(2)	-1(2)	4(2)	1(2)
C(11)	19(3)	18(3)	18(3)	1(2)	4(2)	1(2)
C(12)	19(3)	20(3)	17(3)	-3(2)	-1(2)	-4(2)
C(13)	27(3)	18(3)	30(3)	1(2)	4(2)	-5(2)
C(14)	32(3)	25(3)	23(3)	2(2)	8(3)	-1(2)
C(15)	26(3)	24(3)	13(3)	-2(2)	9(2)	-1(2)
N(21)	16(2)	13(2)	14(2)	-2(2)	0(2)	-1(2)
C(21)	16(2)	16(3)	19(3)	-2(2)	3(2)	0(2)
C(22)	25(3)	19(3)	16(3)	2(2)	4(2)	-1(2)
C(23)	16(2)	21(3)	15(3)	-1(2)	3(2)	3(2)
C(24)	20(3)	16(3)	20(3)	-5(2)	0(2)	-4(2)
C(25)	17(2)	16(3)	17(3)	-2(2)	2(2)	-2(2)
N(31)	16(2)	18(2)	17(2)	-2(2)	-1(2)	-1(2)
C(31)	15(2)	19(3)	18(3)	-3(2)	-1(2)	-1(2)
C(32)	24(3)	29(3)	20(3)	3(2)	4(2)	-6(2)
C(33)	32(3)	26(3)	27(3)	4(3)	3(3)	-12(3)
C(34)	24(3)	26(3)	30(3)	-2(3)	0(3)	-8(2)
C(35)	21(3)	28(3)	17(3)	-3(2)	-1(2)	0(2)
C(41)	18(3)	27(3)	13(3)	-1(2)	3(2)	-5(2)
C(42)	24(3)	28(3)	22(3)	3(2)	1(2)	-1(2)
C(43)	26(3)	42(4)	27(3)	13(3)	-1(3)	1(3)
C(44)	30(3)	59(5)	16(3)	6(3)	-2(3)	-3(3)
C(45)	24(3)	46(4)	23(3)	-10(3)	4(2)	-9(3)
C(46)	19(3)	31(3)	21(3)	-5(2)	5(2)	-1(2)
C(47)	45(4)	33(4)	33(4)	-12(3)	13(3)	1(3)
N(51)	20(2)	23(2)	15(2)	-4(2)	3(2)	-2(2)
C(51)	16(2)	18(3)	19(3)	-2(2)	5(2)	1(2)
C(52)	26(3)	23(3)	18(3)	1(2)	1(2)	5(2)
C(53)	25(3)	23(3)	28(3)	-1(2)	6(2)	2(2)
C(54)	20(3)	27(3)	30(3)	-10(3)	10(2)	-1(2)
C(55)	21(3)	29(3)	21(3)	-6(2)	7(2)	-3(2)
N(61)	14(2)	17(2)	17(2)	2(2)	1(2)	3(2)
C(61)	20(3)	17(3)	19(3)	-3(2)	5(2)	-2(2)
C(62)	25(3)	15(3)	18(3)	-4(2)	2(2)	0(2)
C(63)	25(3)	18(3)	20(3)	0(2)	2(2)	5(2)
C(64)	22(3)	17(3)	17(3)	1(2)	1(2)	6(2)
C(65)	16(2)	14(3)	19(3)	2(2)	1(2)	1(2)
N(71)	15(2)	20(2)	17(2)	0(2)	-3(2)	1(2)
C(71)	17(2)	18(3)	15(3)	-1(2)	0(2)	-2(2)
C(72)	24(3)	24(3)	16(3)	-3(2)	-2(2)	3(2)
C(73)	28(3)	24(3)	28(3)	-1(2)	4(3)	11(2)
C(74)	22(3)	27(3)	22(3)	4(2)	-3(2)	8(2)
C(75)	24(3)	30(3)	16(3)	3(2)	-4(2)	1(2)
C(81)	20(3)	23(3)	16(3)	-5(2)	2(2)	5(2)
C(82)	31(3)	24(3)	23(3)	-1(2)	2(3)	6(2)
C(83)	31(3)	37(4)	15(3)	6(3)	3(2)	6(3)
C(84)	37(3)	44(4)	18(3)	-2(3)	-3(3)	11(3)

C(85)	33(3)	31(3)	28(3)	-5(3)	-4(3)	3(3)
C(86)	25(3)	26(3)	21(3)	1(2)	0(2)	4(2)
C(87)	30(3)	34(4)	35(4)	0(3)	-3(3)	2(3)
Cl(1)	28(1)	23(1)	24(1)	2(1)	5(1)	1(1)
Cl(2)	33(1)	19(1)	20(1)	0(1)	3(1)	-1(1)

---

### 3.5 Table 5.

Hydrogen coordinates ( $\times 10^4$ ) and isotropic displacement parameters ( $\text{Å}^2 \times 10^3$ ) for  $[\text{Co}(\text{ottp})_2 \cdot \text{Cl}_2] \cdot 2.25\text{CH}_3\text{OH}$ .

	x	y	z	U(eq)
H(12)	756	505	-605	24
H(13)	359	192	942	31
H(14)	1715	323	2922	32
H(15)	3440	751	3303	25
H(22)	4112	1605	-2228	24
H(24)	1253	867	-1987	24
H(32)	5894	1966	-1060	30
H(33)	7754	2285	318	36
H(34)	8589	2130	2324	34
H(35)	7474	1689	2959	28
H(42)	1489	1743	-3607	31
H(43)	258	1808	-5653	40
H(44)	-44	1363	-6912	44
H(45)	797	862	-6168	38
H(47A)	3269	673	-3400	55
H(47B)	2294	524	-4657	55
H(47C)	1527	557	-3594	55
H(52)	8220	478	4674	28
H(53)	8724	95	3334	31
H(54)	7771	193	1264	31
H(55)	6329	653	602	28
H(62)	5358	1706	5714	24
H(64)	7996	911	5757	24
H(72)	3690	2045	4566	28
H(73)	1890	2375	3192	33
H(74)	1130	2234	1174	31
H(75)	2135	1775	561	30

H(82)	7015	909	7706	33
H(83)	8298	949	9741	34
H(84)	9701	1409	10495	43
H(85)	9785	1838	9247	40
H(87A)	8484	1868	6164	53
H(87B)	9345	2068	7343	53
H(87C)	7496	2065	6862	53
H(11A)	6287	354	5946	94
H(201)	7645	322	8477	71
H(21A)	5845	-63	8528	80
H(21B)	5262	247	7705	80
H(21C)	5054	231	9014	80
H(301)	1818	2238	8031	109
H(31A)	2990	2477	10200	248
H(31B)	1975	2664	9038	248
H(31C)	3765	2594	9207	248

---

#### 4.1 Table 1. $[(\text{Cl-ottp})\text{Cu}(\mu\text{-Cl})(\mu\text{-Br})\text{Cu}(\text{Cl-ottp})]2\text{PF}_6$

Crystal data and structure refinement for  $[(\text{Cl-ottp})\text{Cu}(\mu\text{-Cl})(\mu\text{-Br})\text{Cu}(\text{Cl-ottp})]2\text{PF}_6$

Identification code	PATBR	
Empirical formula	C <sub>22</sub> H <sub>16</sub> Br <sub>0.50</sub> Cl <sub>1.50</sub> Cu F <sub>6</sub> N <sub>3</sub> P	
Formula weight	624.02	
Temperature	122(2) K	
Wavelength	0.71073 Å	
Crystal system, space group	monoclinic, P2 <sub>1</sub> /n	
Crystal size	0.76 x 0.20 x 0.14 mm	
Crystal colour	blue-green	
Crystal form	needle	
Unit cell dimensions	a = 16.6918(10) Å	alpha = 90 deg.
	b = 7.0247(4) Å	beta = 100.442(3) deg.

	$c = 19.6665(12) \text{ \AA}$	$\gamma = 90 \text{ deg.}$
Volume	2267.8(2) $\text{\AA}^3$	
Z, Calculated density	4, 1.828 $\text{Mg/m}^3$	
Absorption coefficient	2.159 $\text{mm}^{-1}$	
Absorption Correction	multi-scan	
F(000)	1240	
Theta range for data collection	2.48 to 25.05 deg.	
Limiting indices	$-19 \leq h \leq 19, -8 \leq k \leq 8, -23 \leq l \leq 23$	
Reflections collected / unique	40691 / 4016 [R(int) = 0.0476]	
Completeness to theta = 25.05	99.9 %	
Max. and min. transmission	0.7520 and 0.2908	
Refinement method	Full-matrix least-squares on $F^2$	
Data / restraints / parameters	4016 / 0 / 320	
Goodness-of-fit on $F^2$	1.053	
Final R indices [ $I > 2\sigma(I)$ ]	R1 = 0.0458, wR2 = 0.1258	
R indices (all data)	R1 = 0.0594, wR2 = 0.1363	
Largest diff. peak and hole	0.965 and -0.516 $\text{e.\AA}^{-3}$	

## 4.2 Table 2.

Atomic coordinates ( $\times 10^4$ ) and equivalent isotropic displacement parameters ( $\text{\AA}^2 \times 10^3$ ) for  $[(\text{Cl-ottp})\text{Cu}(\mu\text{-Cl})(\mu\text{-Br})\text{Cu}(\text{Cl-ottp})]2\text{PF}_6$

U(eq) is defined as one third of the trace of the orthogonalized  $U_{ij}$  tensor.

	x	y	z	U(eq)
Cu(1)	5313(1)	12645(1)	4990(1)	27(1)
Br(1)	3990(9)	13663(18)	4749(8)	37(1)
Cl(1)	4020(20)	13850(50)	4780(20)	37(1)
Cl(2)	8068(1)	5700(2)	4495(1)	60(1)
N(1)	5581(2)	12787(5)	4026(2)	29(1)

N(2)	6376(2)	11466(4)	5158(2)	25(1)
N(3)	5356(2)	11742(5)	5978(2)	28(1)
C(1)	5108(3)	13504(6)	3465(2)	36(1)
C(2)	5388(3)	13698(7)	2845(2)	42(1)
C(3)	6166(3)	3154(7)	2814(3)	44(1)
C(4)	6652(3)	12385(6)	3389(2)	37(1)
C(5)	6348(3)	12216(6)	3990(2)	30(1)
C(6)	6799(2)	11423(6)	4643(2)	27(1)
C(7)	7587(3)	10693(6)	4766(2)	33(1)
C(8)	7916(2)	10040(6)	5422(2)	32(1)
C(9)	7445(2)	10097(6)	5938(2)	30(1)
C(10)	6670(2)	10811(5)	5785(2)	26(1)
C(11)	6076(2)	10937(5)	6260(2)	27(1)
C(12)	6232(3)	10272(7)	6930(2)	35(1)
C(13)	5629(3)	10454(7)	330(2)	41(1)
C(14)	4899(3)	11290(6)	7043(3)	39(1)
C(15)	4780(3)	11904(6)	6370(2)	34(1)
C(16)	8772(3)	9325(7)	5595(2)	39(1)
C(17)	9400(3)	10613(9)	5781(3)	49(1)
C(18)	10195(3)	10003(11)	5969(3)	57(2)
C(19)	10365(3)	8125(11)	5972(3)	66(2)
C(20)	9764(4)	6843(11)	5799(4)	79(2)
C(21)	8947(3)	7416(9)	608(4)	68(2)
C(22)	8294(4)	5970(9)	5420(6)	101(3)
P(1)	7500	-2097(3)	2500	68(1)
P(2)	7500	5072(3)	7500	54(1)
F(10)	8070(5)	3664(9)	2884(4)	174(3)
F(11)	6924(2)	477(7)	2113(2)	86(1)
F(12)	6996(3)	2086(6)	3114(3)	93(1)
F(20)	7753(4)	3433(7)	7040(3)	119(2)
F(21)	6655(3)	5024(9)	7052(4)	171(3)
F(22)	7771(5)	6690(7)	7048(3)	144(3)

---

### 4.3 Table 3.

Bond lengths [Å] and angles [deg] for [(Cl-ottp)Cu( $\mu$ -Cl)( $\mu$ -Br)Cu(Cl-ottp)]2PF<sub>6</sub>

---

Cu(1)-N(2)	1.931(3)	Cu(1)-N(1)	2.027(4)
Cu(1)-N(3)	2.033(4)	Cu(1)-Cl(1)	2.29(4)
Cu(1)-Br(1)	2.287(15)	Cu(1)-Cl(1)#1	2.71(3)
Cu(1)-Br(1)#1	2.851(12)	Br(1)-Cu(1)#1	2.851(12)
Cl(1)-Cu(1)#1	2.71(3)	Cl(2)-C(22)	1.800(11)
N(1)-C(1)	1.333(6)	N(1)-C(5)	1.355(5)
N(2)-C(10)	1.325(5)	N(2)-C(6)	1.336(5)
N(3)-C(15)	1.343(5)	N(3)-C(11)	1.352(5)
C(1)-C(2)	1.391(7)	C(1)-H(1A)	0.9500
C(2)-C(3)	1.365(7)	C(2)-H(2A)	0.9500
C(3)-C(4)	1.377(7)	C(3)-H(3A)	0.9500
C(4)-C(5)	1.374(6)	C(4)-H(4A)	0.9500
C(5)-C(6)	1.475(6)	C(6)-C(7)	1.391(6)
C(7)-C(8)	1.386(6)	C(7)-H(7A)	0.9500
C(8)-C(9)	1.393(6)	C(8)-C(16)	1.494(6)
C(9)-C(10)	1.369(6)		
C(9)-H(9A)	0.9500	C(10)-C(11)	1.482(5)
C(11)-C(12)	1.378(6)	C(12)-C(13)	1.391(6)
C(12)-H(12A)	0.9500	C(13)-C(14)	1.378(7)
C(13)-H(13A)	0.9500	C(14)-C(15)	1.371(7)
C(14)-H(14A)	0.9500	C(15)-H(15A)	0.9500
C(16)-C(21)	1.372(8)	C(16)-C(17)	1.383(7)
C(17)-C(18)	1.380(7)	C(17)-H(17A)	0.9500

C(18)-C(19)	1.349(10)	C(18)-H(18A)	0.9500
C(19)-C(20)	1.345(10)	C(19)-H(19A)	0.9500
C(20)-C(21)	1.406(8)	C(20)-H(20A)	0.9500
C(21)-C(22)	1.486(9)	C(22)-H(22A)	0.9900
C(22)-H(22B)	0.9900	P(1)-F(10)#2	1.558(5)
P(1)-F(10)	1.558(5)		
P(1)-F(11)#2	1.591(4)		
P(1)-F(11)	1.591(4)		
P(1)-F(12)#2	1.591(4)		
P(1)-F(12)	1.591(4)		
P(2)-F(21)	1.522(4)		
P(2)-F(21)#3	1.522(5)		
P(2)-F(22)	1.559(5)		
P(2)-F(22)#3	1.559(5)		
P(2)-F(20)	1.569(5)		
P(2)-F(20)#3	1.569(5)		
N(2)-Cu(1)-N(1)	80.19(14)		
N(2)-Cu(1)-N(3)	80.21(14)		
N(1)-Cu(1)-N(3)	158.97(13)		
N(2)-Cu(1)-Cl(1)	176.3(8)		
N(1)-Cu(1)-Cl(1)	100.2(11)		
N(3)-Cu(1)-Cl(1)	98.9(11)		
N(2)-Cu(1)-Br(1)	172.7(3)		
N(1)-Cu(1)-Br(1)	99.2(4)		
N(3)-Cu(1)-Br(1)	99.3(4)		
Cl(1)-Cu(1)-Br(1)	3.7(10)		
N(2)-Cu(1)-Cl(1)#1	91.4(8)		
N(1)-Cu(1)-Cl(1)#1	87.5(9)		
N(3)-Cu(1)-Cl(1)#1	100.6(9)		
Cl(1)-Cu(1)-Cl(1)#1	92.3(11)		
Br(1)-Cu(1)-Cl(1)#1	95.9(9)		

N(2)-Cu(1)-Br(1)#1	91.6(3)
N(1)-Cu(1)-Br(1)#1	88.4(4)
N(3)-Cu(1)-Br(1)#1	99.7(4)
Cl(1)-Cu(1)-Br(1)#1	92.2(8)
Br(1)-Cu(1)-Br(1)#1	95.7(4)
Cl(1)#1-Cu(1)-Br(1)#1	90.9(12)
Cu(1)-Br(1)-Cu(1)#1	84.3(4)
Cu(1)-Cl(1)-Cu(1)#1	87.7(11)
C(1)-N(1)-C(5)	119.5(4)
C(1)-N(1)-Cu(1)	126.4(3)
C(5)-N(1)-Cu(1)	113.9(3)
C(10)-N(2)-C(6)	122.7(3)
C(10)-N(2)-Cu(1)	118.8(3)
C(6)-N(2)-Cu(1)	118.4(3)
C(15)-N(3)-C(11)	118.4(4)
C(15)-N(3)-Cu(1)	128.2(3)
C(11)-N(3)-Cu(1)	113.4(3)
N(1)-C(1)-C(2)	121.4(4)
N(1)-C(1)-H(1A)	119.3
C(2)-C(1)-H(1A)	119.3
C(3)-C(2)-C(1)	119.0(4)
C(3)-C(2)-H(2A)	120.5
C(1)-C(2)-H(2A)	120.5
C(2)-C(3)-C(4)	119.8(5)
C(2)-C(3)-H(3A)	120.1
C(4)-C(3)-H(3A)	120.1
C(5)-C(4)-C(3)	119.1(5)
C(5)-C(4)-H(4A)	120.5
C(3)-C(4)-H(4A)	120.5
N(1)-C(5)-C(4)	121.2(4)
N(1)-C(5)-C(6)	113.9(4)
C(4)-C(5)-C(6)	124.9(4)

N(2)-C(6)-C(7)	119.4(4)
N(2)-C(6)-C(5)	113.2(3)
C(7)-C(6)-C(5)	127.5(4)
C(8)-C(7)-C(6)	119.1(4)
C(8)-C(7)-H(7A)	120.4
C(6)-C(7)-H(7A)	120.5
C(7)-C(8)-C(9)	119.2(4)
C(7)-C(8)-C(16)	121.7(4)
C(9)-C(8)-C(16)	119.1(4)
C(10)-C(9)-C(8)	119.1(4)
C(10)-C(9)-H(9A)	120.4
C(8)-C(9)-H(9A)	120.4
N(2)-C(10)-C(9)	120.5(4)
N(2)-C(10)-C(11)	112.9(3)
C(9)-C(10)-C(11)	126.7(4)
N(3)-C(11)-C(12)	122.3(4)
N(3)-C(11)-C(10)	114.4(4)
C(12)-C(11)-C(10)	123.3(4)
C(11)-C(12)-C(13)	118.6(4)
C(11)-C(12)-H(12A)	120.7
C(13)-C(12)-H(12A)	120.7
C(14)-C(13)-C(12)	119.0(4)
C(14)-C(13)-H(13A)	120.5
C(12)-C(13)-H(13A)	120.5
C(15)-C(14)-C(13)	119.4(4)
C(15)-C(14)-H(14A)	120.3
C(13)-C(14)-H(14A)	120.3
N(3)-C(15)-C(14)	122.3(4)
N(3)-C(15)-H(15A)	118.8
C(14)-C(15)-H(15A)	118.8
C(21)-C(16)-C(17)	119.1(5)
C(21)-C(16)-C(8)	121.6(5)

C(17)-C(16)-C(8)	119.2(5)
C(18)-C(17)-C(16)	120.9(6)
C(18)-C(17)-H(17A)	119.5
C(16)-C(17)-H(17A)	119.5
C(19)-C(18)-C(17)	119.7(6)
C(19)-C(18)-H(18A)	120.1
C(17)-C(18)-H(18A)	120.1
C(20)-C(19)-C(18)	120.5(5)
C(20)-C(19)-H(19A)	119.8
C(18)-C(19)-H(19A)	119.8
C(19)-C(20)-C(21)	121.3(7)
C(19)-C(20)-H(20A)	119.4
C(21)-C(20)-H(20A)	119.4
C(16)-C(21)-C(20)	118.5(6)
C(16)-C(21)-C(22)	121.3(5)
C(20)-C(21)-C(22)	120.2(6)
C(21)-C(22)-Cl(2)	109.5(6)
C(21)-C(22)-H(22A)	109.8
Cl(2)-C(22)-H(22A)	109.8
C(21)-C(22)-H(22B)	109.8
Cl(2)-C(22)-H(22B)	109.8
H(22A)-C(22)-H(22B)	108.2
F(10)#2-P(1)-F(10)	90.0(7)
F(10)#2-P(1)-F(11)#2	179.3(4)
F(10)-P(1)-F(11)#2	90.6(4)
F(10)#2-P(1)-F(11)	90.6(4)
F(10)-P(1)-F(11)	179.3(4)
F(11)#2-P(1)-F(11)	88.7(3)
F(10)#2-P(1)-F(12)#2	89.7(3)
F(10)-P(1)-F(12)#2	90.7(3)
F(11)#2-P(1)-F(12)#2	90.2(2)
F(11)-P(1)-F(12)#2	89.4(2)

F(10)#2-P(1)-F(12)	90.7(3)
F(10)-P(1)-F(12)	89.7(3)
F(11)#2-P(1)-F(12)	89.4(2)
F(11)-P(1)-F(12)	90.2(2)
F(12)#2-P(1)-F(12)	179.4(4)
F(21)-P(2)-F(21)#3	177.5(5)
F(21)-P(2)-F(22)	91.1(4)
F(21)#3-P(2)-F(22)	90.7(4)
F(21)-P(2)-F(22)#3	90.7(4)
F(21)#3-P(2)-F(22)#3	91.1(4)
F(22)-P(2)-F(22)#3	86.4(4)
F(21)-P(2)-F(20)	88.2(4)
F(21)#3-P(2)-F(20)	90.0(4)
F(22)-P(2)-F(20)	94.1(3)
F(22)#3-P(2)-F(20)	178.8(4)
F(21)-P(2)-F(20)#3	90.0(4)
F(21)#3-P(2)-F(20)#3	88.2(4)
F(22)-P(2)-F(20)#3	178.8(4)
F(22)#3-P(2)-F(20)#3	94.1(3)
F(20)-P(2)-F(20)#3	85.6(5)

---

Symmetry transformations used to generate equivalent atoms:

#1  $-x+1, -y+3, -z+1$

#2  $-x+3/2, y, -z+1/2$

#3  $-x+3/2, y, -z+3/2$

#### 4.4 Table 4.

Anisotropic displacement parameters ( $\text{\AA}^2 \times 10^3$ ) for  $[(\text{Cl-ottp})\text{Cu}(\mu\text{-Cl})(\mu\text{-Br})\text{Cu}(\text{Cl-ottp})]2\text{PF}_6$

The anisotropic displacement factor exponent takes the form:

$$-2 \pi^2 [ h^2 a^{*2} U_{11} + \dots + 2 h k a^* b^* U_{12} ]$$

---

	U11	U22	U33	U23	U13	U12
Cu(1)	23(1)	24(1)	35(1)	-4(1)	4(1)	2(1)
Br(1)	28(1)	29(2)	53(2)	-11(2)	1(1)	0(1)
Cl(1)	28(1)	29(2)	53(2)	-11(2)	1(1)	0(1)
Cl(2)	52(1)	44(1)	82(1)	-22(1)	8(1)	-7(1)
N(1)	30(2)	23(2)	32(2)	-5(1)	3(2)	1(1)
N(2)	24(2)	22(2)	30(2)	-1(1)	7(1)	0(1)
N(3)	24(2)	21(2)	39(2)	-3(1)	8(2)	0(1)
C(1)	39(2)	25(2)	39(2)	-5(2)	-4(2)	3(2)
C(2)	56(3)	33(2)	34(2)	1(2)	-2(2)	3(2)
C(3)	58(3)	39(3)	34(2)	3(2)	8(2)	-5(2)
C(4)	41(3)	36(2)	37(2)	-1(2)	13(2)	-4(2)
C(5)	32(2)	23(2)	34(2)	-2(2)	5(2)	-1(2)
C(6)	28(2)	24(2)	31(2)	-3(2)	8(2)	-1(2)
C(7)	26(2)	37(2)	38(2)	0(2)	13(2)	1(2)
C(8)	23(2)	33(2)	40(2)	1(2)	7(2)	0(2)
C(9)	27(2)	33(2)	30(2)	3(2)	2(2)	-1(2)
C(10)	25(2)	23(2)	29(2)	-2(2)	6(2)	-3(2)
C(11)	25(2)	23(2)	34(2)	-7(2)	7(2)	-5(2)
C(12)	32(2)	37(2)	36(2)	-1(2)	8(2)	-1(2)
C(13)	45(3)	45(3)	35(2)	-5(2)	14(2)	-7(2)
C(14)	37(2)	37(2)	48(3)	-12(2)	22(2)	-8(2)
C(15)	27(2)	29(2)	49(3)	-10(2)	13(2)	3(2)
C(16)	25(2)	55(3)	38(3)	9(2)	9(2)	4(2)
C(17)	31(3)	68(3)	48(3)	-5(3)	7(2)	-3(2)
C(18)	30(3)	98(5)	43(3)	-3(3)	3(2)	-5(3)
C(19)	26(3)	114(6)	60(4)	33(4)	12(2)	15(3)

---

C(20)	39(3)	73(4)	127(6)	36(4)	17(4)	22(3)
C(21)	30(3)	62(4)	113(6)	24(4)	17(3)	10(3)
C(22)	42(4)	45(4)	217(11)	13(5)	25(5)	10(3)
P(1)	52(1)	51(1)	112(2)	0	45(1)	0
P(2)	58(1)	33(1)	60(1)	0	-21(1)	0
F(10)	246(7)	122(4)	193(7)	76(4)	142(6)	127(5)
F(11)	45(2)	108(3)	102(3)	-2(3)	10(2)	13(2)
F(12)	74(3)	88(3)	133(4)	7(3)	64(3)	1(2)
F(20)	149(5)	75(3)	130(4)	-28(3)	12(4)	25(3)
F(21)	118(4)	126(5)	219(7)	-8(5)	-100(5)	40(4)
F(22)	261(8)	69(3)	118(4)	22(3)	77(5)	-7(4)

#### 4.5 Table 5.

Hydrogen coordinates ( $\times 10^4$ ) and isotropic displacement parameters ( $\text{Å}^2 \times 10^3$ ) for  $[(\text{Cl-ottp})\text{Cu}(\mu\text{-Cl})(\mu\text{-Br})\text{Cu}(\text{Cl-ottp})]2\text{PF}_6$

	x	y	z	U(eq)
H(1A)	4569	13890	3490	43
H(2A)	5043	14202	2448	51
H(3A)	6371	13306	2397	53
H(4A)	7190	11976	3370	45
H(7A)	7896	10644	4405	39
H(9A)	7659	9647	6390	36
H(12A)	6741	9702	7115	42
H(13A)	5719	10009	7794	49

H(14A)	4481	11440	7309	46
H(15A)	4273	12464	6175	41
H(17A)	9283	11936	5778	59
H(18A)	10622	10901	6095	69
H(19A)	10912	7704	6099	79
H(20A)	9894	5526	5806	95
H(22A)	7798	6377	5590	122
H(22B)	8474	4736	5638	122

---

---

<sup>1</sup> *S*AINT-Plus, Bruker AXS Inc., Madison, Wisconsin, U.S.A.

<sup>2</sup> Sheldrick, G. M. *SHELXS-97*, Bruker, University of Göttingen, Germany, **1997**.

<sup>3</sup> Sheldrick, G. M. *SHELXL-97*, Bruker, University of Göttingen, Germany, **1997**.

<sup>4</sup> Sheldrick, G. M. *SHELXTL*, Bruker, University of Göttingen, Germany, **1997**.